INTERNUCLEAR COMPANY

INTERNUC - 55

STUDIES OF CONTROL, POWER SHAPING, AND BURNOUT BEHAVIOR FOR AETR

Work Performed for the
Chicago Operations Office
U. S. Atomic Energy Commission
Contract No. AT(11-1)688

by

T. L. Francis
W. S. Delicate
A. M. Larson, Jr.

April 5, 1960

DISCLAIMER

PREFACE

Since December 1956, Internuclear Company has prepared for the U.S. Atomic Energy Commission a series of reports[1-7] on the use of the "flux-trap" type reactor for high flux testing requirements. Among these reports was included a conceptual design of a seven reactor complex (INTERNUC-23, "An Advanced Engineering Test Reactor").

In October, 1958, the Commission requested Internuclear Company to a) make a prelimnary hazards evaluation of the reactor facility described in INTERNUC-23, b) design, construct and operate pilot models of the reflector safety and power regulation control systems and c) make a detailed engineering design of a "flux-trap" type nuclear mockup facility incorporating a reflector control system. During the course of the work the Commission requested Internuclear Company to investigate briefly the use of the AETR for the Naval Reactors testing requirements and to determine, in so far as possible, the test requirements of other AEC branches. Four reports covering this work were submitted.

In October, 1959, the Commision extended the above mentioned contract to perform additional experimental studies with the AETR reflector control mockup and additional analytical studies in certain areas important to the concept. These analytical studies include a) use of burnable poisons in the fuel assemblies, b) changes of nuclear characteristics with fuel burnup, c) evaluation of safety reflector worth with two-dimensional calculations and d) power flattening with non-uniform fuel distribution. This report is submitted in fulfillment of that portion of the contract relating to these analytical studies.

TABLE OF CONTENTS

TABLE OF CONTENTS (Continued)

LIST OF TABLES

LIST OF TABLES (Continued)

LIST OF FIGURES

LIST OF FIGURES (Continued)

LIST OF FIGURES (Continued)

LIST OF FIGURES (Continued)

1.0 INTRODUCTION

In previous work on the AETR design concept, certain characteristics of the reactor were studied only in a cursory manner. Further studies were deemed necessary to optimize its performance and to obtain a clearer understanding of its nuclear characteristics. In this report four of the more important parameters have been investigated further, namely:

1) worth of the droppable safety reflector

2) radial power flattening using a graded fuel distribution

3) variation of reactor characteristics with fuel burnup, and

4) use of burnable poisons in fuel assemblies.

In the previous work[2,3], the safety reflector worth was evaluated using one-dimensional diffusion theory calculations. This method is inherently limited because the end leakage of neutrons is not adequately treated and the relationship between the reactivity removed and the level of the drop is not established. In the present study, two-dimensional diffusion theory calculations are performed to obtain better information concerning the nuclear behavior of the droppable safety reflector.

The design power level of the AETR was established on the premise that considerable flattening of the radial power density distribution is achieved.[2] The principal method proposed for shaping the radial power distribution consists of grading the fuel radially by varying the thickness of the meat. In the present work a technique for calculating the graded fuel distribution is developed and the graded fuel distribution is determined.

The reactivity lifetime has been estimated assuming uniform flux, poisoning and fuel depletion effects.[2] In this report, the spatial variations of the reactor behavior with operating time are investigated. Of particular interest are the effects of the burnup and the changes in shim reflector poison concentration on radial power peaking during the cycle.

The use of burnable core poisons has been suggested[3] but not explored. For a fuel cycle of 19 days at 170 Mw as proposed in the preliminary conceptual design report[2], the necessity for a control method to supplement the reflector control systems seems probable. In this work, the effectiveness of a burnable core poison is investigated.

In addition to the above analytical investigations, the feasibility for fabricating the AETR fuel assembly with graded fuel and burnable poisons was explored with fuel element manufacturers and ORNL.

The reactor configuration considered for the above studies corresponds to the Type "A" reactor proposed in the preliminary conceptual design report(2) with slight changes to adjust for further optimization of the reflector control system.(3) Figures 1.A, 1.B and 1.C show the reactor elevation and plan views of the reactor-midplane and core-midplane, respectively. The droppable D_2O safety reflector adjacent to the core is 4 inches thick and is followed by a 3-inch thick shim reflector containing D_2O and soluble poison. Figures 1.D and 1.E show the elevation and plan models which are used throughout this report for nuclear calculations.

Figure 1.A Reactor Elevation

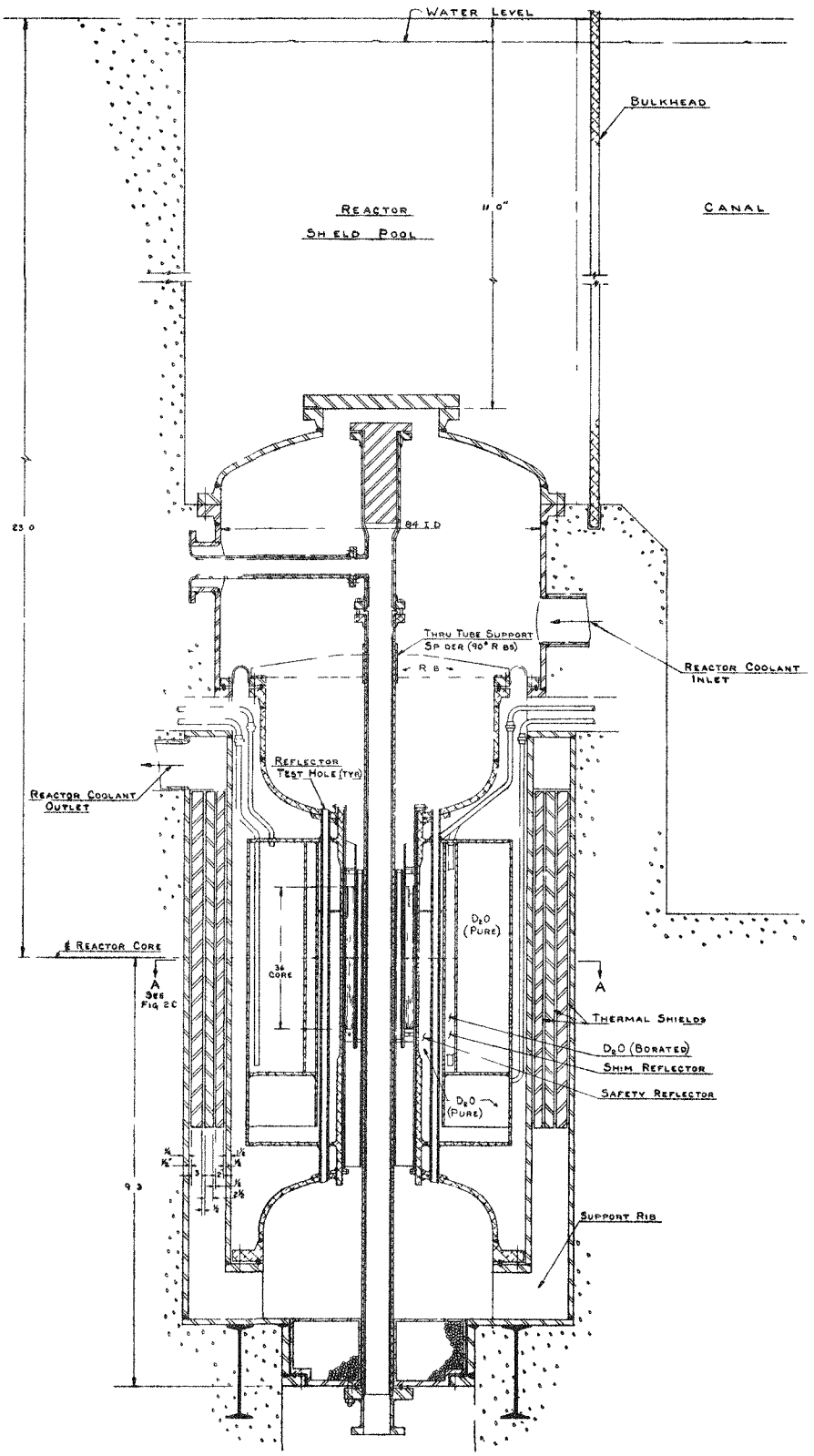

Figure 1.A

Figure 1 B Reactor Mid-Plane Cross Section

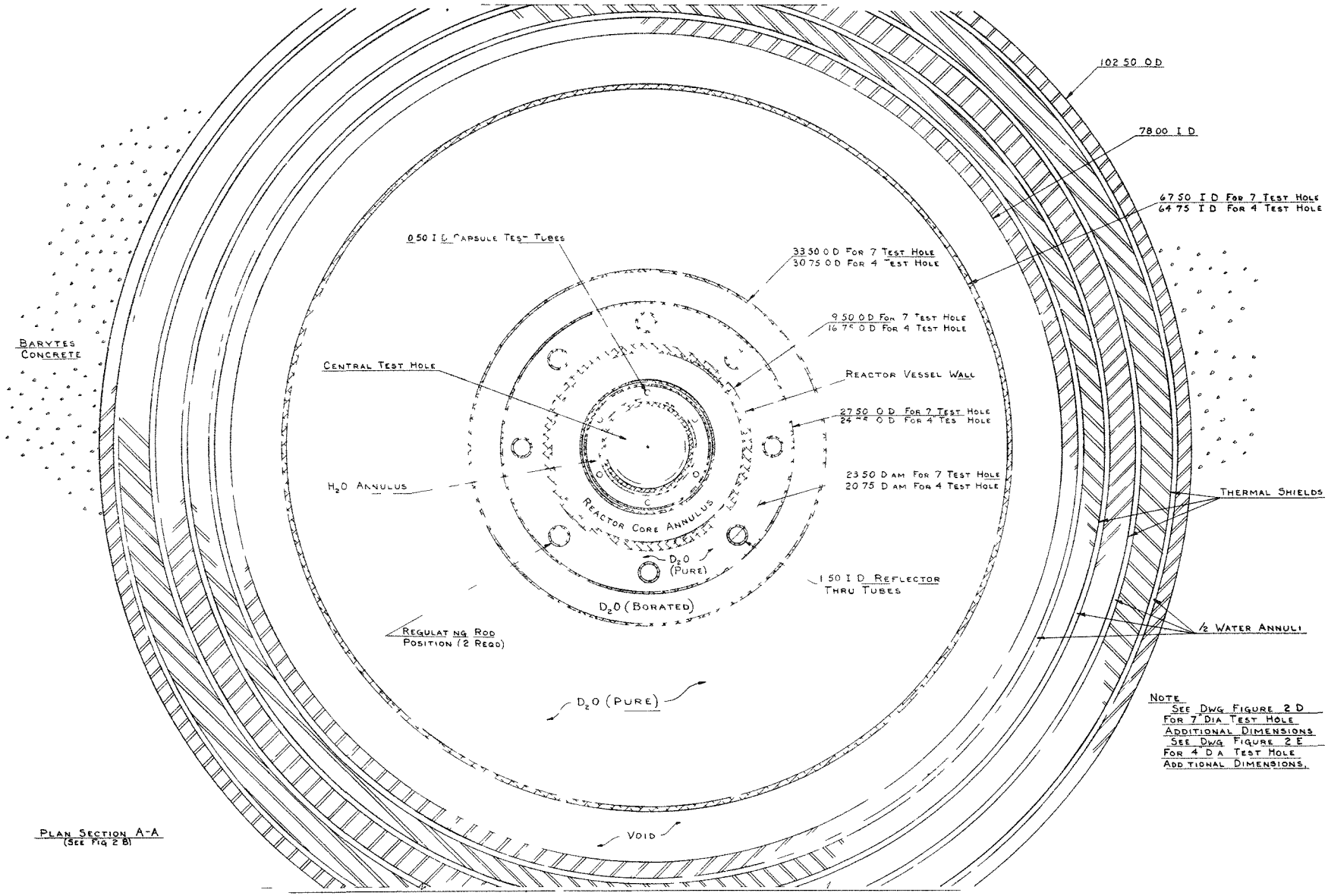

Figure 1 B

Figure 1.C Reactor-Core Cross Section

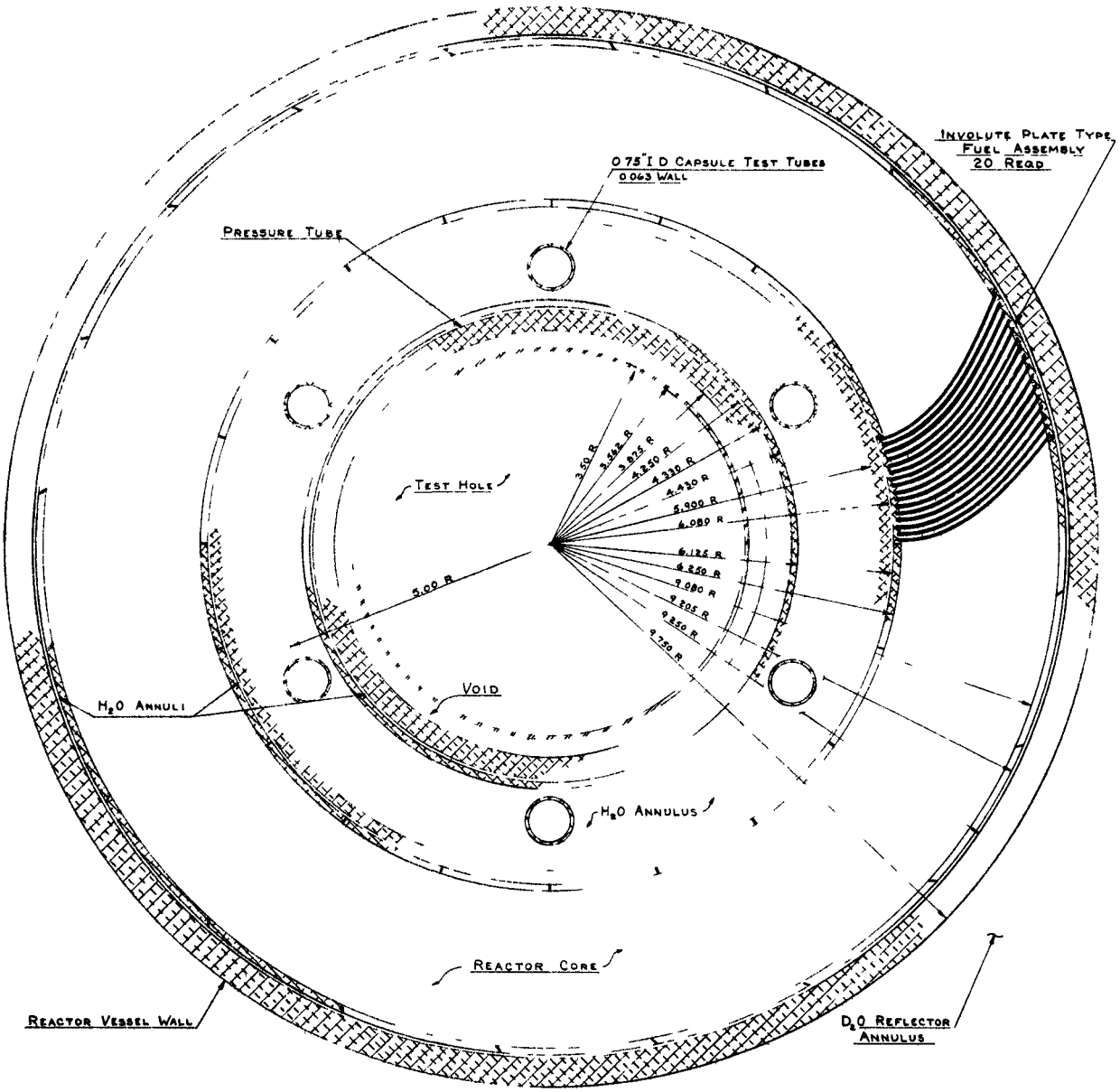

Figure 1 C

Figure 1.D

Sketch of Reactor Elevation for
Nuclear Calculations

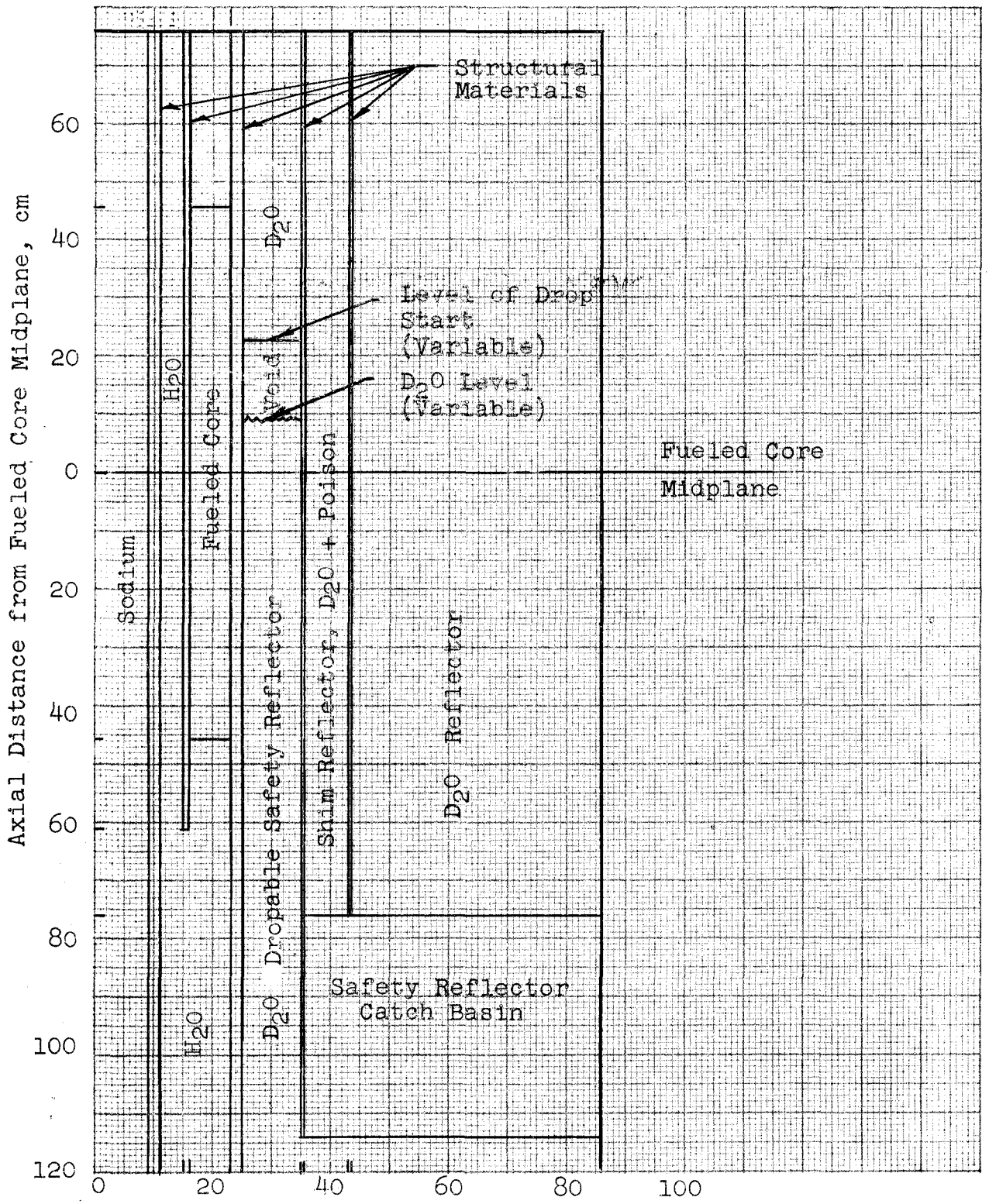

Fig. 1.D

Figure 1.E

Sketch of Reactor Midplane Cross Section
for Nuclear Calculations

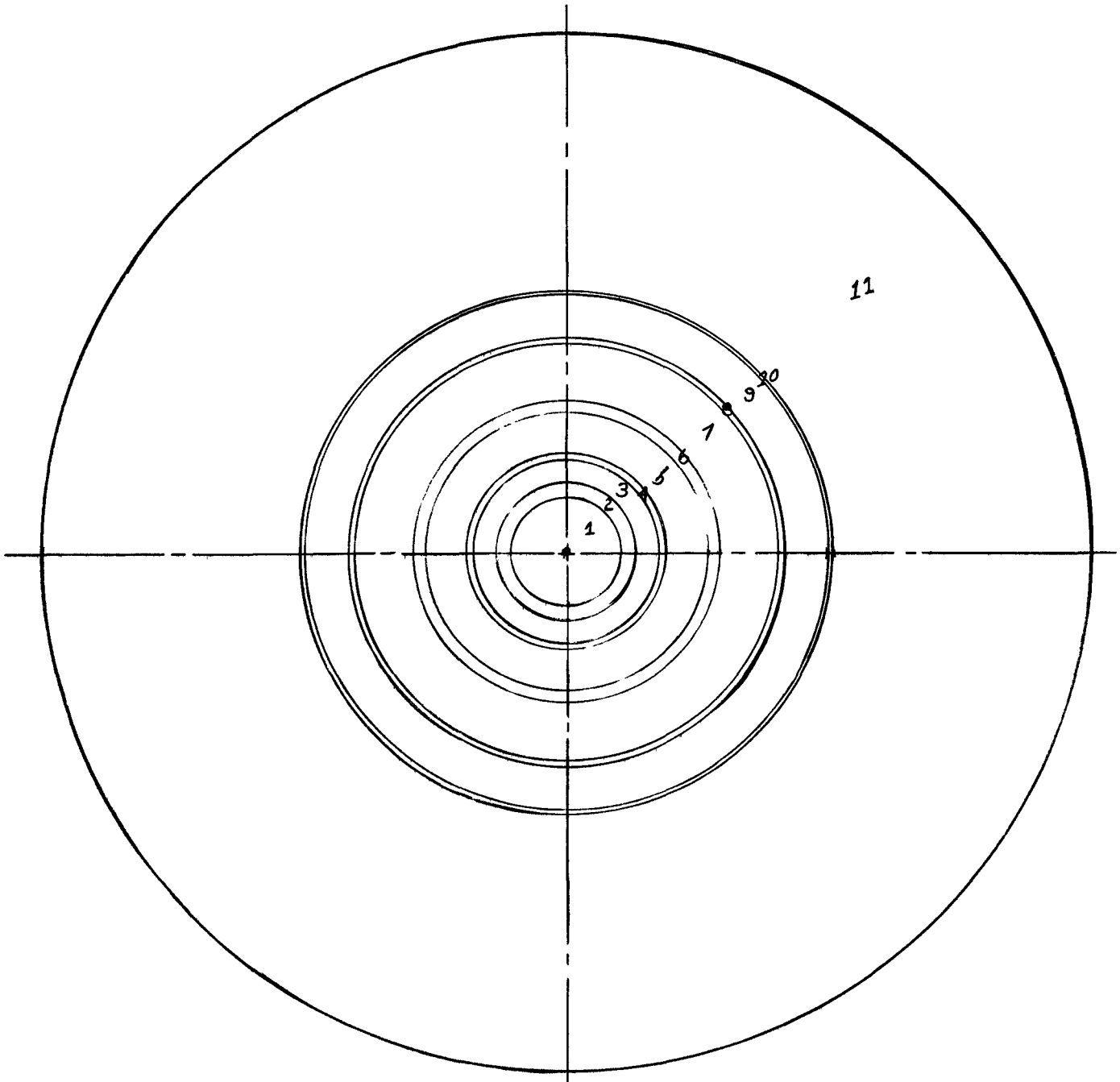

Identification	Content	O.R., cm	Identification	Content	O.R., cm
1	Sodium	8.8899	7	D_2O Dropable Safety	34.9256
2	Structure	11.2519			
3	H_2O	14.2519	8	Structure	35.4016
4	Structure	16.0326	9	D_2O+Poison, Shim	43,0216
5	Fueled Core	22.9066			
6	Structure	24.7656	10	Structure	43,4976
			11	D_2O	85.7256

Fig. 1.E

2.0 SUMMARY

Two-dimensional two-group diffusion theory calculations were performed for the purpose of evaluating the worth of the droppable safety reflector. Removal of the D_2O from the 4-inch thick safety reflector region from the level of the top of the active core to the level of the bottom of the active core with a fully poisoned shim reflector region results in a decrease in the multiplication factor from 0.9911 to 0.7515. This corresponds to 31.9% $(k'-k)/k'$ which is much greater than the value of 18.7% $(k'-k)/k'$ previously obtained using one-dimensional analysis. Removal of the D_2O from the 4-inch thick safety reflector region with a clean D_2O shim reflector results in a decrease in the multiplication factor from 1.18 to about 1.04. This corresponds to 13% $(k'-k)/k'$ and indicates the safety reflector worth decreases as the boron poison is removed from the shim reflector during the core life. The variation of the reactivity removed with the drop level is much flatter than the typical "S" shaped curve predicted by first order bare core perturbation theory, and the reactivity removed during the early stages of the drop is greater than previously estimated.

An iterative procedure using one-dimensional three-group diffusion theory calculations was performed to determine a graded fuel distribution which produces a flat radial power density. Without fuel grading the maximum-to-average power density is 1.98. The continuous fuel grading is approximated by 12 equally-thick annular fuel regions each of which contains a homogeneous fuel distribution. The calculations were terminated when the maximum-to-average power density was reduced to 1.018. To achieve this degree of power shaping, a radial maximum-to-average fuel concentration of about 1.5 is required and the maximum-to-minimum concentration is about 3.5.

Burnup calculations, using the CANDLE one-dimensional, four-group diffusion theory depletion code for the IBM-704, were performed for flat and graded fuel cores, each containing 12 kg U(235) initially. The reactivity lifetime is 500 hours for the core with initial flat fuel distribution and 425 hours for the graded core. The initial multiplication factors are 1.202 and 1.175, respectively. The radial variations in the fuel distributions and the power density distributions during the fuel cycle were determined at several times. The maximum-to-average radial power density for the flat fuel distribution decreases during the burnup from its initial value of 1.98 to a value of 1.62 after about half the cycle is complete. The fuel grading produces an initial maximum-to-average power density of 1.14 occuring at the inner edge of the core (this value differs from the value achieved in the power flattening calculations because of the different nuclear

constants used in each of the programs). In this case, the maximum-to-average power density decreases to a minimum of 1.08 during the cycle and increases to 1.20 at the end of the cycle. Variations of the flux level in the sodium test volume are very small during the cycle with the thermal flux varying by less than 1%.

The effectiveness of a burnable core poison to supplement the soluble-poison shim control in the reflector was investigated. Using a boron(10) poisoning (defined as the ratio of the thermal macroscopic absorption cross section of the poison to that of the fuel) of 0.075 reduces the initial multiplication factor by 5.9%. Near the end of the fuel cycle, the residual burnable poison accounts for a reduction in the multiplication factor of 0.9%, which reduces the reactivity lifetime of the cycle. For the graded core, the net result is to reduce the initial multiplication factor from 1.175 to 1.116 and shorten the cycle from 425 hours to 395 hours. An initial excess multiplication of 1.13-1.14 can be readily handled by the shim control reflector. By adjusting the fuel loading and optimizing the burnable poison, it appears the 19 day fuel cycle is feasible.

In response to letters of inquiry, three commercial fuel fabricators and ORNL were unanimous in the opinion that practical fabrication of AETR fuel assemblies with variable radial and axial fuel distributions with burnable poisons is feasible. Some preferred the concentric plate-type to the involute plate-type assemblies. ORNL has performed considerable development work toward achieving radial non-uniform fuel distribution in an involute plate. In view of the technological background, the cost of the fuel element development program should not be excessive.

3.0 EVALUATION OF SAFETY REFLECTOR WORTH WITH TWO-DIMENSIONAL CALCULATIONS

In previous studies, the reactivity worth of the D_2O level-control safety reflector has been estimated from one-dimensional few-group diffusion theory calculations using the radial geometry illustrated in Figure 1.E. The variation of the multiplication factor with the density of the D_2O in the safety reflector was determined and extrapolated to zero density to find the effective multiplication factor when the reflector is void. The method is reasonable for slightly reduced D_2O densities but the leakage effects approach infinity in the limit of zero D_2O density. This is incorrect because the neutrons are actually transmitted through and reflected back across the void. A lower limit of 6.8% reactivity worth was established by neglecting completely the axial leakage effects. By a conservative extrapolation method which included end-leakage effects, 18.7% reactivity worth was found. The one-dimensional calculations are not applicable for determining the relationship between the reflector level and the reactivity removed and previous estimates of this behavior are based on first order perturbation theory for bare reactors.

In order to provide a more reliable estimate of the safety reflector worth and to determine more accurately the relation between the worth and the drop level, several calculations were performed utilizing the PDQ[8] two-dimensional few-group neutron-diffusion code for the IBM-704. Effective two-group diffusion constants were synthesized from the original three-group constants to reduce the machine calculation time. The calculational model discussed in Section 1.0 and illustrated in Figure 1.D is used. Details of the calculations such as synthesis of the constants and division of the geometrical model into mesh widths are summarized in Appendix 1.0.

The results for the seven cases considered are summarized in Table 3.a. Case 1 is the reference case having the safety reflector raised and the shim reflector poisoned to yield an effective multiplication factor of about 1.00. Cases 2, 3, and 6 give the multiplication factor when the D_2O in the safety reflector is dropped from the top of the active core to some lower position, the lowest being the level of the bottom of the fueled core. Cases 4 and 5 give the multiplication factors when the drop starts at a position 9 inches below the top of the active core. In all cases the D_2O in the volume above the point at which the drop commences is undisturbed. Case 7 indicates the reactor becomes supercritical if the poison is removed from the D_2O in the shim reflector with the safety reflector lowered. Since the multiplication factor is about 1.18 with a clean shim reflector and the

safety reflector raised, Case 7 indicates the safety reflector worth drops to ~13% at the end of core life when boron poison is removed from shim reflector. The latter case was not run to completion because of excessive computation time requirements and the accuracy is questionable. The reactivities are all calculated with respect to Case 1. The times required for the drop to various levels are typical values quoted from the results of the experimental program[3,7] and are given here for convenience. The improvement in the time response of the reactivity removal by starting the drop below the top of the core is obvious.

The principal results are shown graphically in Figure 3.A. The variation of the reactivity removed with the level of the safety reflector is shown in Figure 3.B.

Table 3.a

Safety Reflector Worth

Problem Number	Safety Reflector Void*	Boric Acid In Shim Reflector	k	Reactivity, % $\frac{k'-k}{k'}$	Time Req'd For Drop** (sec)
1	None	Saturated Solution	0.99109	-	-
2	0 ⟶ 9	Saturated Solution	0.95650	-3.62	.32
3	0 ⟶ 18	Saturated Solution	0.8939	-10.9	.48
4	9 ⟶ 18	Saturated Solution	0.9103	-8.88	.32
5	9 ⟶ 36	Saturated Solution	0.8011	-23.7	.73
6	0 ⟶ 36	Saturated Solution	0.7515	-31.9	1.15
7	0 ⟶ 36	None	1.03	~+4.0	-

* Measured in Inches from top of core; e.g., 0⟶ 9 indicates a void from top of core to a point 9 inches from top of core.

** Based upon data of Test 23, INTERNUC-47[3].

Figure 3.A

Safety Reflector Worth

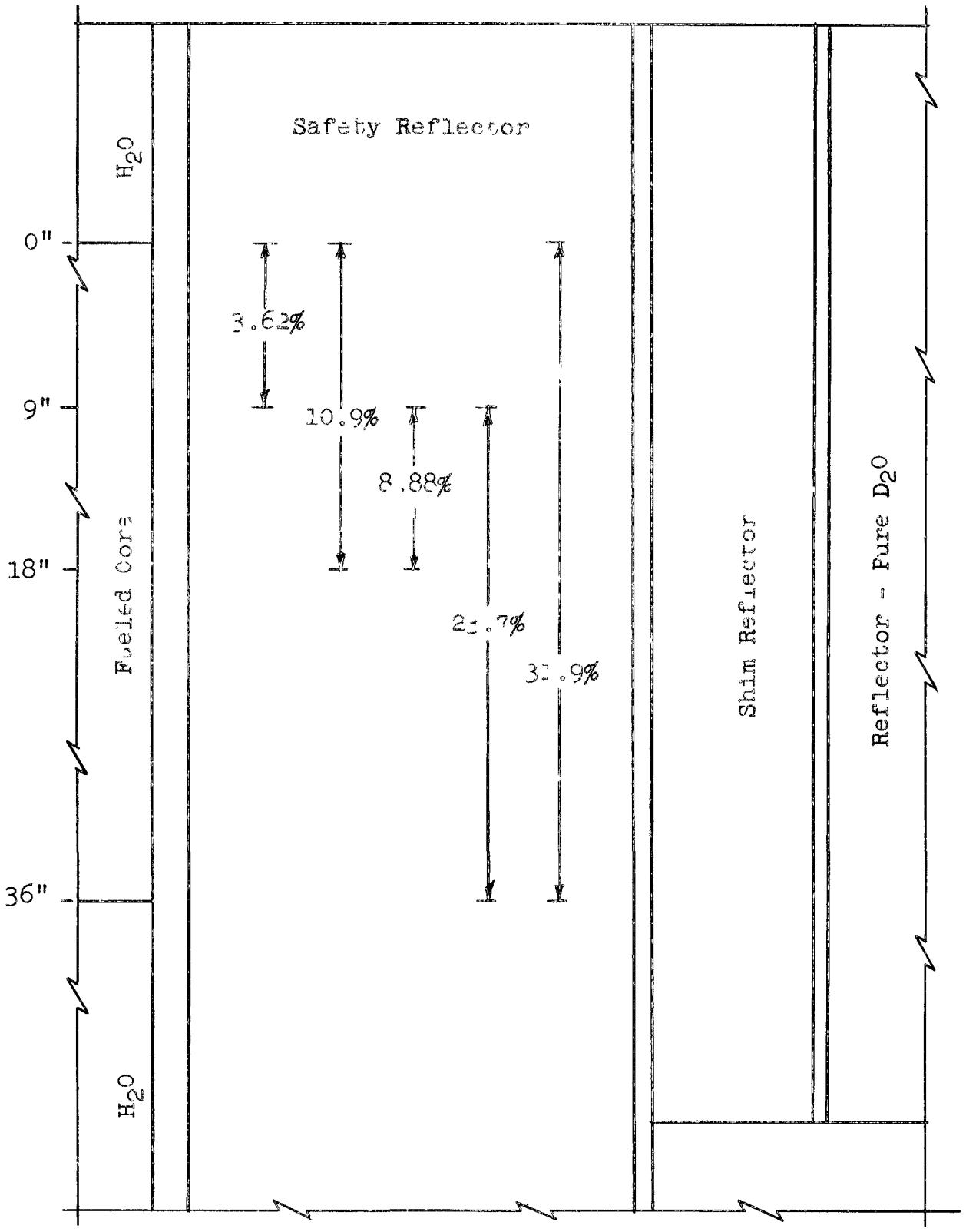

Fig. 3.A

Figure 3.B

Variation of Reactivity Removed with Distance of Safety Reflector Drop

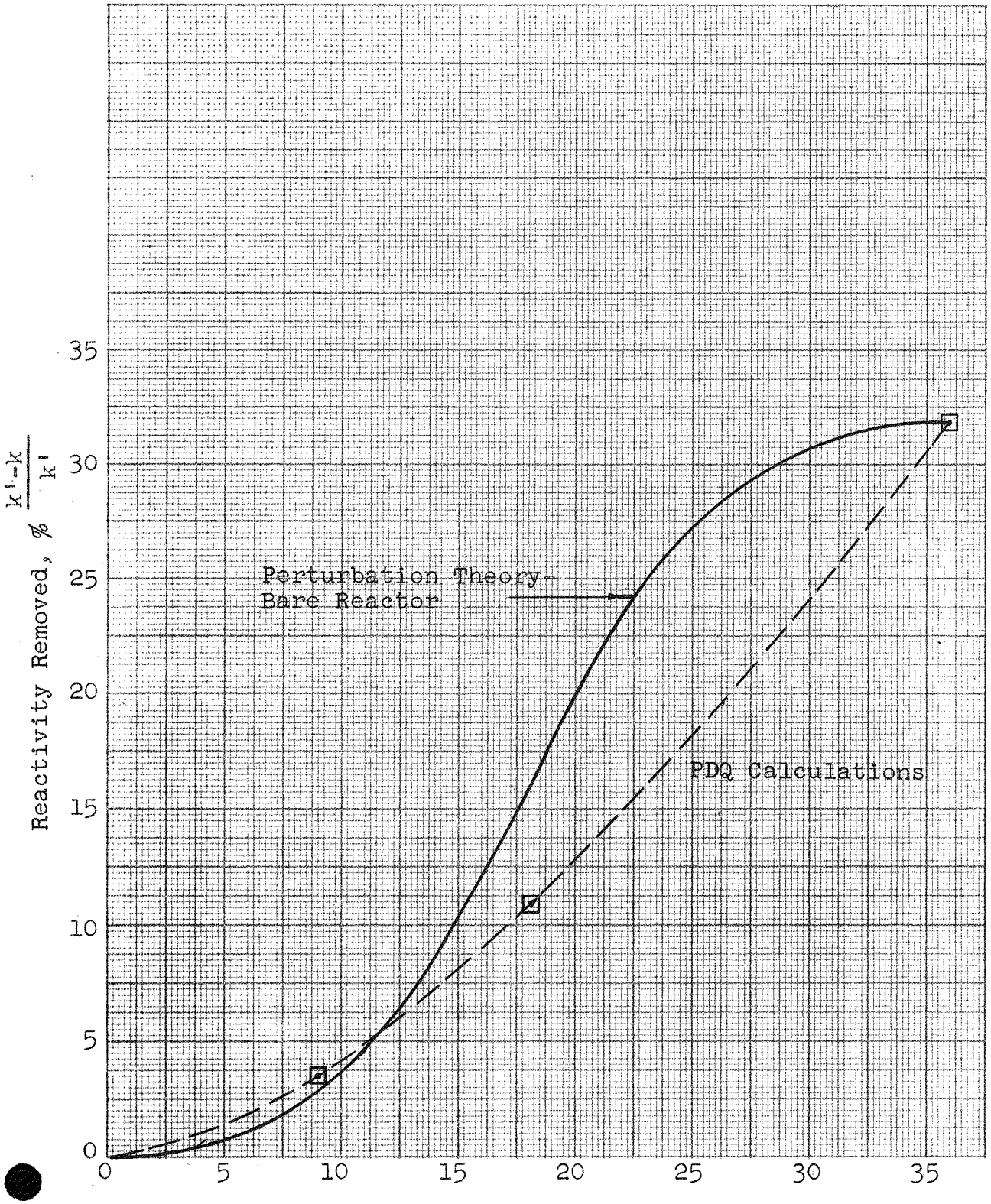

Fig. 3.B

4.0 RADIAL POWER FLATTENING USING A NON-UNIFORM FUEL DISTRIBUTION

In establishing the power level of the AETR, the assumption was made that the distribution of the radial power density is flattened considerably by the use of a variable or graded fuel loading in the core.(2) The purpose of the present work is to demonstrate the feasibility of this power shaping by determining a radial fuel distribution which yields a uniform radial power density in the core.

An iterative technique using the WANDA(9) one-dimensional diffusion theory program for the IBM-704 is used to determine the correct fuel distribution. Basically, the fueled core region is divided into 12 regions of equal thickness, each containing uniform fuel concentrations. Starting with a flat fuel distribution, the relative power densities are calculated in each of the regions with WANDA. A new fuel distribution inversely proportional to the power density is calculated and normalized to the desired loading. Using the new fuel distribution, another WANDA computation is performed. The procedure is repeated until the desired accuracy is achieved. Appendix 2.0 contains a more detailed discussion of the method and a summary of the geometrical data and the three-group nuclear constants. The configuration is consistent with the calculational model illustrated in Figure 1.E, and the three-group cross sections were developed in earlier AETR studies.

The power distribution varies during the fuel cycle because of non-uniform fission product poisoning and fuel depletion. Also, a tilting effect is caused by the removal of the soluble poison in the shim reflector. The initial hot clean case was selected rather arbitrarily and the flattened power distribution and corresponding fuel distribution is given in Table 4.a. The average fuel concentration of 4×10^{20} atoms U(235)/cc corresponds to a loading of 12 kg U(235). The relative power generated in each region increases from inside-out since the volume in each of the equally thick regions also increases. The initial maximum-to-average power density before fuel grading is 1.98. Figure 4.A shows the fuel distribution graphically and the ideal distribution can be closely approximated by drawing a smooth curve through the steps.

Table 4.a

Flattened Core Power Density

Region	U(235) Concentration (Atoms/ccx10^{-20})	Region Power Output* (Megawatts)	Power Density* (kw/cc)
7	1.7576	.070967	1.2083
8	2.2230	.073694	1.2121
9	2.7916	.075874	1.2071
10	3.4498	.077945	1.2006
11	4.1460	.080120	1.1961
12	4.7808	.082384	1.1932
13	5.2242	.084681	1.1909
14	5.3666	.086940	1.1882
15	5.1736	.089085	1.1842
16	4.7036	.091054	1.1781
17	4.0756	.092829	1.1698
18	3.4114	.094427	1.1598
Avg.	4.0000	-	1.1907
Max/Avg.	1.3417	-	1.0180
Max/Min.	3.0534	-	1.0451

* Normalized to a Total Reactor Power at One Megawatt and Height of One Centimeter.

Figure 4.A

Graded Fuel Distribution

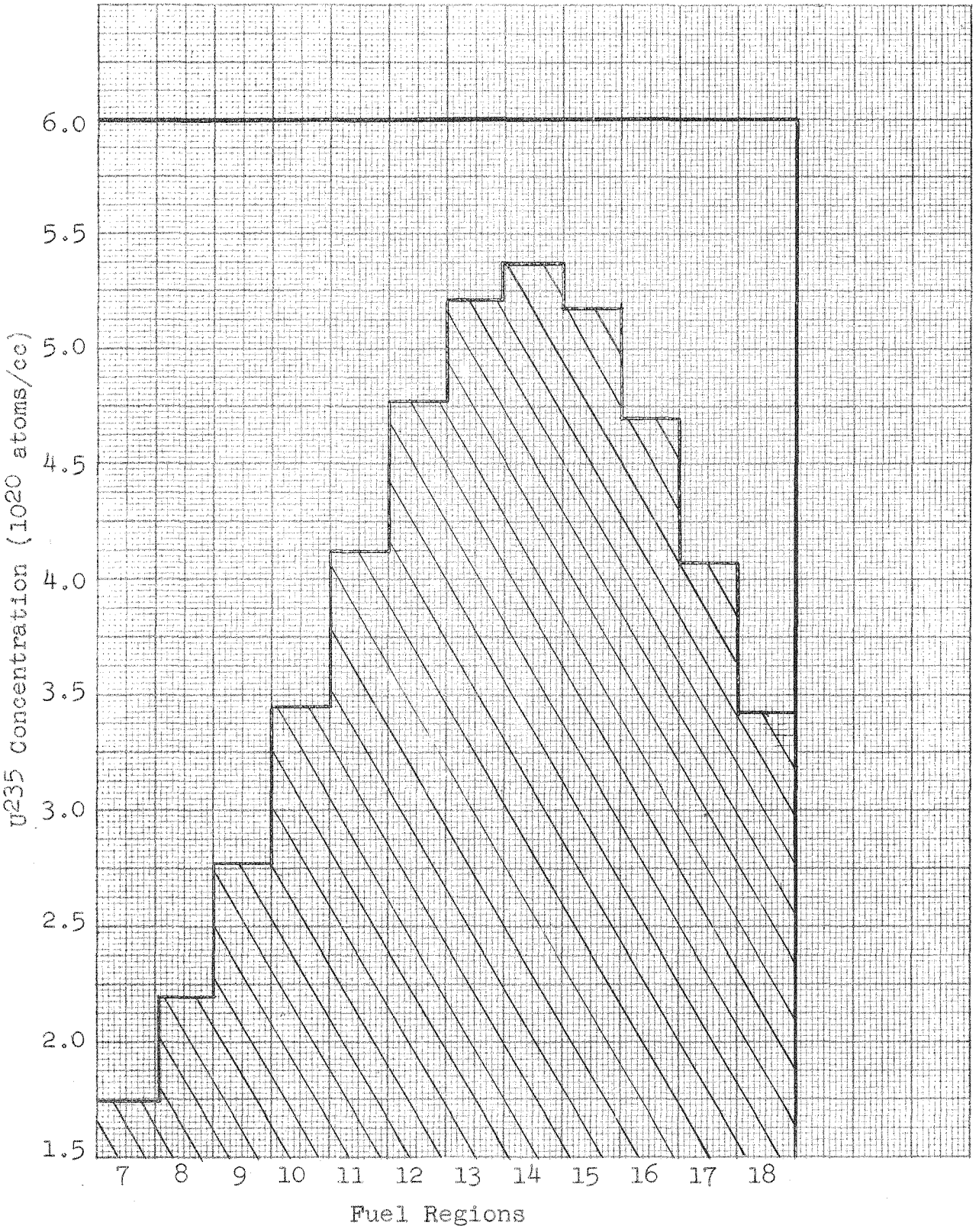

Fig. 4.A

5.0 VARIATION OF REACTOR CHARACTERISTICS WITH FUEL BURNUP

The nuclear burnup effects have been given only cursory treatment in previous AETR studies. The reactivity lifetime was estimated assuming homogeneous fission product poisoning and fuel depletion effects. Small flux variations in the test during the reactor life were predicted but no calculations of the actual variations were performed. The maximum operating power level of the reactor was established on the assumption that considerable initial radial power flattening is achieved and that the radial maximum-to-average power density does not increase prohibitively during the fuel cycle.

The purpose of the present study is to establish the validity of many of the assumptions mentioned above, and to examine the behavior of the nuclear characteristics during the burnup. For the most part the assumptions made in the previous studies were confirmed. With an initial fuel loading of 12 kg U(235), corresponding to about 30 weight percent U in the U-Aℓ alloy meat, the core with power flattening becomes subcritical after 425 hours of operation at 170 Mw and the core without power flattening becomes subcritical after 500 hours of operation at 170 Mw. The proposed cycle is 19 days or 456 hours. Without power shaping, the maximum-to-average power density is 1.98 initially and decreases to 1.61 after 180 hours of operation. With power flattening, the maximum-to-average power density is 1.14 initially, decreasing to a minimum of about 1.09 and increasing to a value of 1.20 after 420 hours of operation. This small variation of power density during the cycle is very encouraging. The flux levels in the test space are very constant during the burnout cycle, as predicted.

The burnout calculations were performed utilizing the CANDLE-2[10,11] one-dimensional few-group depletion code for the IBM-704. Two cases were studied, the first having an initial flat radial distribution of fuel and the second having an initial graded fuel distribution. The fuel loading is 12 kg U(235) in each case and the graded distribution is identical to that given in Table 4.a. The power level is constant at 170 Mw. Because of limitations in funds, the CANDLE calculation on the IBM-704 were run to complete burnout for the graded case only, and the calculation was stopped after 180 hours of burnup for the first case. Details of the CANDLE calculations including input concentrations and cross section data are given in Appendix 3.0.

5.1 Reactivity Lifetime and Shim Control

The variation of the available reactivity with time is shown in Figure 5.A and 5.B for each of the two cases. One obvious effect of the graded fuel distribution is the reduction of the initial excess reactivity by about 0.027. The reactivity lifetime for the

graded core is about 425 hours and by extrapolation it is estimated the reactivity lifetime for the non-graded core is about 500 hours. Thus some sacrifice in fuel loading or reactivity lifetime is made by grading the fuel.

Since the epithermal constants in the CANDLE program are different than those used in previous AETR studies, the value of the initial multiplication factor determined by the two methods differ. The old constants yield an initial multiplication factor of 1.1789 for the non-graded case as compared to 1.2022 from the CANDLE constants. If the former constants are correct, it is estimated the reactivity lifetime is about 350 hours and 440 hours for the graded and non-graded fuel cases, respectively. The CANDLE constants are assumed to be valid for discussion of the study.

The time variation of the poison absorption cross section in the shim reflector is shown in Figures 5.C and 5.D for the flat and graded fuel cases, respectively. The shim cleanup system must be capable of removing the poison at a rapid rate initially to compensate for the Xe(135) buildup. After the Xe(135) builds in, however, the removal rate requirements are much less severe. After the first day of operation, a reduction of the poison concentration by a factor of ten handles the shim requirements for the next 11.5 days. The use of an additional mechanical shim control system capable of handling the Xe(135) buildup may be desirable if difficulty is encountered with the soluble poison system.

The intitial concentration of the soluble poison in the shim control region is dependent primarily on the excess reactivity controlled, as shown in Figure 5.E. The effective absorption cross section of a saturated solution of boric acid at 170°F is about 0.28 cm^{-1}. Unless a more suitable soluble poison is found or the reflector design is modified, the maximum permissible initial excess multiplication factor is .151 and .158 for flat and graded initial fuel distributions, respectively, as determined from Figure 5.E. This is lower than the excess available in each of the cases studied. In an attempt to achieve the proposed 19 day cycle, the use of a burnable poison in the fuel meat appears to be a logical selection for examination (see Section 6.0).

5.2 Time Variation of Radial Power and Fuel Distributions

The results from the CANDLE calculations, include fuel and power distributions after each time step. These results were plotted as histograms for each of the 12 radial increments into which the fueled regions are divided. Figures 5.F through 5.M show the radial fuel distribution and the radial power density distribution initially and for each of the calculated time steps, starting with the flat fuel distribution. Figures 5.N through 5.Y

show the radial fuel distribution and the radial power density distribution initially and for each of the calculated time steps, starting with the graded fuel distribution. The effectiveness of the fuel grading in reducing the maximum-to-average power density initially and during the burnup is clearly demonstrated, although no attempt was made to minimize the variation during the cycle. Figure 5.P shows the initial power density distribution for the CANDLE graded-fuel case is tilted somewhat upward toward the center. This is caused by the greater than anticipated poison content in the reflector shim control region required for control. The inward tilt is fortuitous since it tends to minimize the maximum-to-average power density during the cycle.

Figure 5.Z shows the radial burnup for the graded fuel in terms of percent of initial fuel consumed and Figure 5.AA shows the radial burnup for the graded fuel in terms of atoms/cc. Although the overall burnup is 30.8%, it is shown in Figure 5.Z that local burnups at the inner edge where the initial fuel concentration is low is on the order of 60%. This raises a question concerning fuel element performance although certain MTR fuel plates have shown ~100% burnup. If the grading is accomplished by varying the meat thickness and the plate thickness is constant, the higher percentage burnups occur where the cladding is thickest.

5.3 Time Variations of Neutron Flux

As pointed out in previous reports, the relative insensitivity of the flux levels in the test volume to perturbations of the thermal neutron flux in the core is one of the advantages of the flux-trap reactor. The neutron flux levels in the test are primarily dependent on the power level since the source of thermal neutrons in the test space depends on the thermalization of fast neutrons in the water moderator region. The reactor design, therefore, is particularly suited to irradiations requiring minimum variation in flux levels during the irradiation cycle.

The stability of the flux levels are demonstrated most dramatically by the results from the CANDLE burnup calculations given in Tables 5.a and 5.b. The reactor power has been maintained constant at 170 Mw during the burnup.

Table 5.a

Neutron Flux Variations in Sodium Test
During Burnup for Initial Flat Fuel Distribution

Time Hrs.	Mwd	Average Fluxes at Centerline, 10^{15}n/cm^2-sec Ø1	Ø2	Ø3	Øth
0	0	0.3978	0.6129	0.6232	1.541
10	71	0.3930	0.6065	0.6187	1.530
60	425	0.3871	0.5985	0.6125	1.521
180	1275	0.3793	0.5882	0.6045	1.518

Table 5.b

Neutron Flux Variations in Sodium Test
During Burnup for Initial Variable Fuel Distribution

Time Hrs.	Mwd	Average Fluxes at Centerline, 10^{15}n/cm^2-sec Ø1	Ø2	Ø3	Øth	Test Vol. Avg. Thermal Flux, 10^{15}n/cm^2-sec
0	0	0.3727	0.5796	0.5972	1.546	1.569
10	71	0.3684	0.5737	0.5926	1.534	1.559
60	425	0.3622	0.5653	0.5857	1.524	1.548
180	1275	0.3537	0.5539	0.5767	1.521	1.545
300	2125	0.3459	0.5435	0.5684	1.521	1.545
420	2975	0.3386	0.5337	0.5607	1.522	1.547

The radial flux distributions are plotted for the inital clean reactor and for the last calculated burnout time step. Figures 5.BB and 5.CC give the thermal and epithermal distributions for the case with initial flat fuel distribution, and Figures 5.DD and 5.EE gives the distributions after 180 hours of operation. Figures 5.FF and 5.GG give the thermal and epithermal distributions for the case with initial power flattening by fuel grading and Figures 5.HH and 5.II gives the distributions after 420 hours of operation.

Each case has the same initial fuel loading of 12 kg U(235) but the initial excess reactivity is greater for the case with flat fuel distribution. The large differences of the flux depression in the shim control region in the clean reactors is caused by the rather large differences in shim poison concentration required to control the initial excess multiplication. The reflector flux levels vary considerably during the cycle because of the variation in the soluble shim poison concentration during the cycle.

Figure 5.A

Variation of Available Reactivity with Operating Time for Flat Initial Fuel Distribution

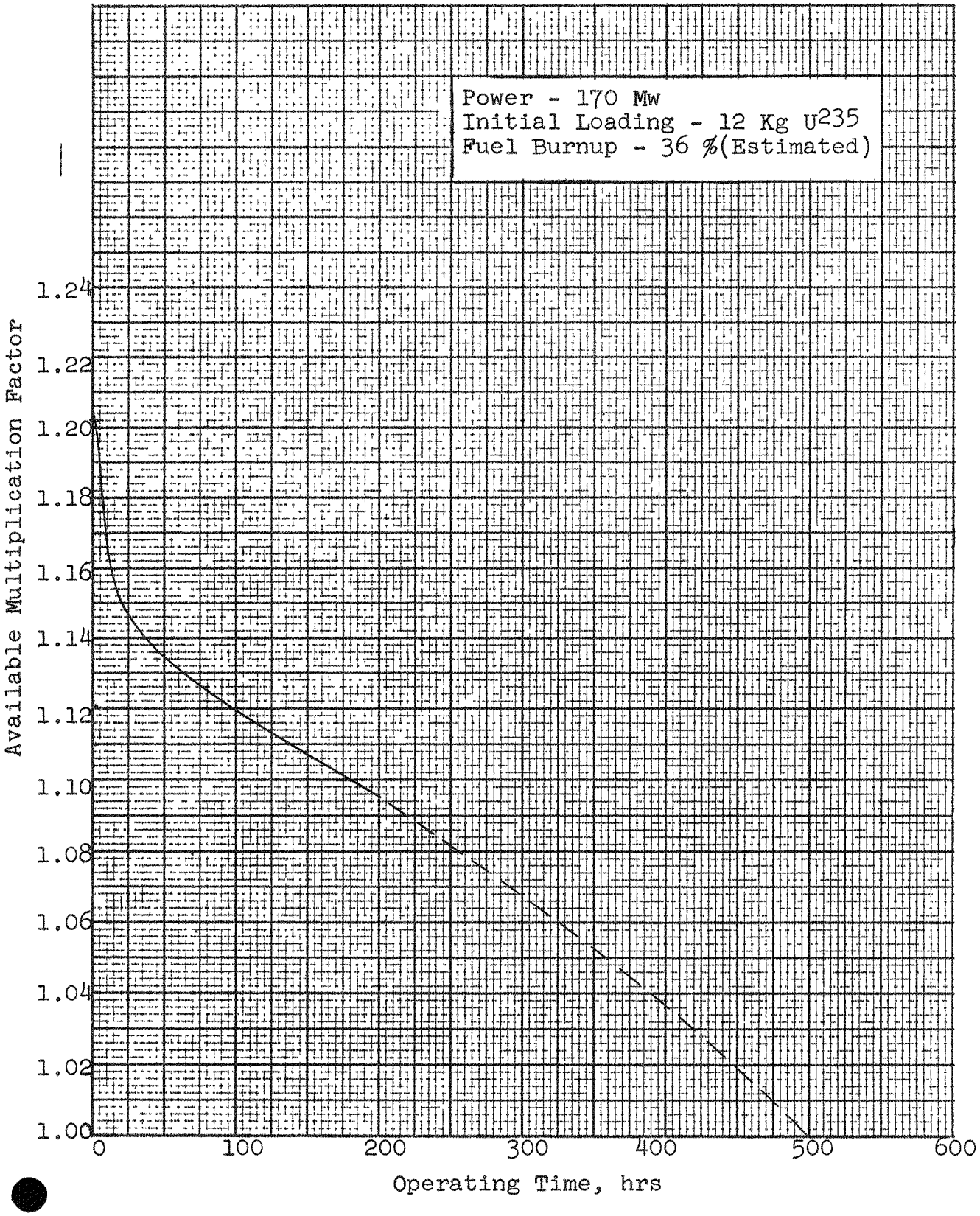

Fig. 5.A

Figure 5.B

Variation of Available Reactivity with Operating Time for Variable Initial Fuel Distribution

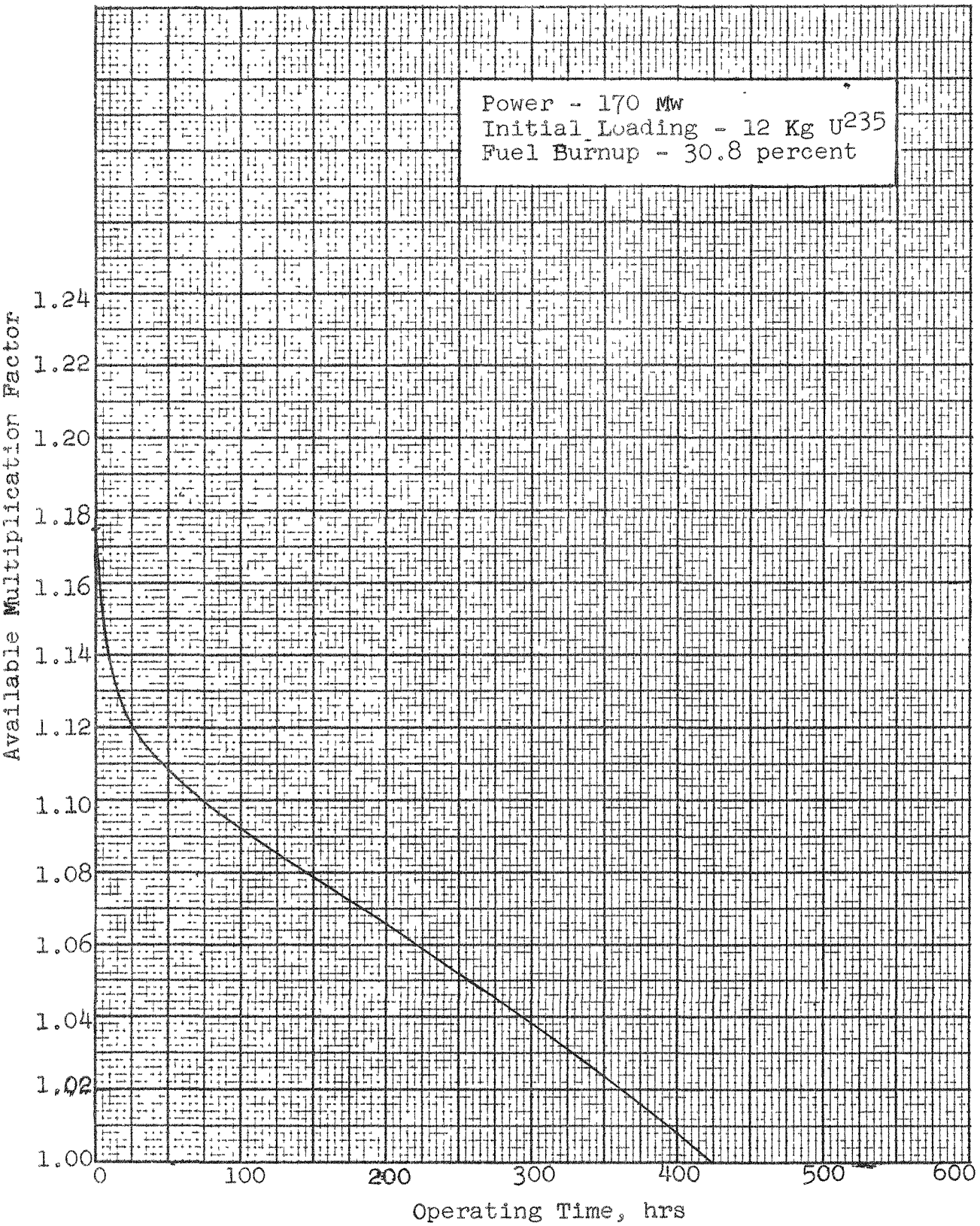

Fig. 5.B

Figure 5.C

Time Variation of Shim Control Requirements
for Flat Initial Fuel Distribution

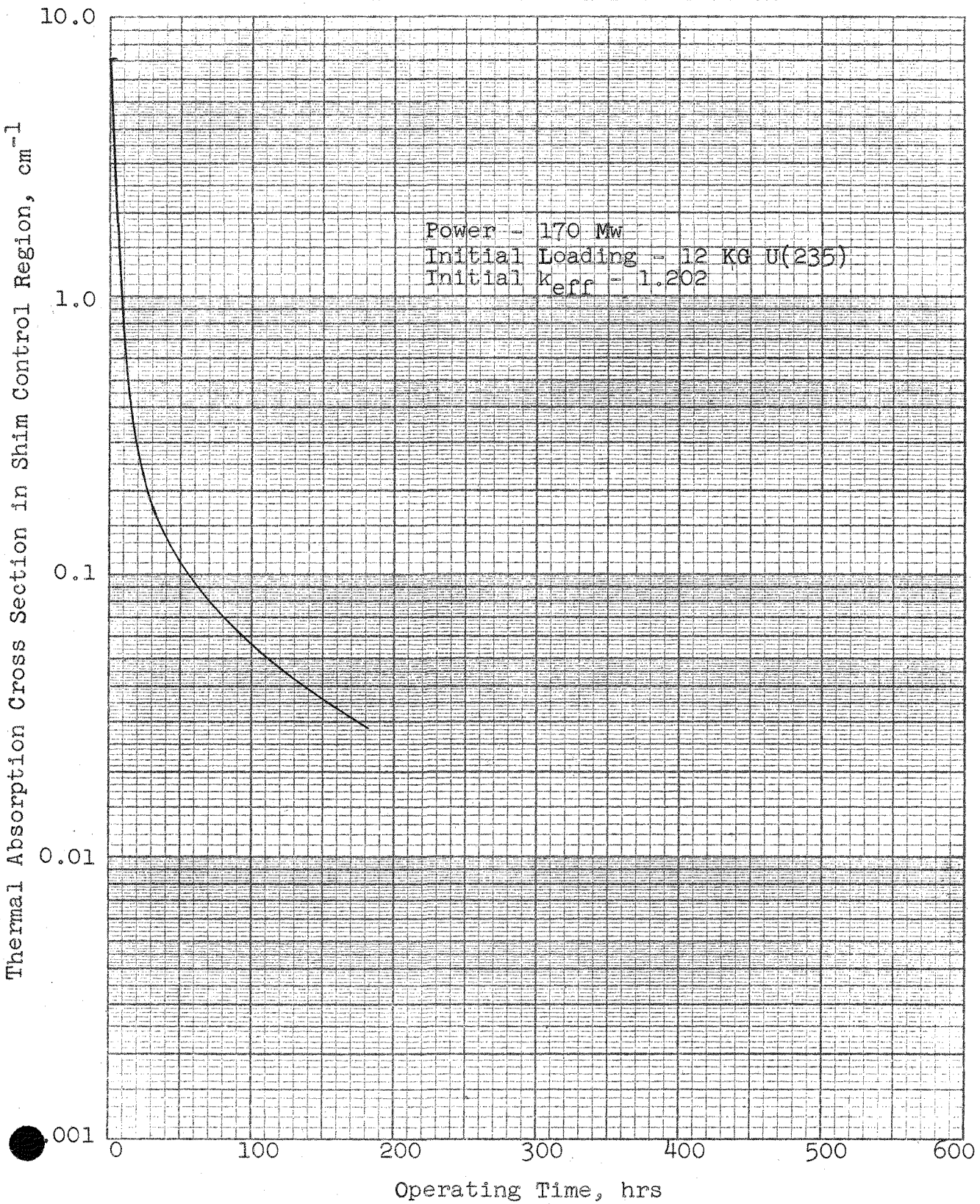

Fig. 5.C

Figure 5.D

Time Variation of Shim Control Requirements
for Variable Initial Fuel Distribution

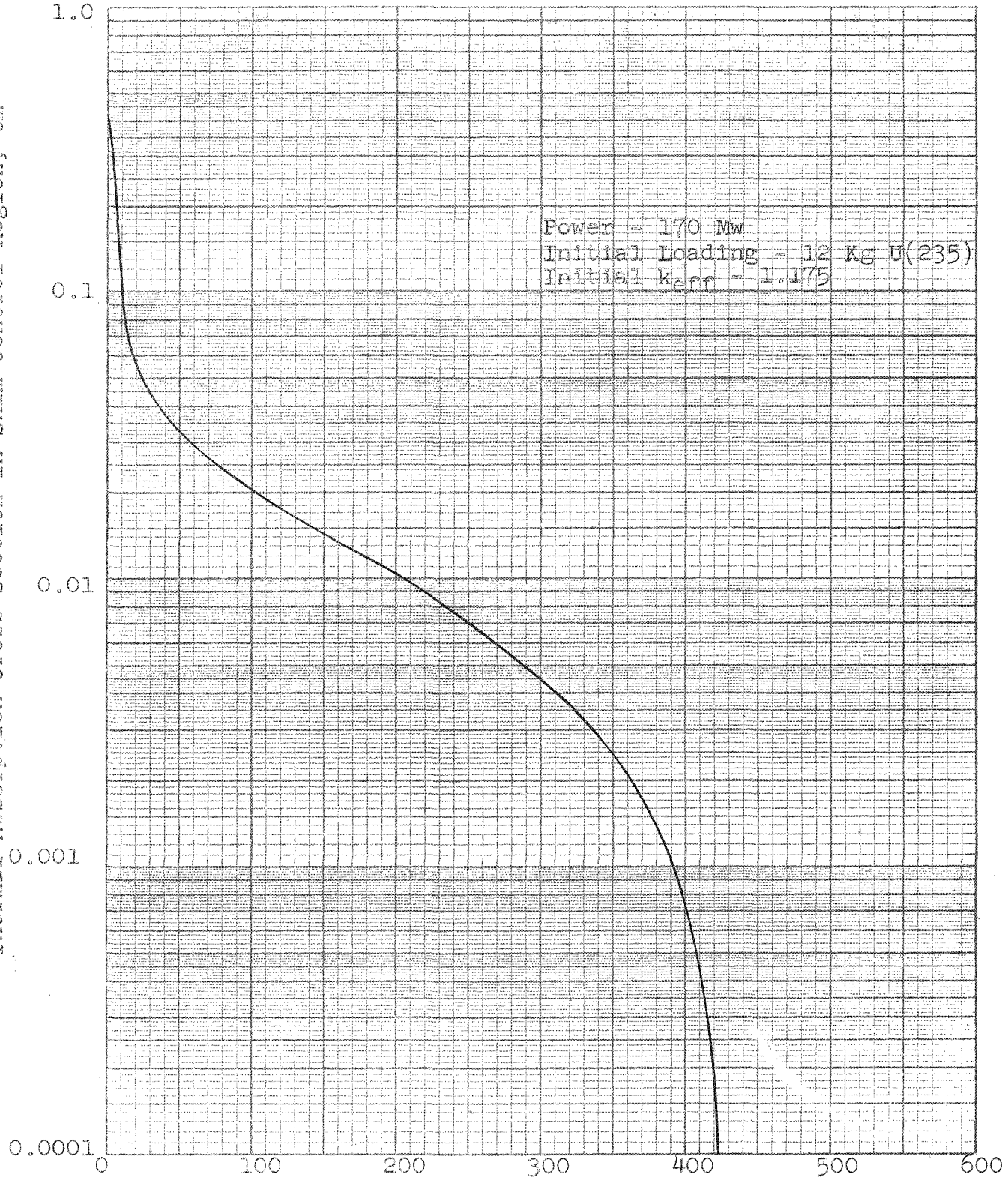

Fig. 5.D

Figure 5.E

Shim Absorber Requirements as Function of Excess Reactivity

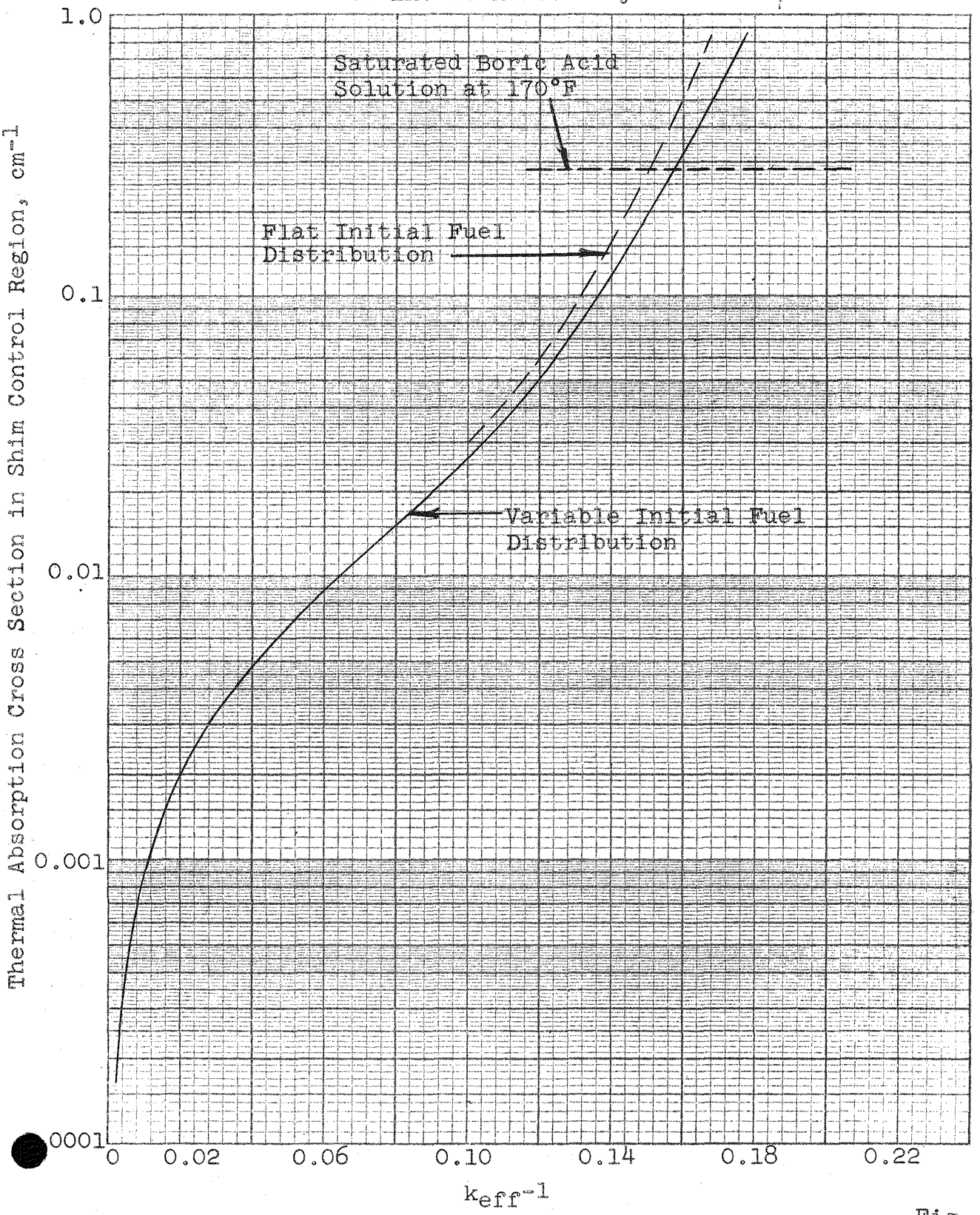

Fig. 5.E

Figure 5.F

Initial Radial Fuel Distribution for
Uniformly Loaded Core

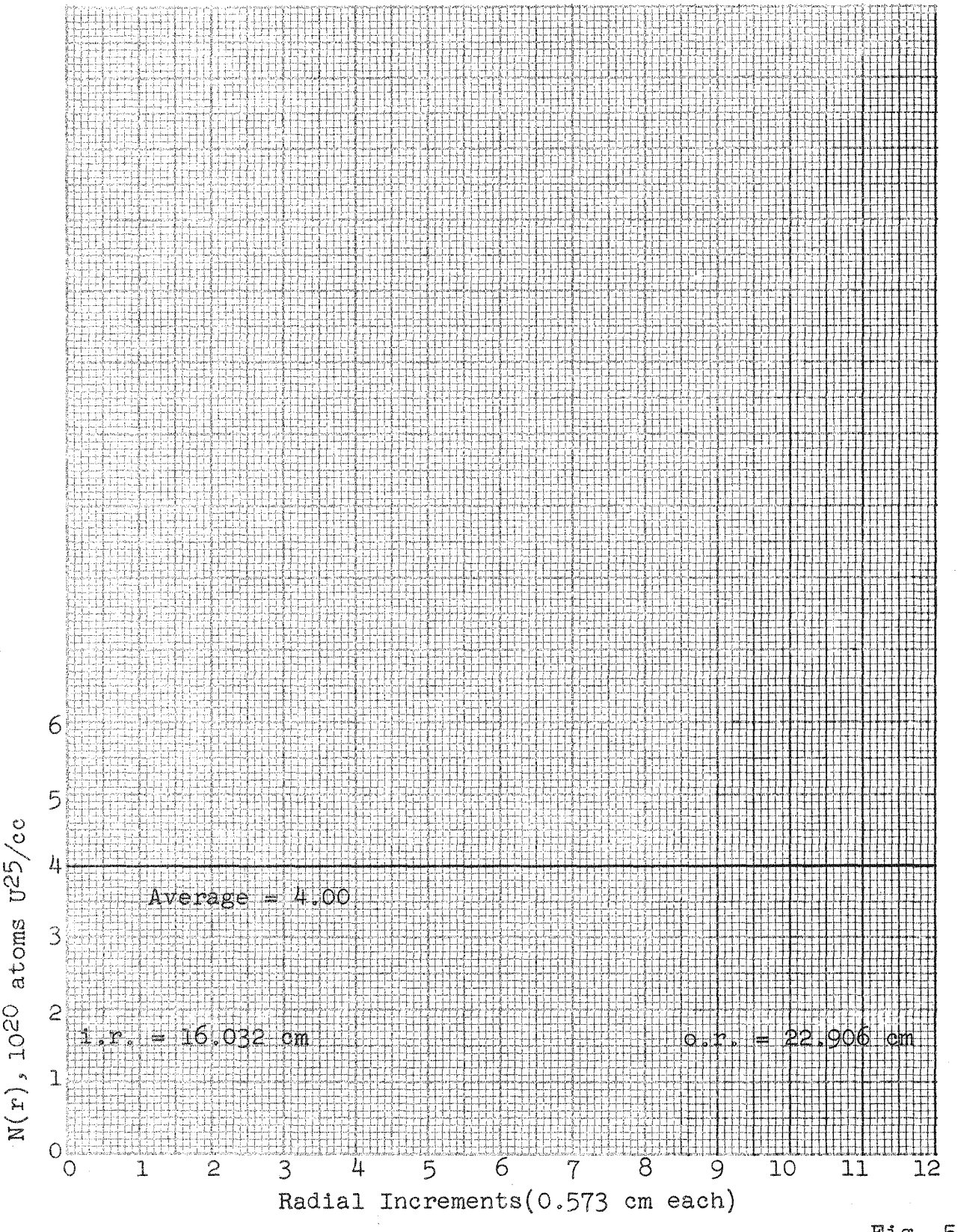

Fig. 5.F

Figure 5.G

Initial Radial Distribution of Power Density for Uniformly Loaded Core

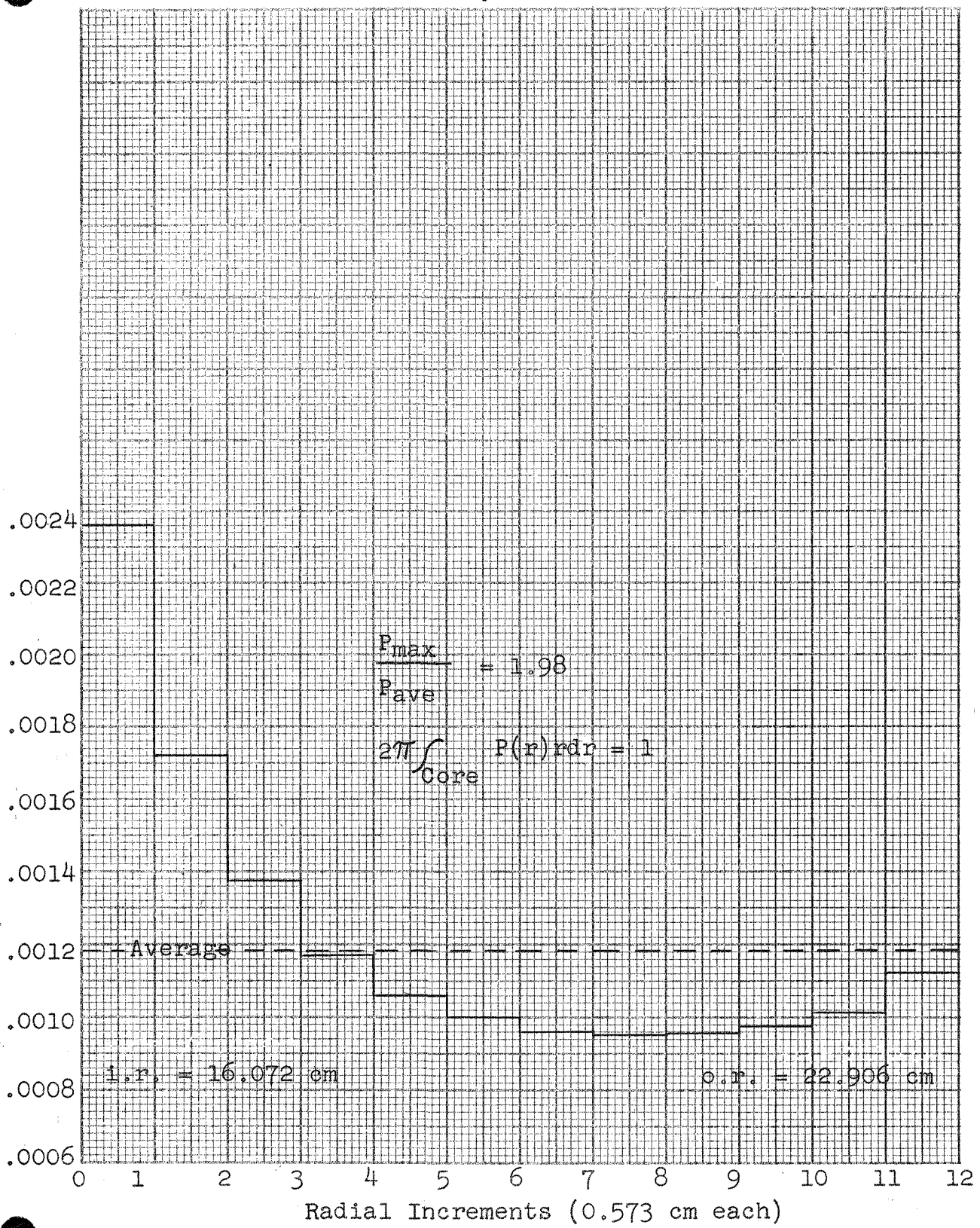

Fig. 5.G

Figure 5.H

Radial Fuel Distribution After 10 Hours
for Initial Uniform Fuel Loading

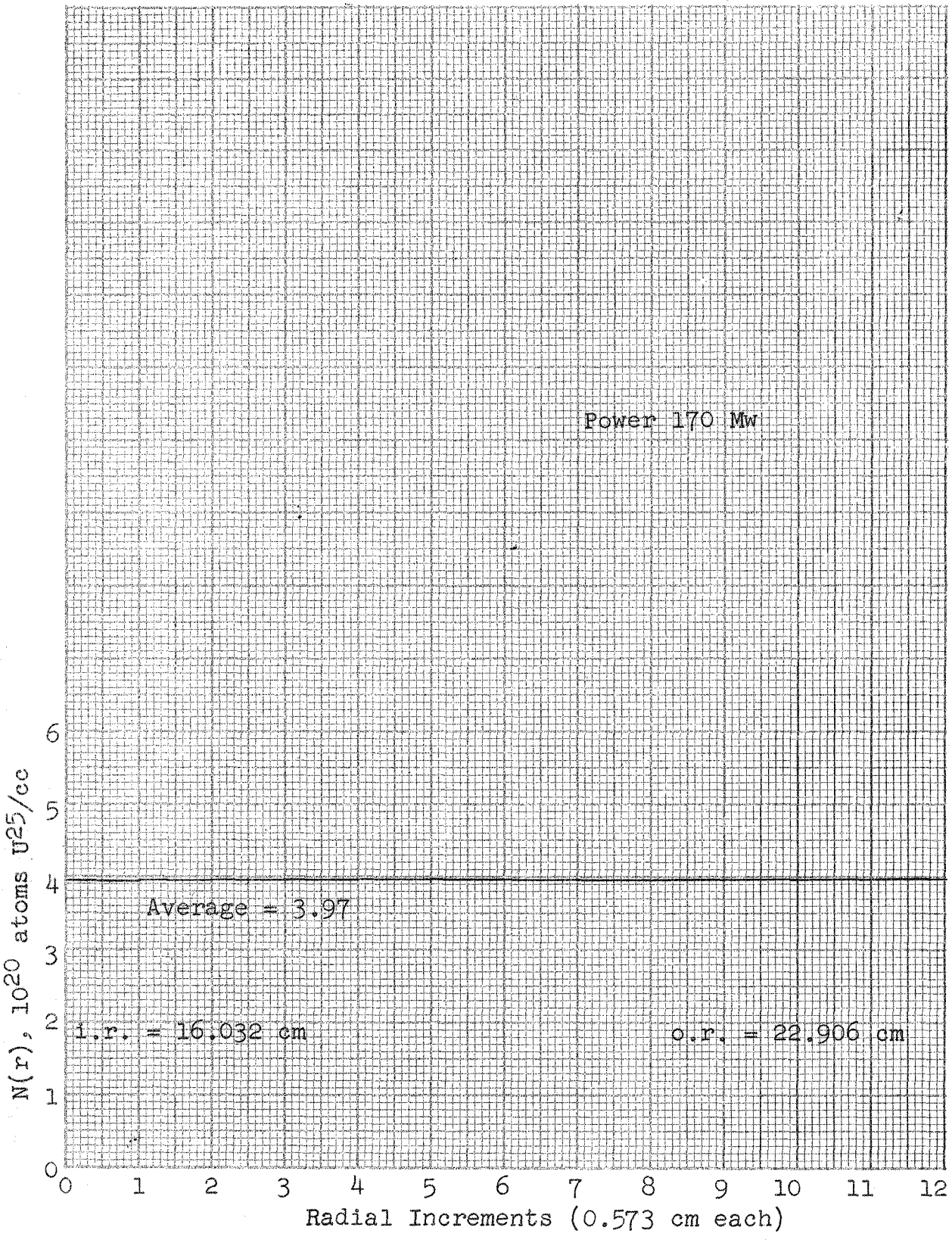

Fig. 5.H

Figure 5.I

Radial Distribution of Power Density After
10 Hours for Initial Uniform Fuel Loading

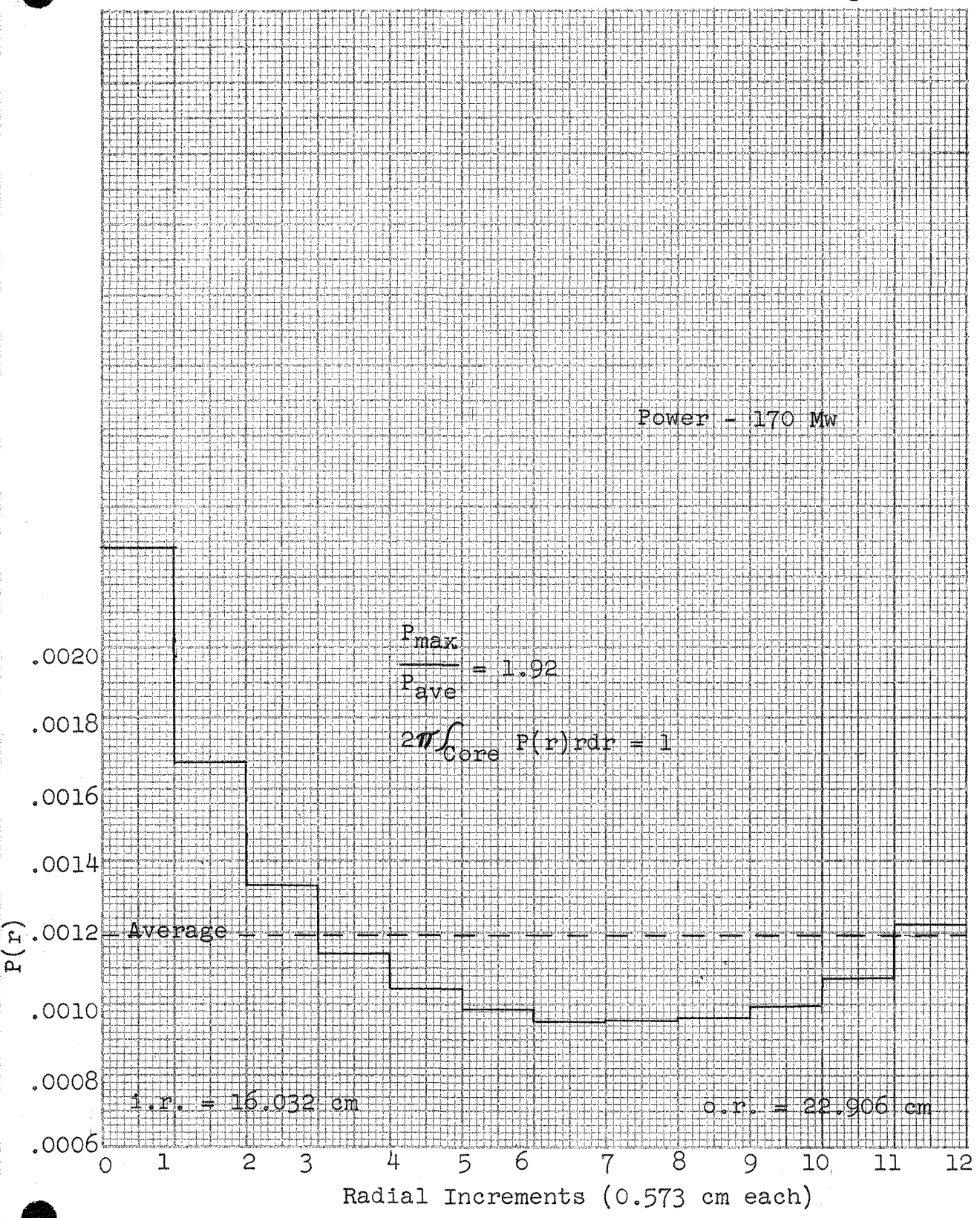

Fig. 5.I

Figure 5.J

Radial Fuel Distribution After 60 Hours for Initial Uniform Fuel Loading

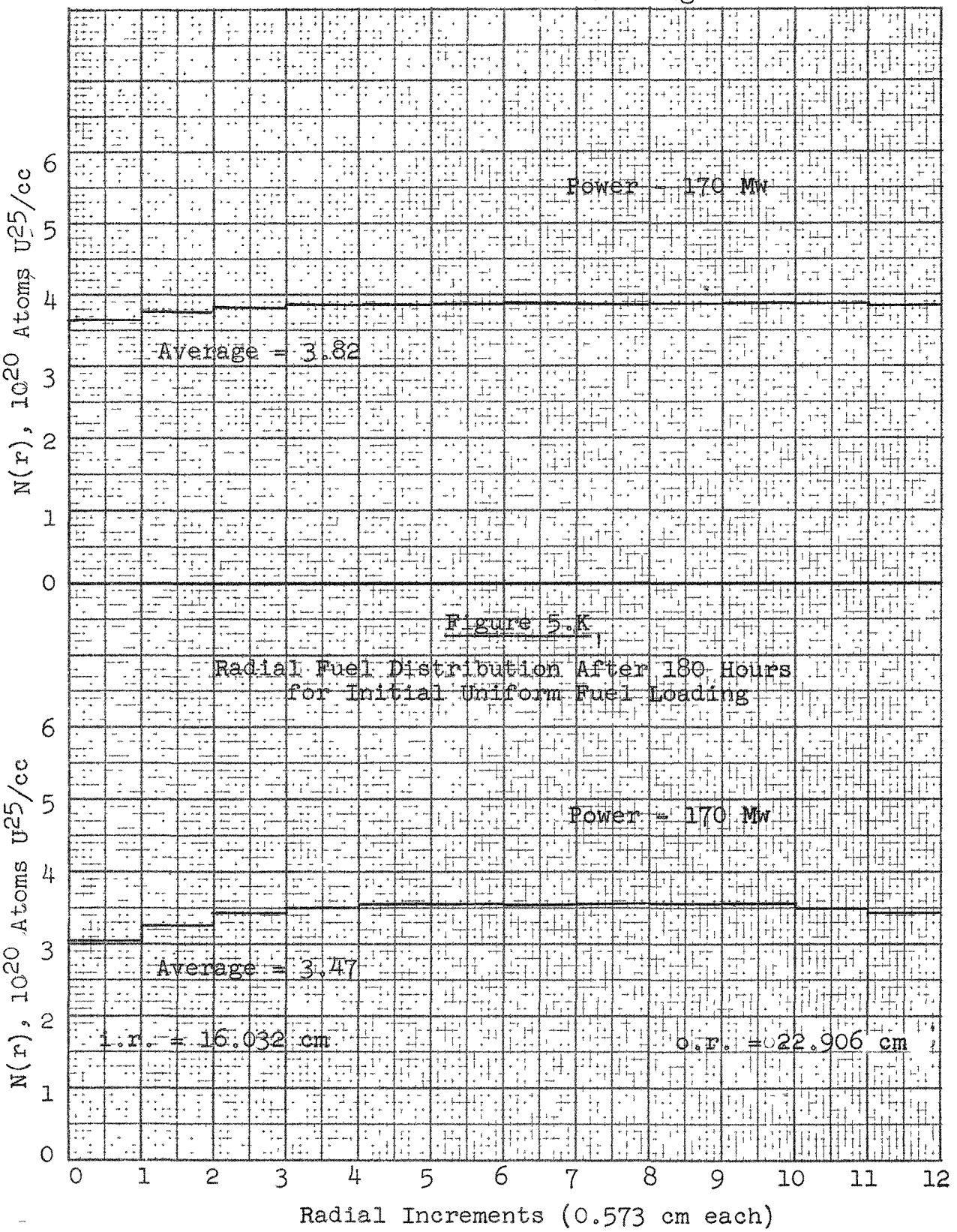

Figure 5.K

Radial Fuel Distribution After 180 Hours for Initial Uniform Fuel Loading

Figs. 5.J and 5.K

Figure 5.L

Radial Distribution of Power Density After 60 Hours for Initial Uniform Fuel Loading

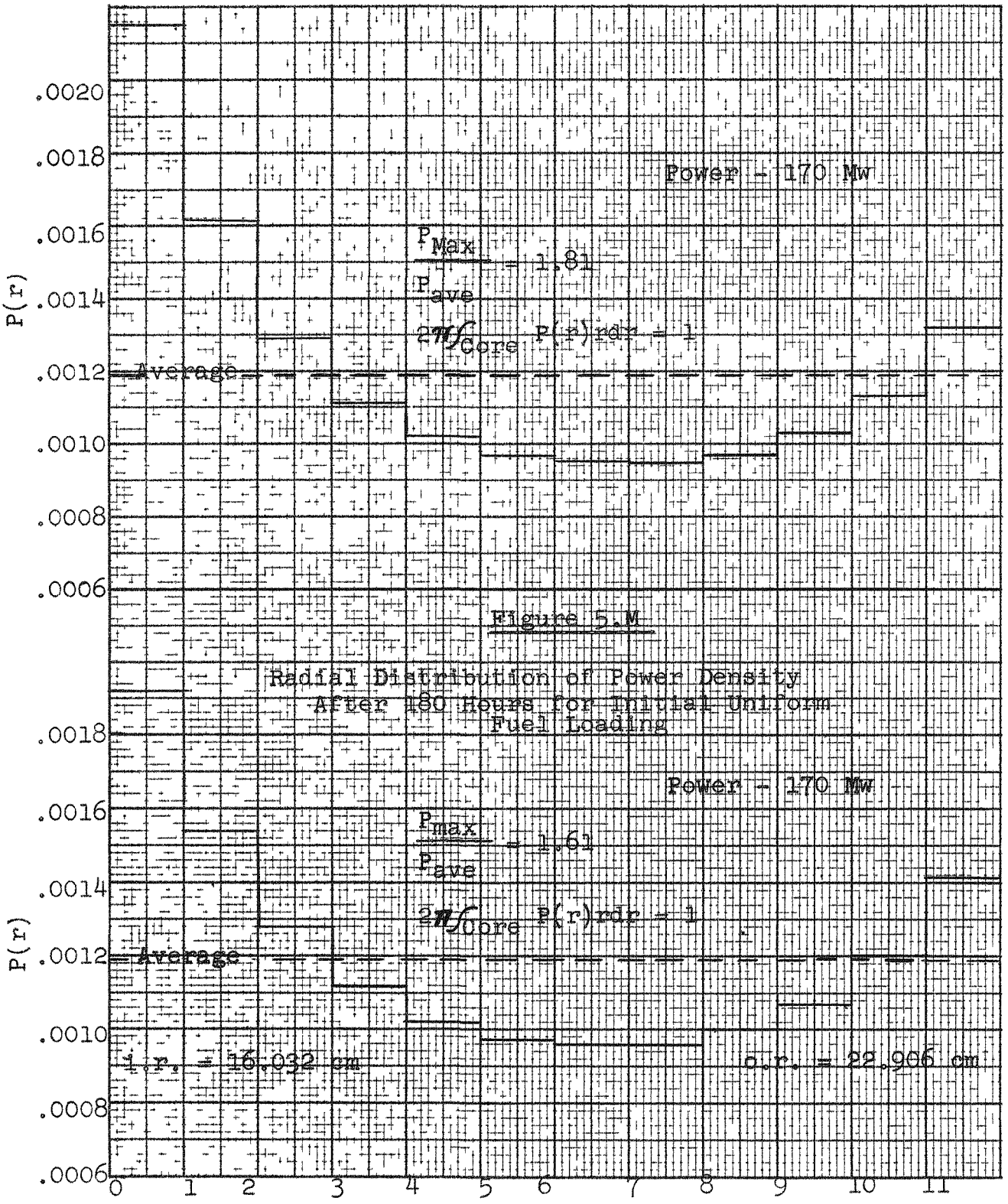

Figure 5.M

Radial Distribution of Power Density After 180 Hours for Initial Uniform Fuel Loading

Figs. 5.L and 5.M

Figure 5.N

Initial Radial Fuel Distribution
for Variable Fuel Loading

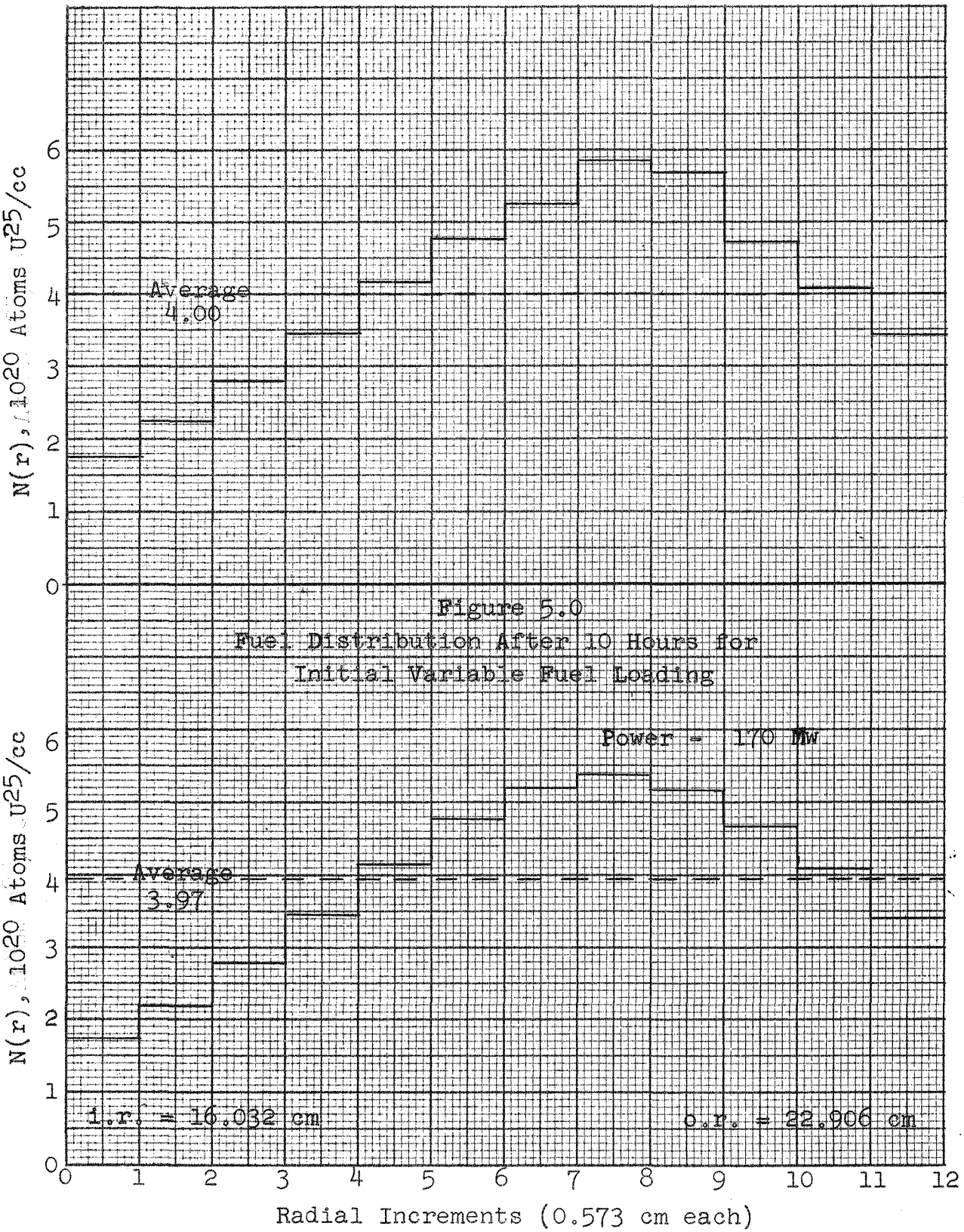

Figs. 5.N and 5.0

Figure 5.P

Initial Radial Distribution of Power Density
for Variable Fuel Loading of Core

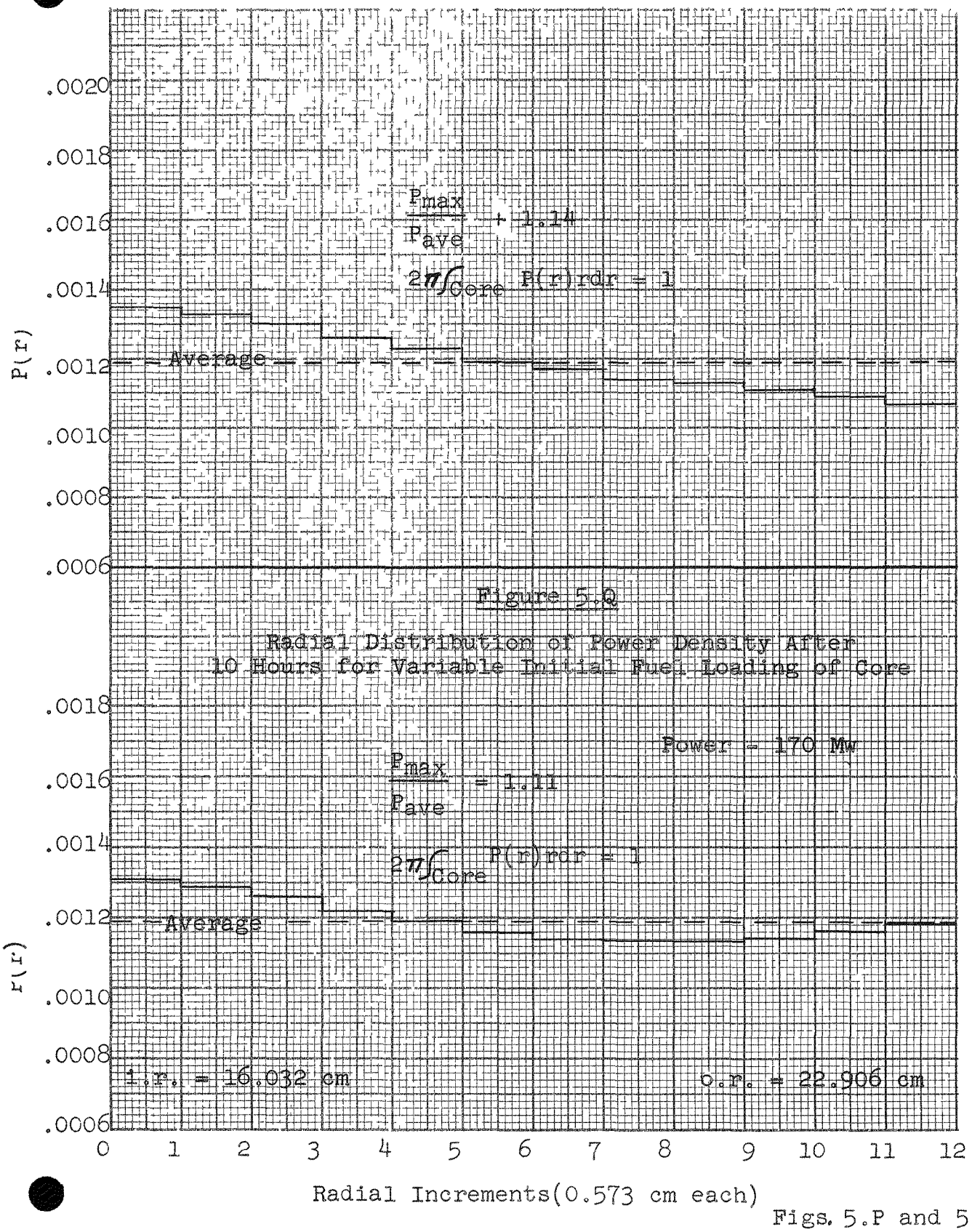

Figure 5.Q

Radial Distribution of Power Density After
10 Hours for Variable Initial Fuel Loading of Core

Figs. 5.P and 5.Q

Figure 5.R

Radial Fuel Distribution After 60 Hours
for Initial Variable Fuel Loading

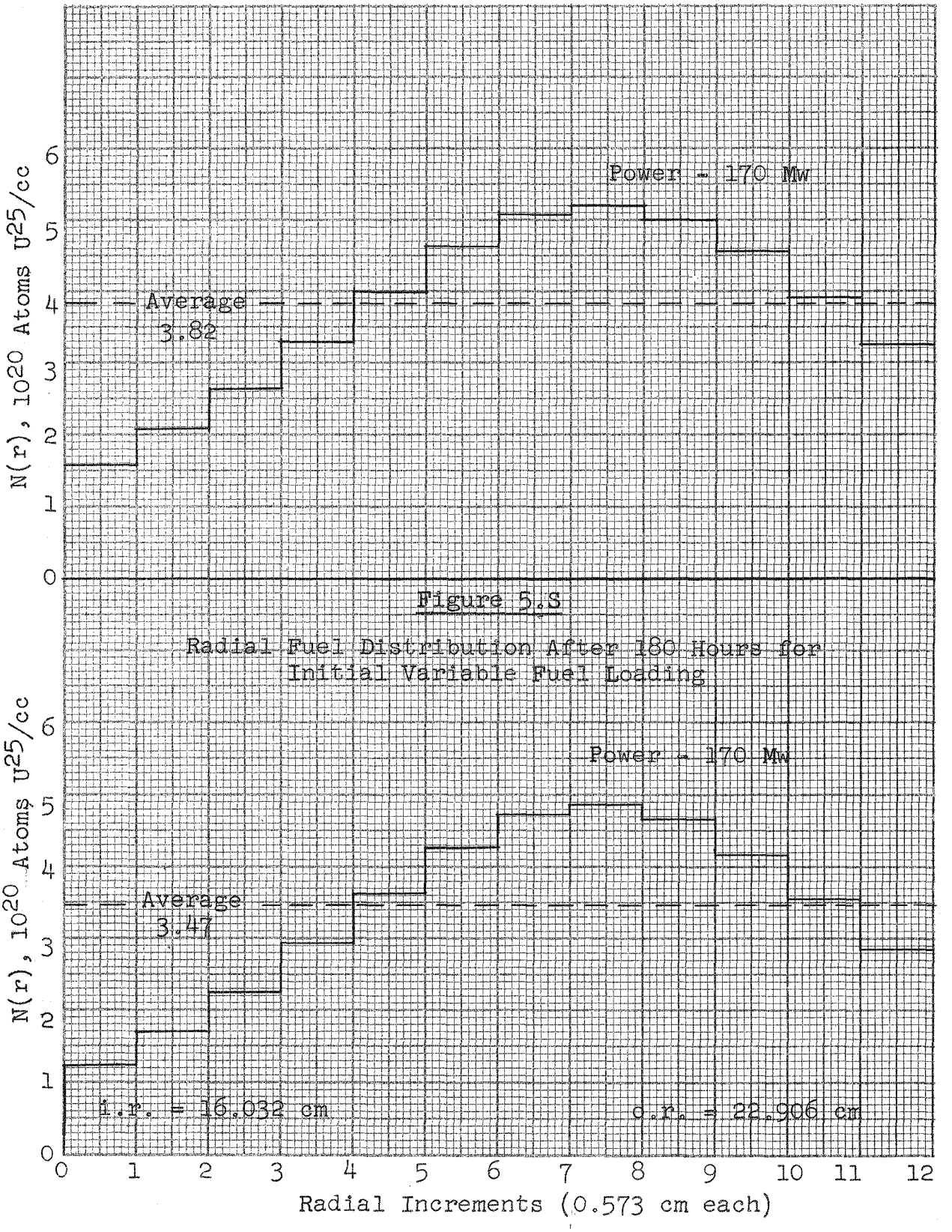

Figure 5.S

Radial Fuel Distribution After 180 Hours for
Initial Variable Fuel Loading

Figs. 5.R and 5.S

Figure 5.T

Distribution of Power Density After 60 Hours
for Variable Initial Fuel Loading of Core

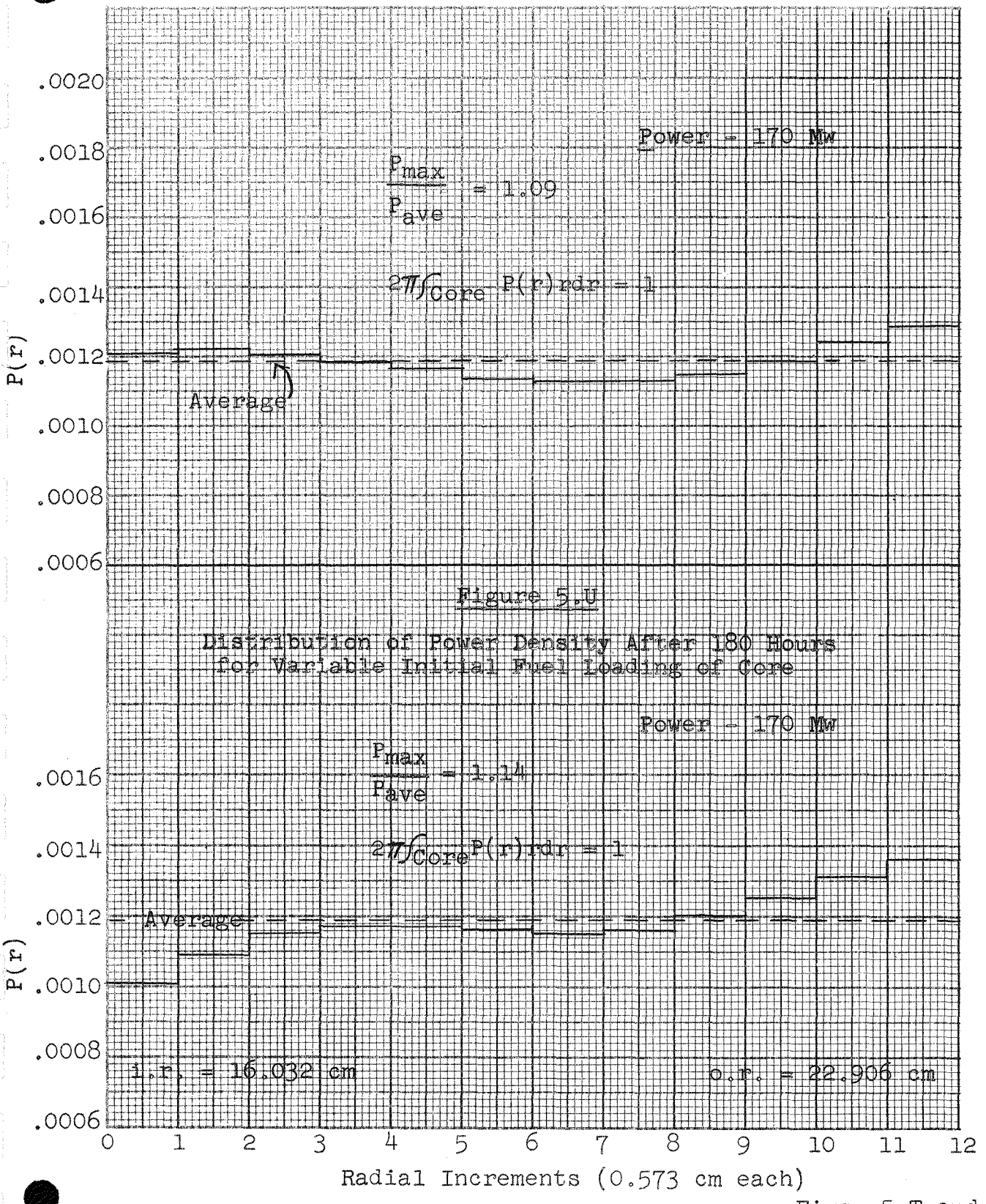

Figure 5.U

Distribution of Power Density After 180 Hours
for Variable Initial Fuel Loading of Core

Figs. 5.T and 5.U

Figure 5.V

Radial Fuel Distribution After 300 Hours
for Initial Variable Fuel Loading

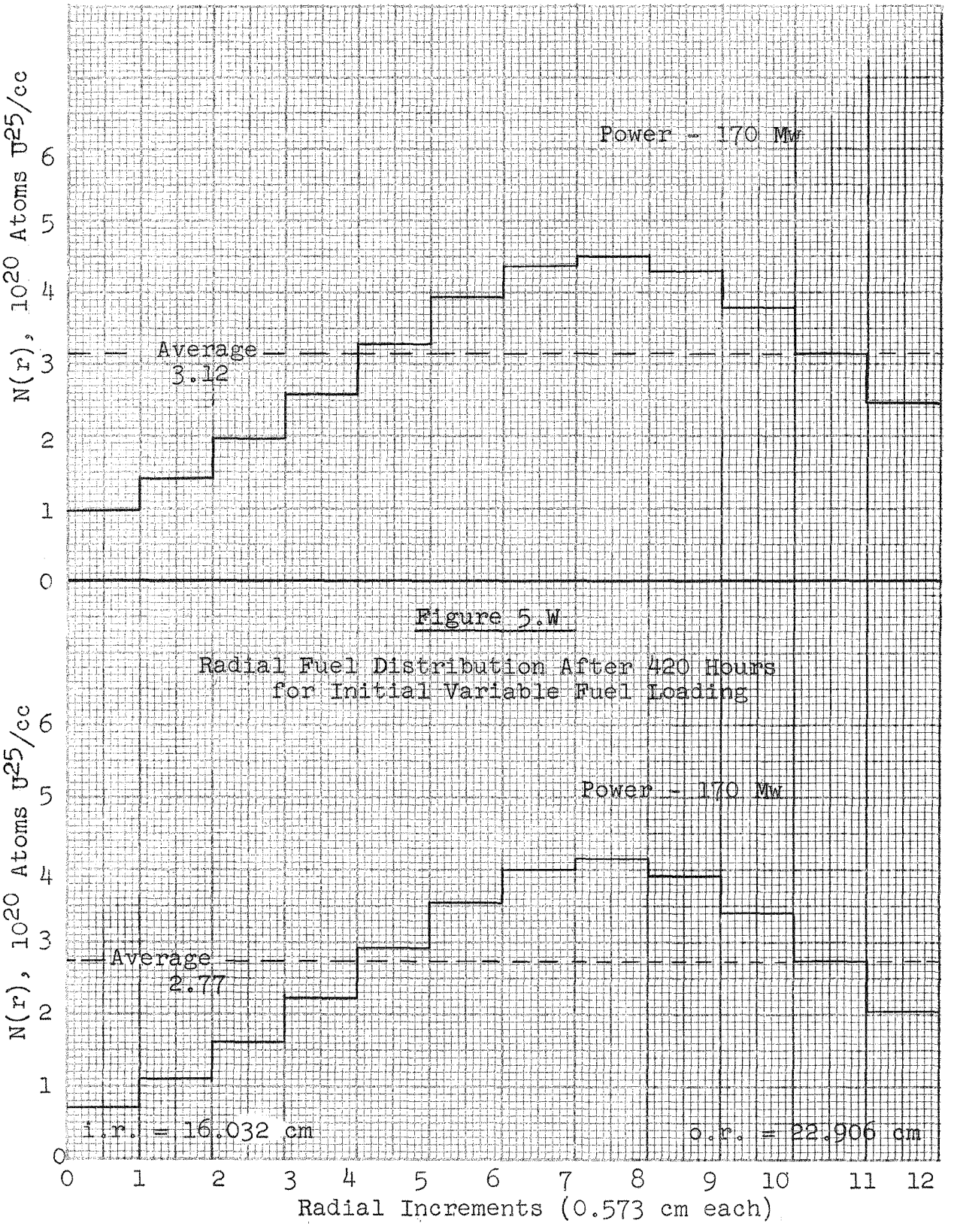

Figure 5.W

Radial Fuel Distribution After 420 Hours
for Initial Variable Fuel Loading

Figs.5.V and 5.W

Figure 5.X

Distribution of Power Density After 300 Hours
for Variable Initial Fuel loading of Core

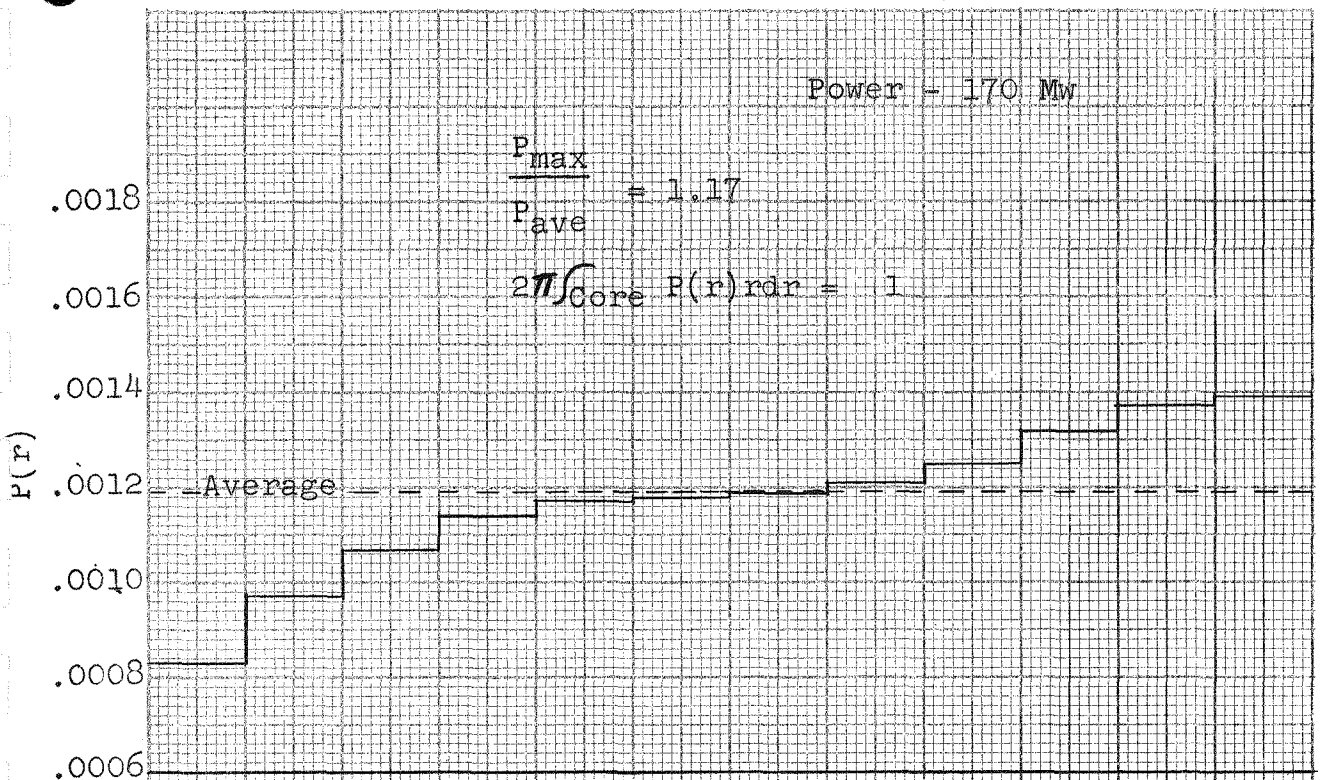

Figure 5.Y

Distribution of Power Density After 420 Hours
for Variable Initial Fuel Loading at Core

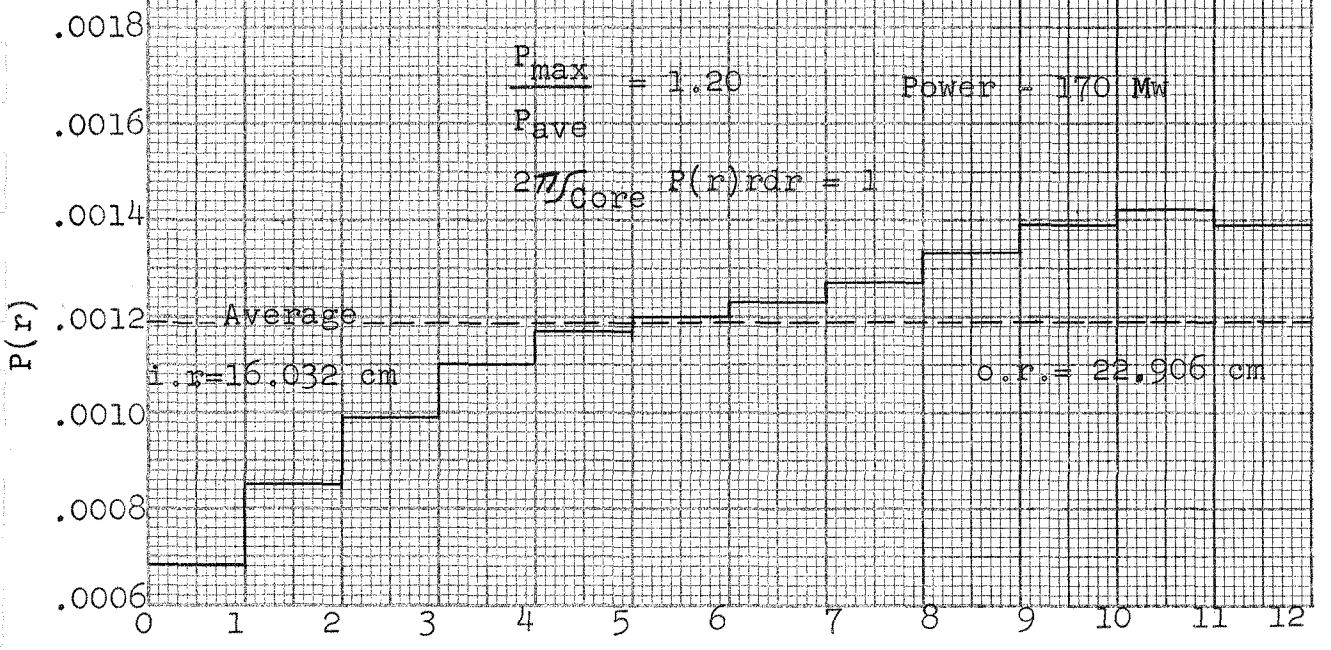

Figs. 5.X and 5.Y

Figure 5.Z

Local Burnup After 420 Hours for
Initial Variable Fuel Loading

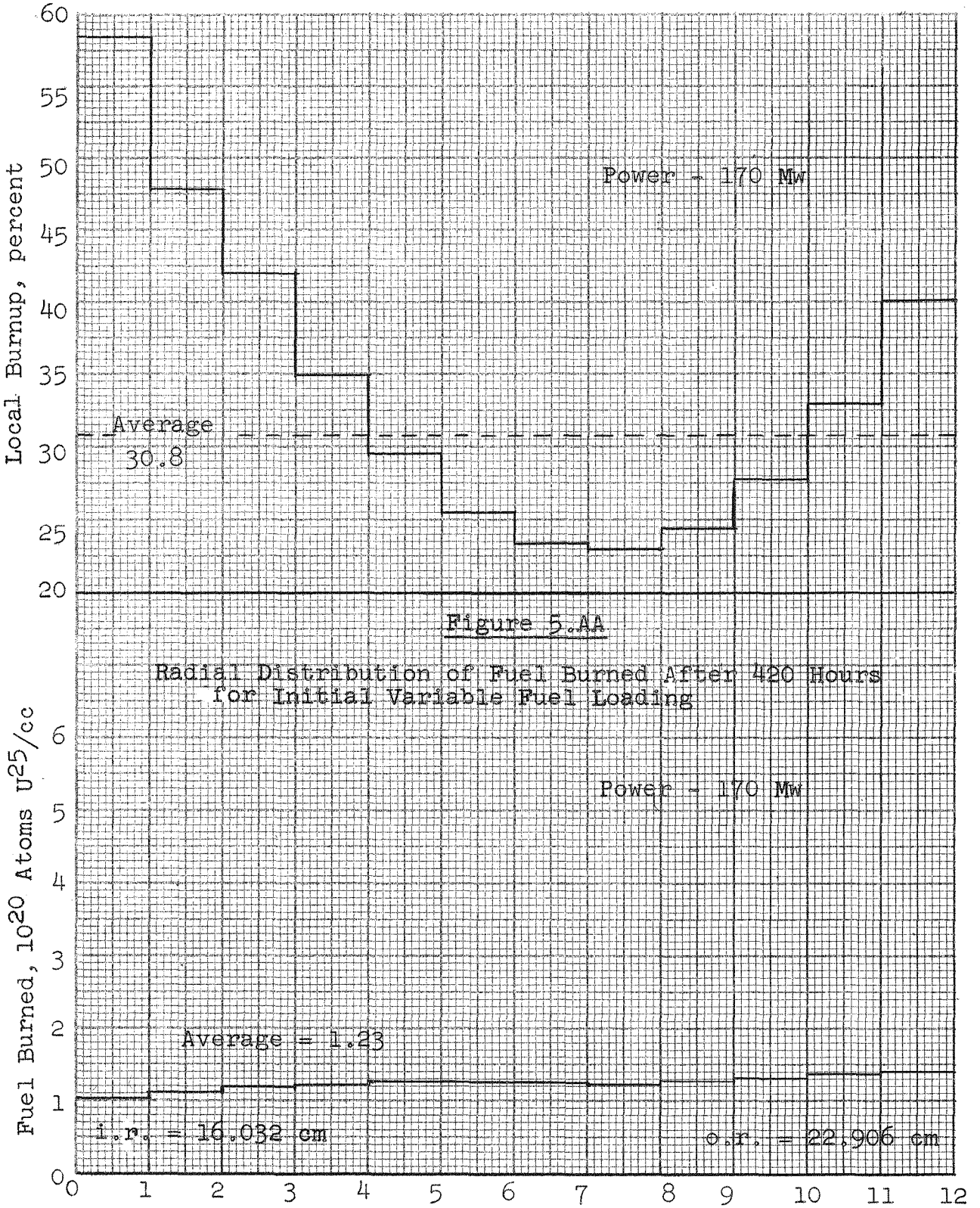

Figure 5.AA

Radial Distribution of Fuel Burned After 420 Hours
for Initial Variable Fuel Loading

Figs.5.Z and 5.AA

Figure 5.BB

Initial Radial Thermal Nuetron Flux Distribution
for Flat Fuel Loading

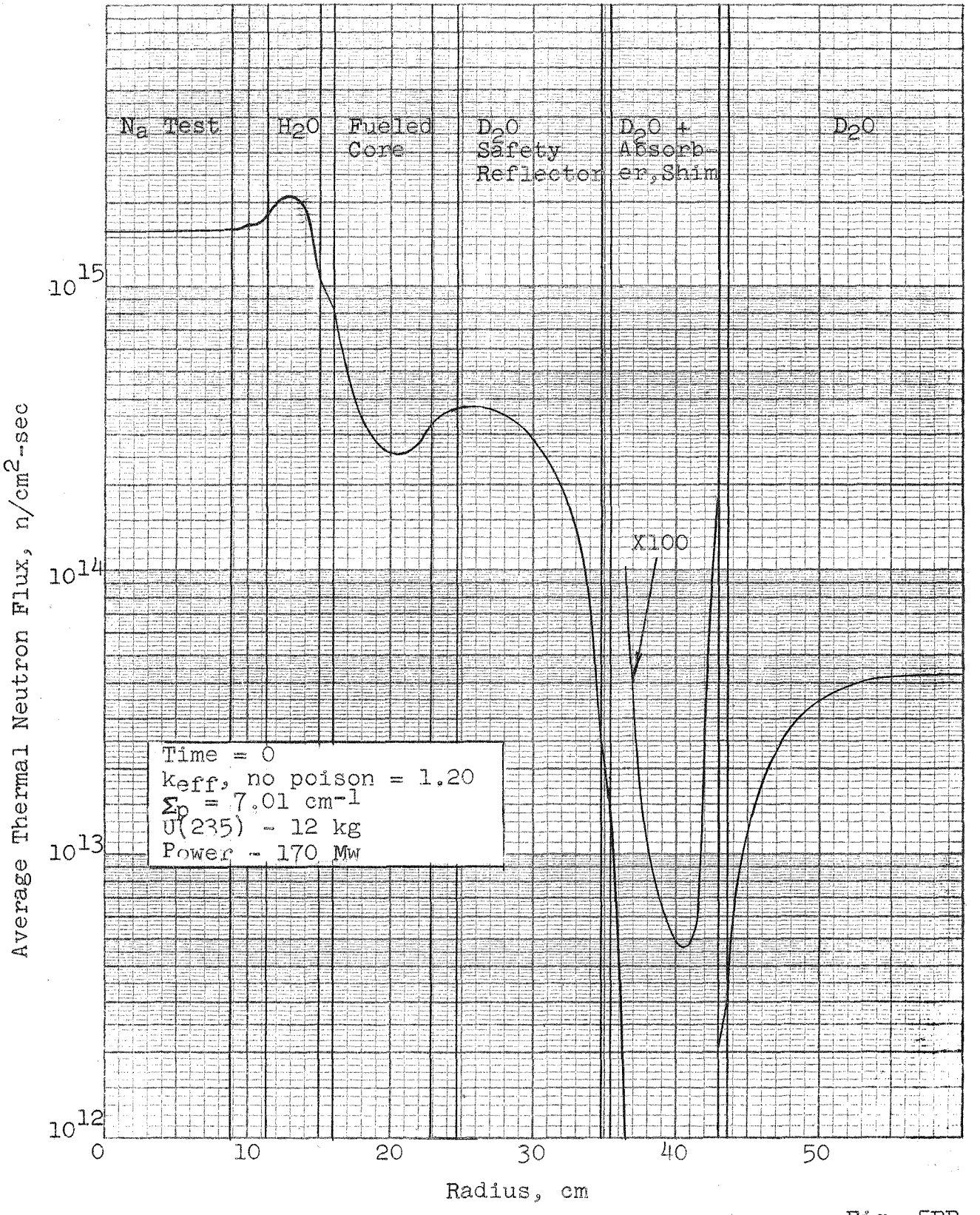

Fig. 5BB

Figure 5.CC

Initial Radial Epithermal Neutron Flux Distributions for Flat Fuel Distribution

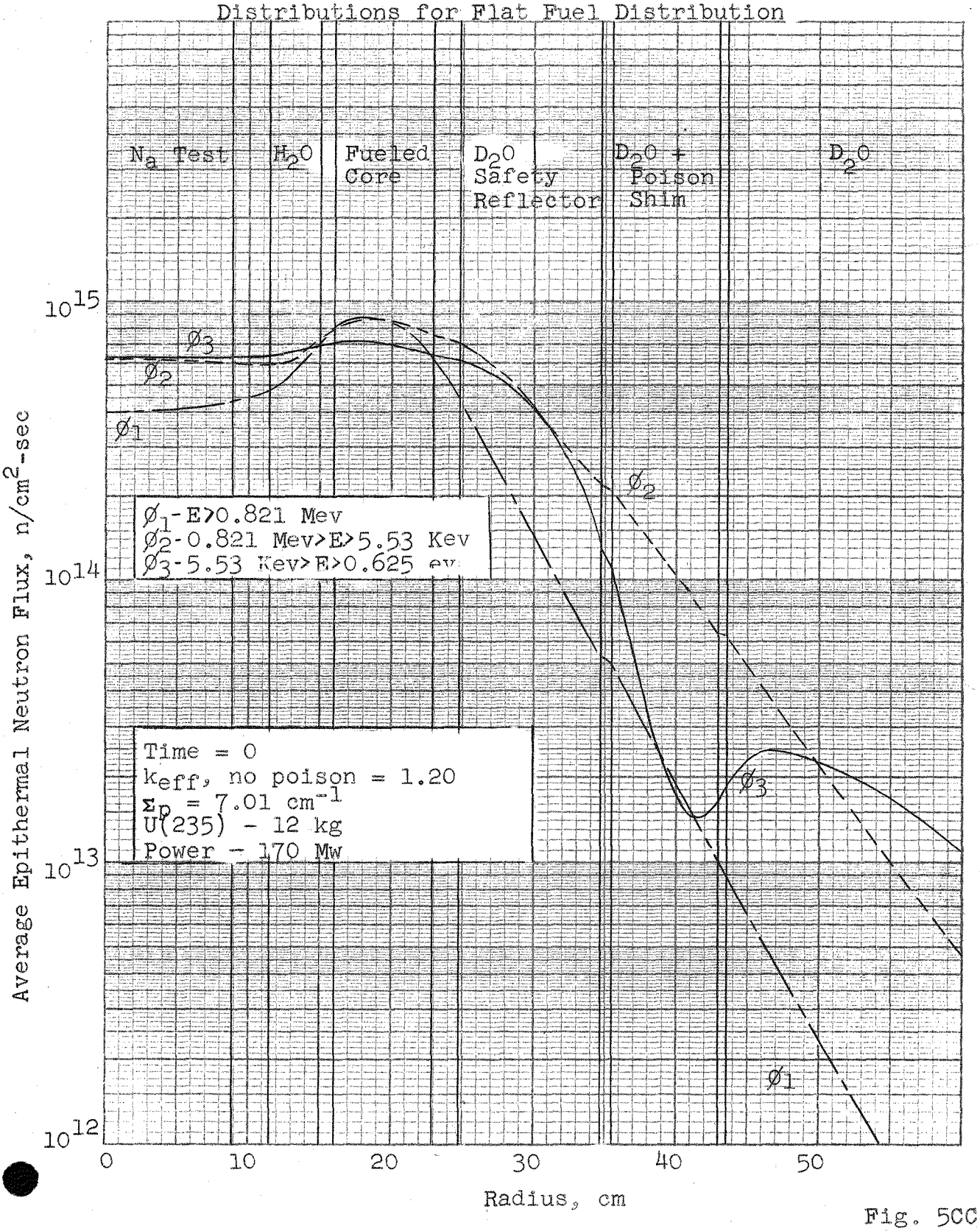

Fig. 5CC

Figure 5.DD

Radial Thermal Neutron Flux Distribution
After 180 Hours for Initial Flat Fuel Distribution

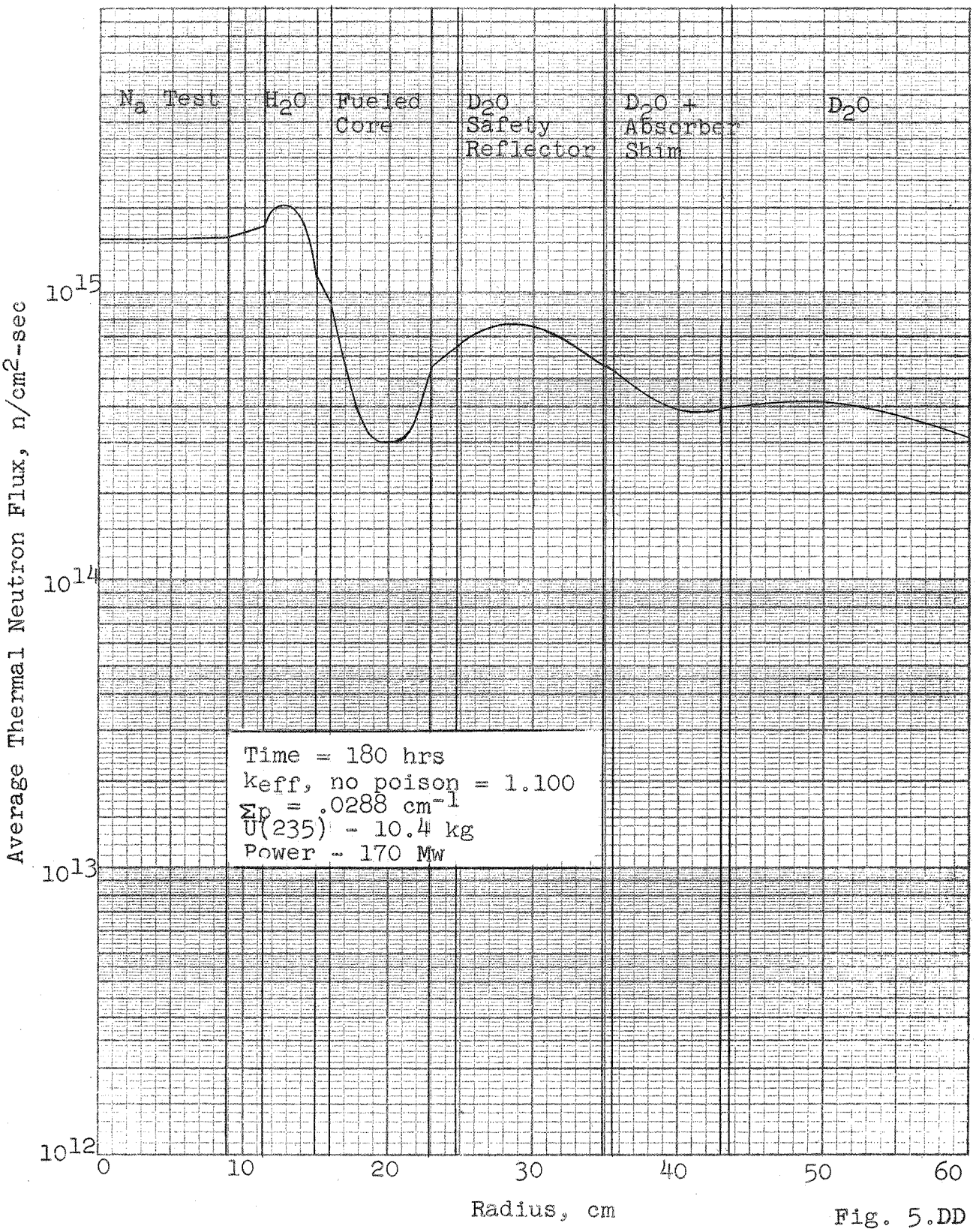

Fig. 5.DD

Figure 5.EE

Radial Epi-Thermal Neutron Flux Distributions After 180 Hours for Initial Flat Fuel Distribution

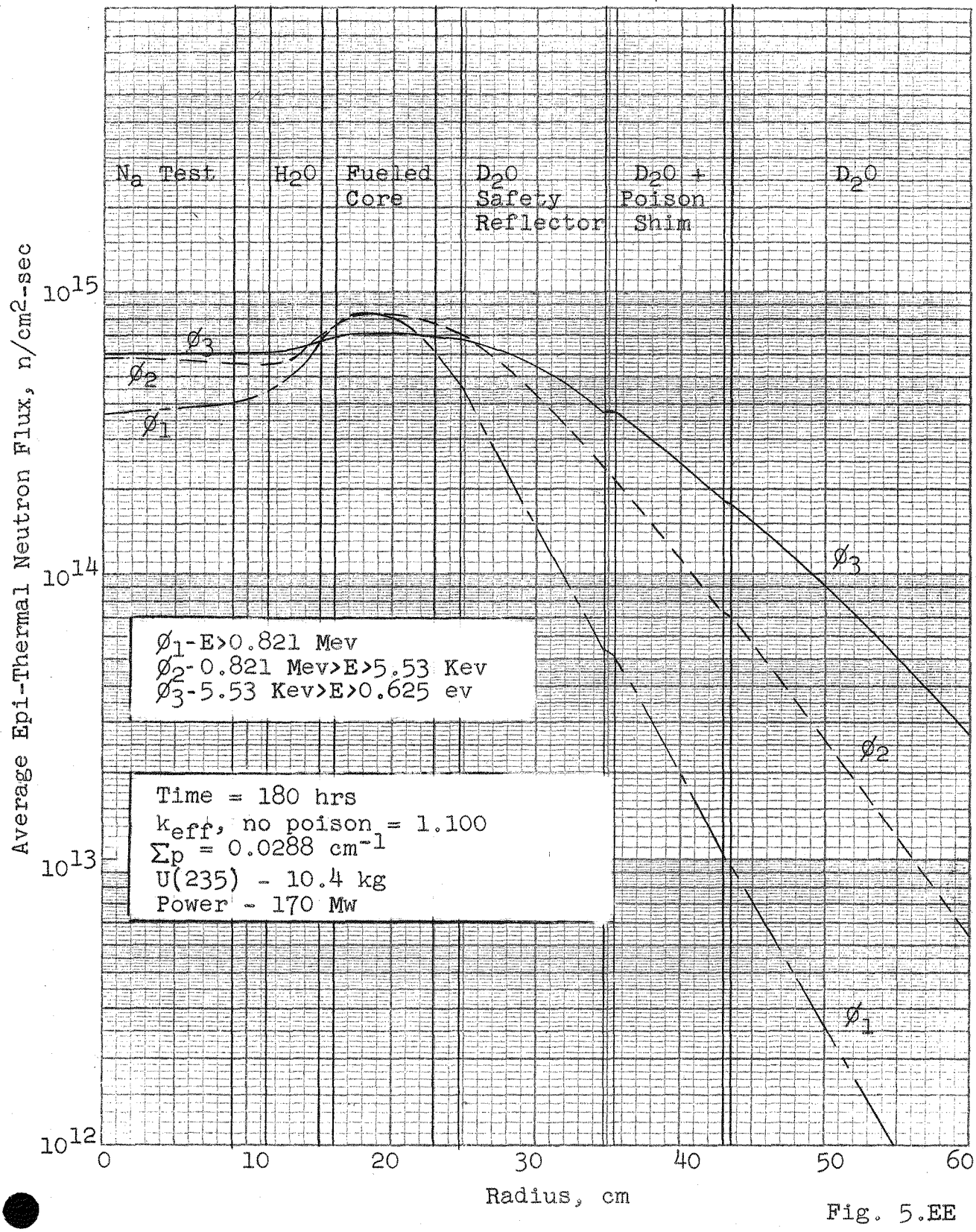

Fig. 5.EE

Figure 5.FF

Initial Radial Thermal Neutron Flux Distribution
for Variable Fuel Loading

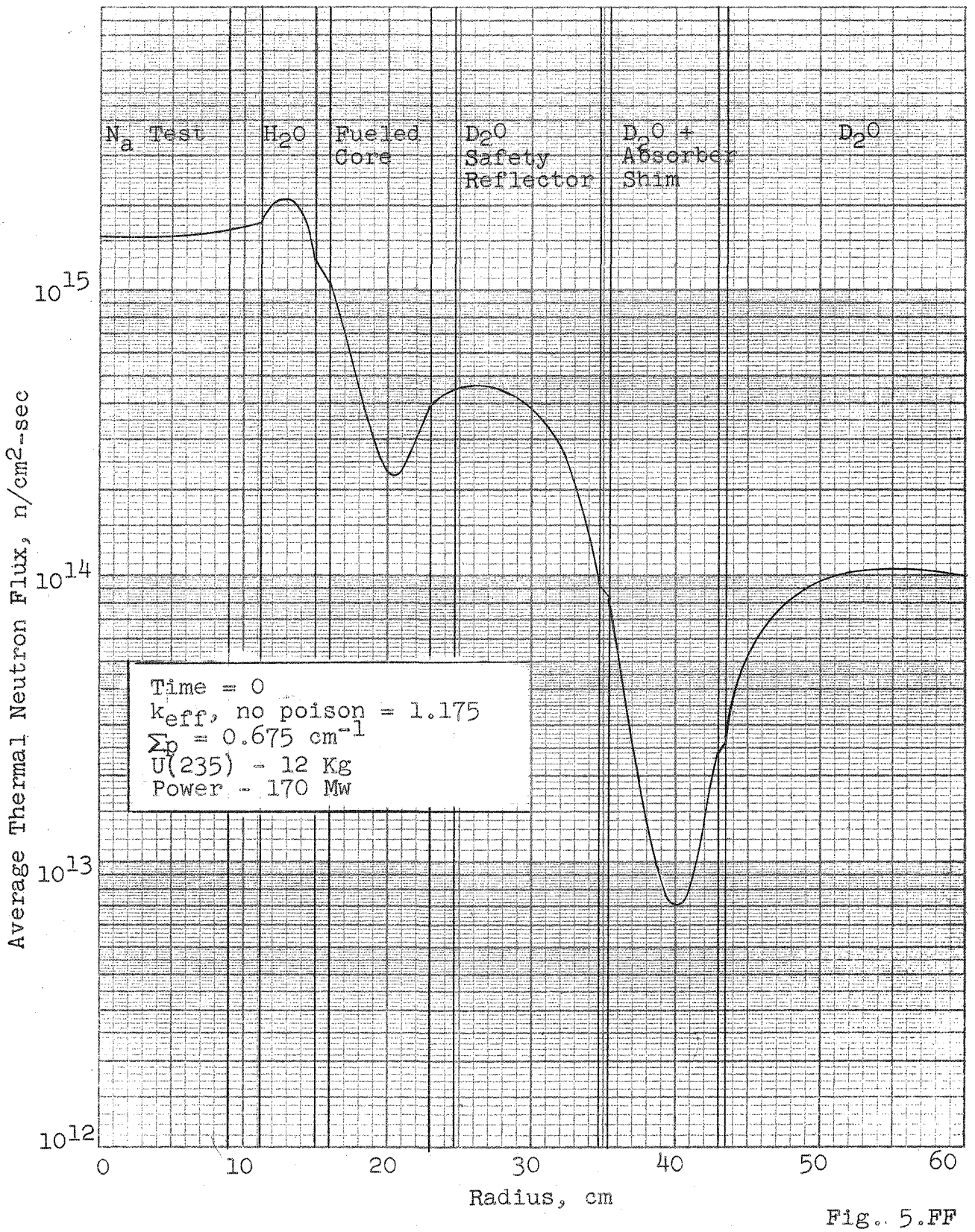

Fig. 5.FF

Figure 5.GG

Initial Radial Epi-Thermal Neutron Flux
Distribution for Variable Fuel Loading

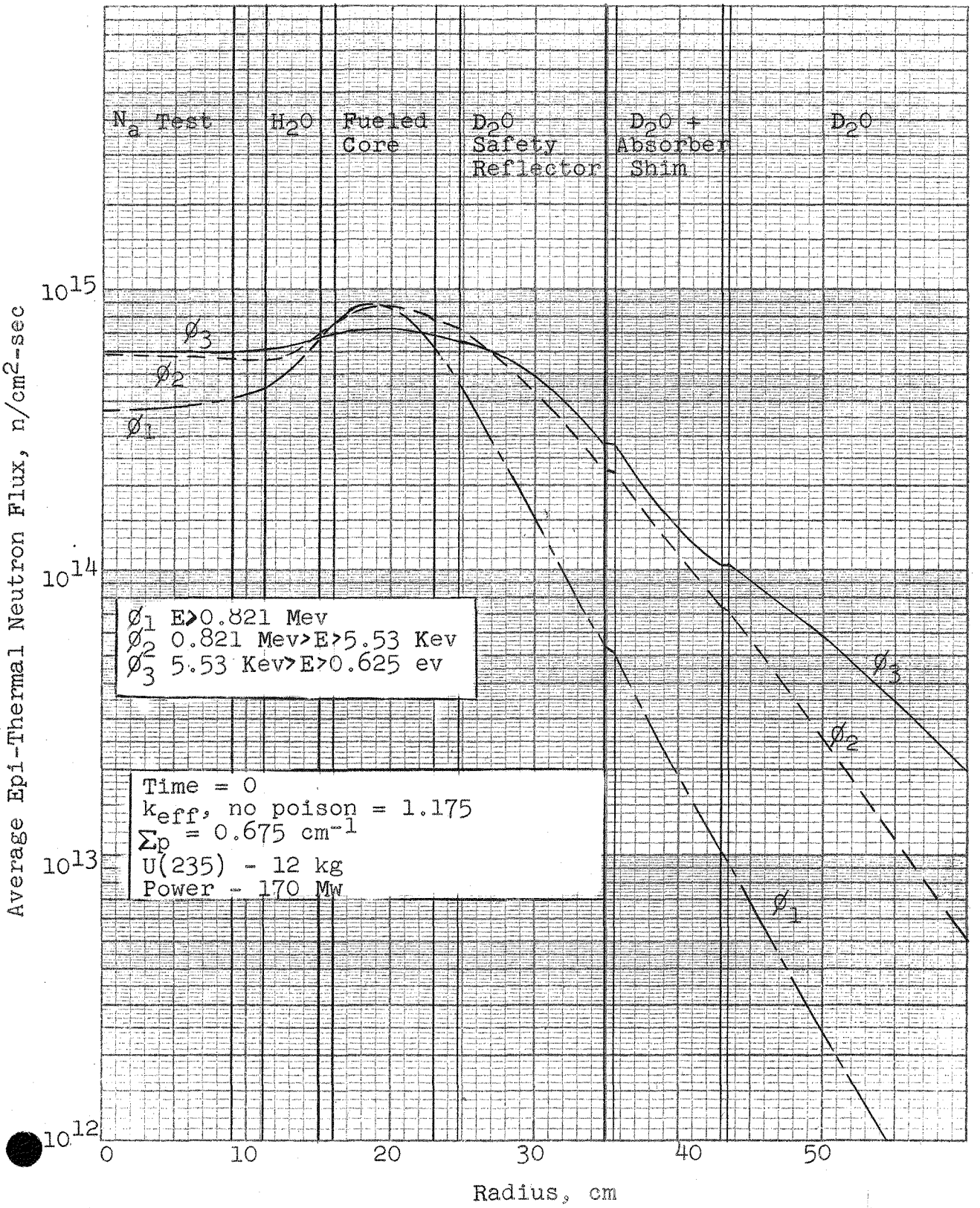

Fig. 5.GG

Figure 5.HH

End of Life Radial Thermal Neutron
Flux Distribution for Initial Variable Fuel Loading

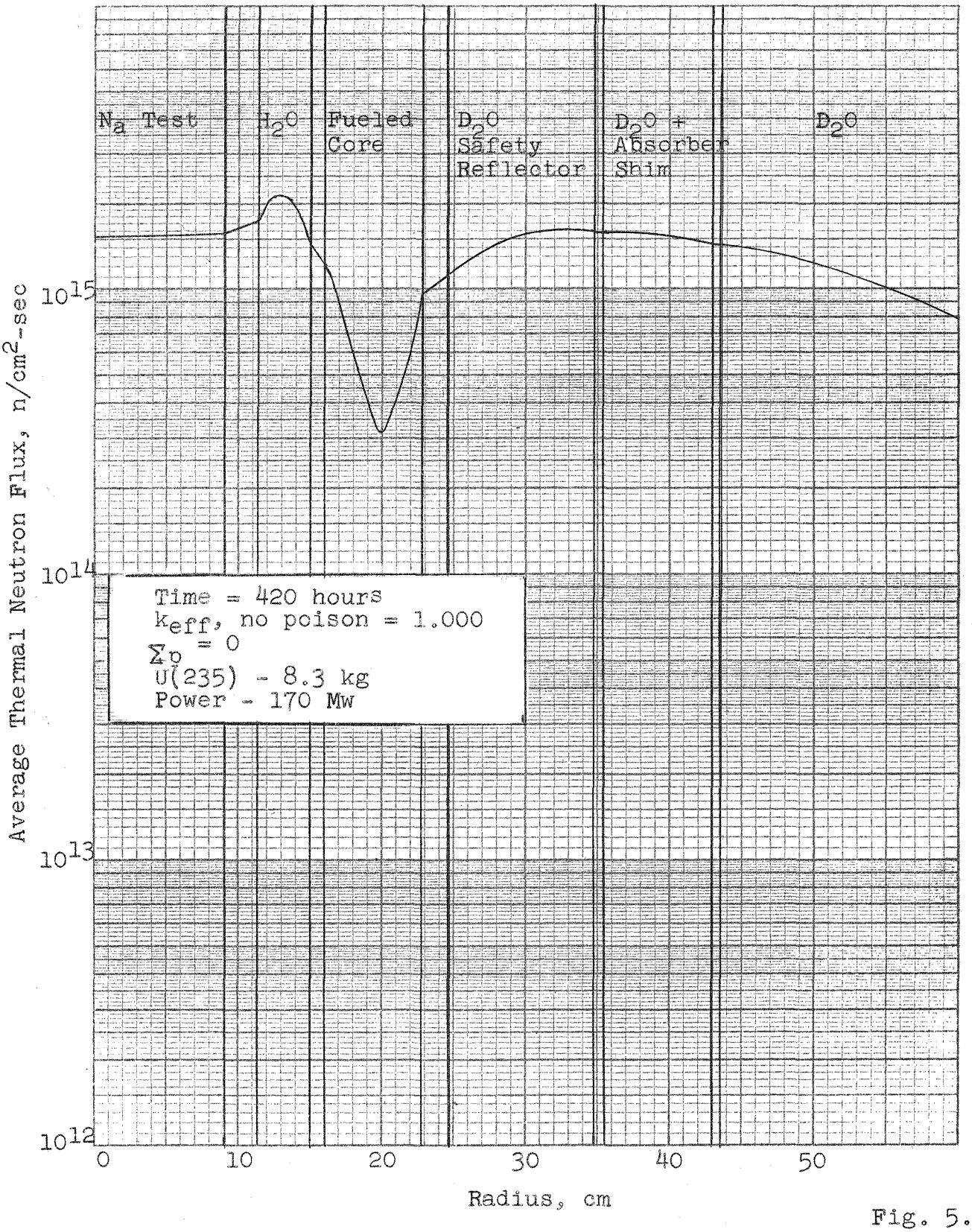

Fig. 5.HH

Figure 5.II

End of Life Radial Epi-Thermal Neutron Flux
Distributions for Initial Variable Fuel Loading

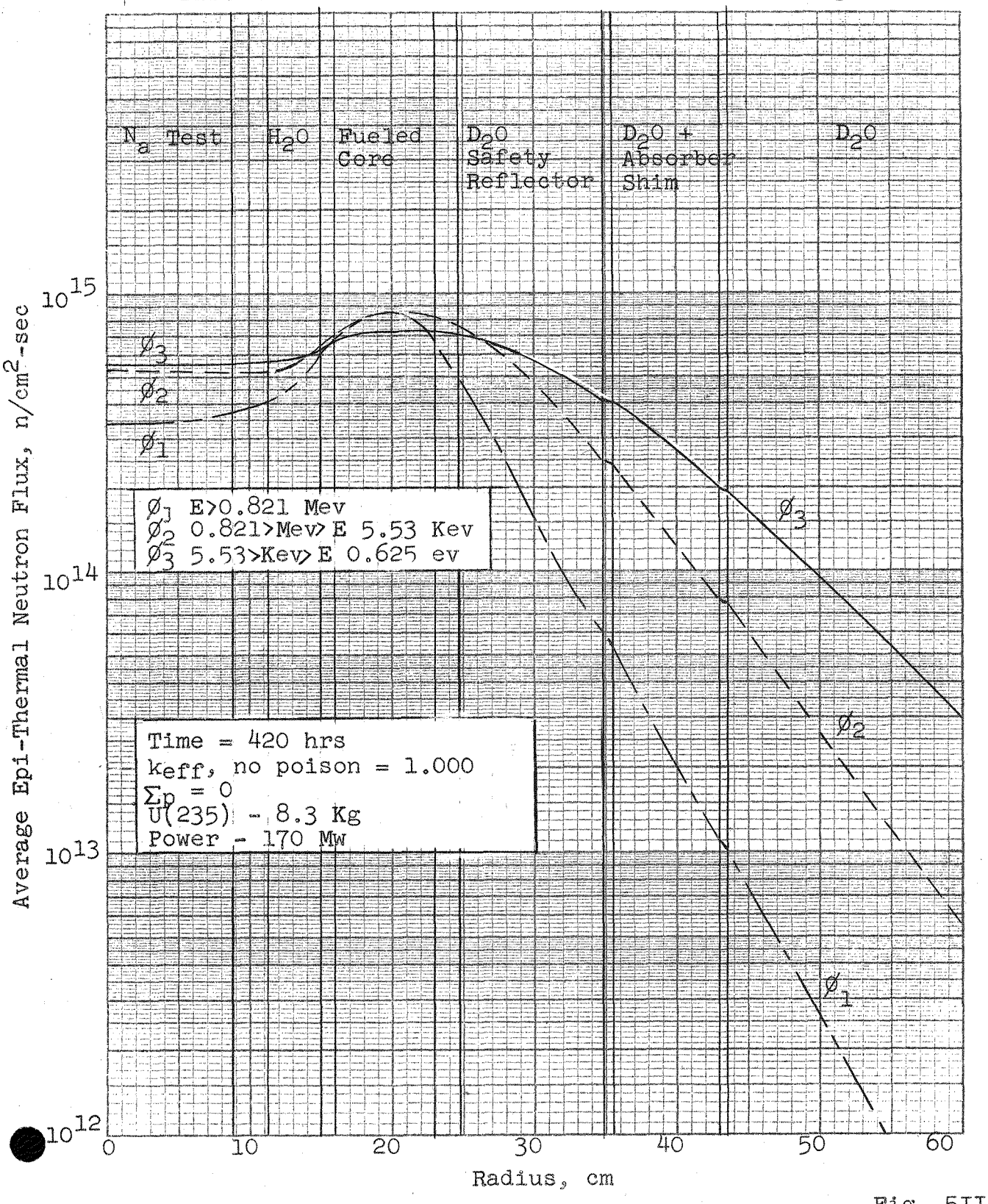

Fig. 5II

6.0 SUPPLEMENTAL SHIM CONTROL WITH BURNABLE POISONS

As indicated in the previous section, the desired 19 day fuel cycle at 170 Mw power level appears to be difficult to achieve because of the high shim control demands at reactor startup. The maximum excess reactivity which can be controlled is limited by the solubility of the poison in the shim region and the approach to infinite neutron blackness in the region. Additional shim control could be achieved by redesign of the reflector so that the annular shim region is closer to the core. However, this reduces the reactivity worth of the safety reflector adjacent to the core. The present arrangement represents a compromise between optimum safety and shim reflector performance. The selection of this configuration is discussed in more detail in a previous report.(3)

One possible solution to the problem is the use of burnable poisons in the fuel. If a burnable element having an absorption cross section larger than that of U(235), such as boron(10), is added to the fuel meat during fabrication, the initial available excess reactivity for a given fuel loading is reduced. Thus, the initial control requirements of the shim reflector are reduced. As the fuel is depleted the available excess reactivity does not fall off as rapidly as it did previously because of the counter-effects of the depletion of burnable poison.

The effectiveness of a burnable core poison in controlling excess reactivity is illustrated in Figure 6.A. The poisoning is defined as the ratio of the macroscopic absorption cross section of the poison to that of the U(235). The data for Figure 6.A were obtained from one-dimensional diffusion theory calculations using WANDA in one of the previous studies.(2)

Relatively simple calculations are adequate to show the general effects of burnup. More precise values would require additional computer calculations which could not be justified at present. The time dependent concentration of the fuel or burnable poison is described by the equation:

$$\frac{dN}{dt} = -N \sigma_a \phi \qquad (1)$$

where N is the time dependent concentration,

σ_a is the microscopic absorption cross section, and

ϕ is the thermal flux.

Integration of (1) yields

$$\ell n \left[\frac{N}{No}\right] = -\sigma_a \int_o^t \phi \, dt' \qquad (2)$$

where No is the concentration of the isotope at time zero. Equation (2) is written for the U(235) fuel and for the boron(10) burnable poison. Since the poison is mixed intimately with the fuel, the flux integrals are identical for each material. Equating the expressions, canceling and rearranging yields the expression for the time dependent poisoning:

$$P(t) = \frac{\sigma_a{}^{10} N_o{}^{10}}{\sigma_a{}^{25} N^{25}} \left[\frac{N^{25}}{N_o{}^{25}}\right]^{\sigma_a{}^{25}/\sigma_a{}^{10}} \qquad (3)$$

where the superscript 10 and 25 represent the poison and fuel, respectively.

A reduction of the initial excess multiplication factor by 0.05 or 0.06 appears desirable and, according to Figure 6.A, a poisoning equal to 0.075 is sufficient. Solving equation (3) at time 0 when $N^{25} = N_o{}^{25} = 4 \times 10^{20}$ atoms/cc, the initial concentration of poison is $N_o{}^{10} = 0.0528 \times 10^{20}$ atoms/cc. The microscopic cross sections for U(235) and boron(10) are 545.3 and 3100.3 barns, respectively, as reported in Table A3.c. With these constants, the poisoning is calculated using equation (3) at the various time steps of the CANDLE calculations. The poisoning values are converted to excess multiplication values using the relationship given in Figure 6.A, and the results are summarized in Table 6.a. Figure 6.B shows the time-reactivity relationship for the graded fuel case which was obtained by combining the time dependent reactivity effects due to the poisoning with the CANDLE results. Thus, for a reduction in initial reactivity of 0.059, a loss in reactivity lifetime of about 30 hours results. The initial reactivity, however, is easily controlled with the shim reflector. With a slight increase in the initial fuel loading, the burnable poison appears to make the soluble poison shim control for the 19 day fuel cycle feasible.

Table 6.a

Intermediate Values in Calculation of Reactivity Effect of Burnable Poisons

Reactor Operation hours	$N^{25}(t)$	$P(t)$	$\Delta k(t)$
0	4.0000	0.0750	-0.059
10	3.9699	0.0725	-0.057
60	3.8213	0.0606	-0.047
180	3.4691	0.0387	-0.029
300	3.1183	0.0235	-0.016
420	2.7691	0.0133	-0.009

Figure 6.A

Compensation of Excess Multiplication
with Core Poisoning

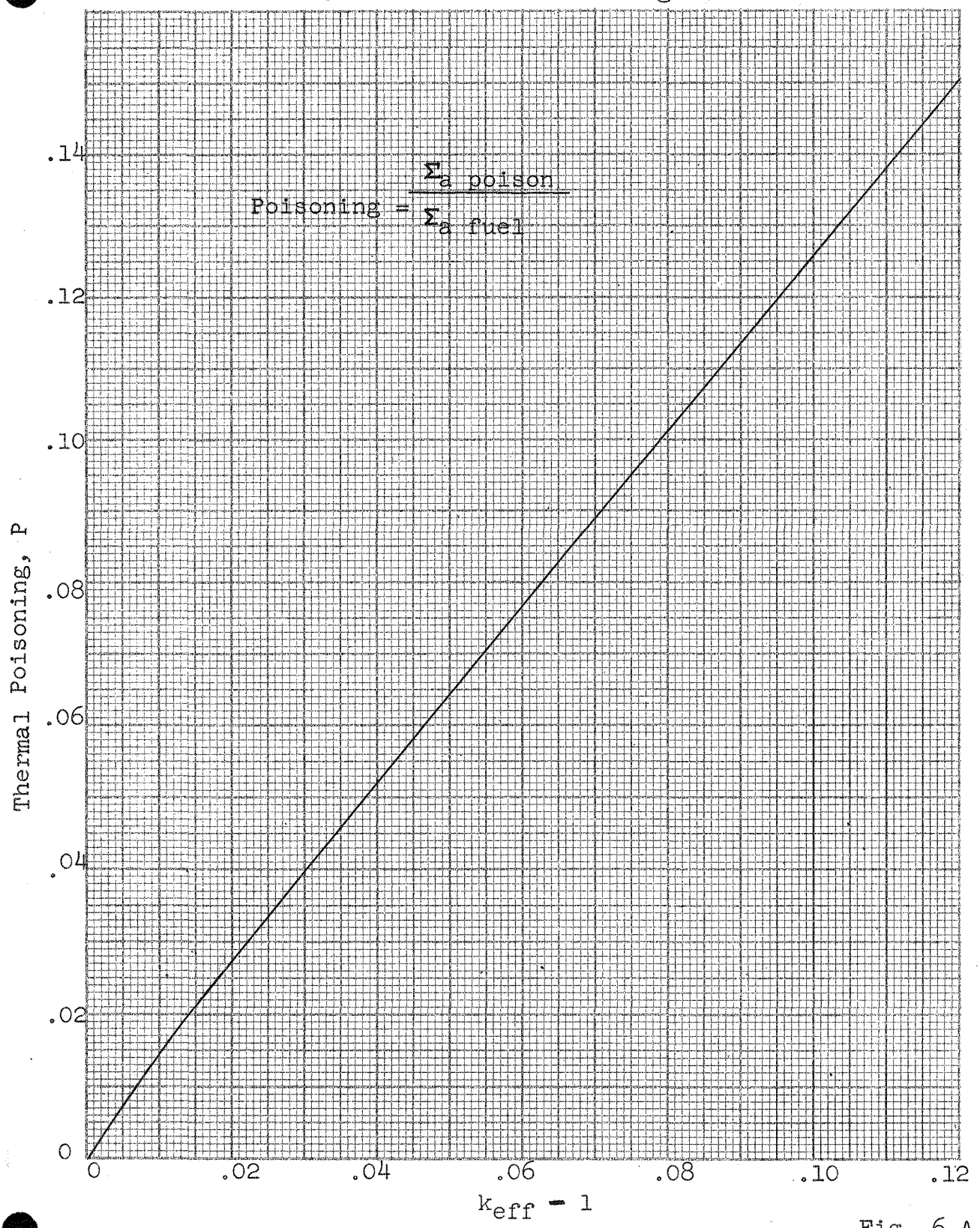

Fig. 6.A

Figure 6.B

Effect of Burnable Poison in Graded Core on Excess Reactivity

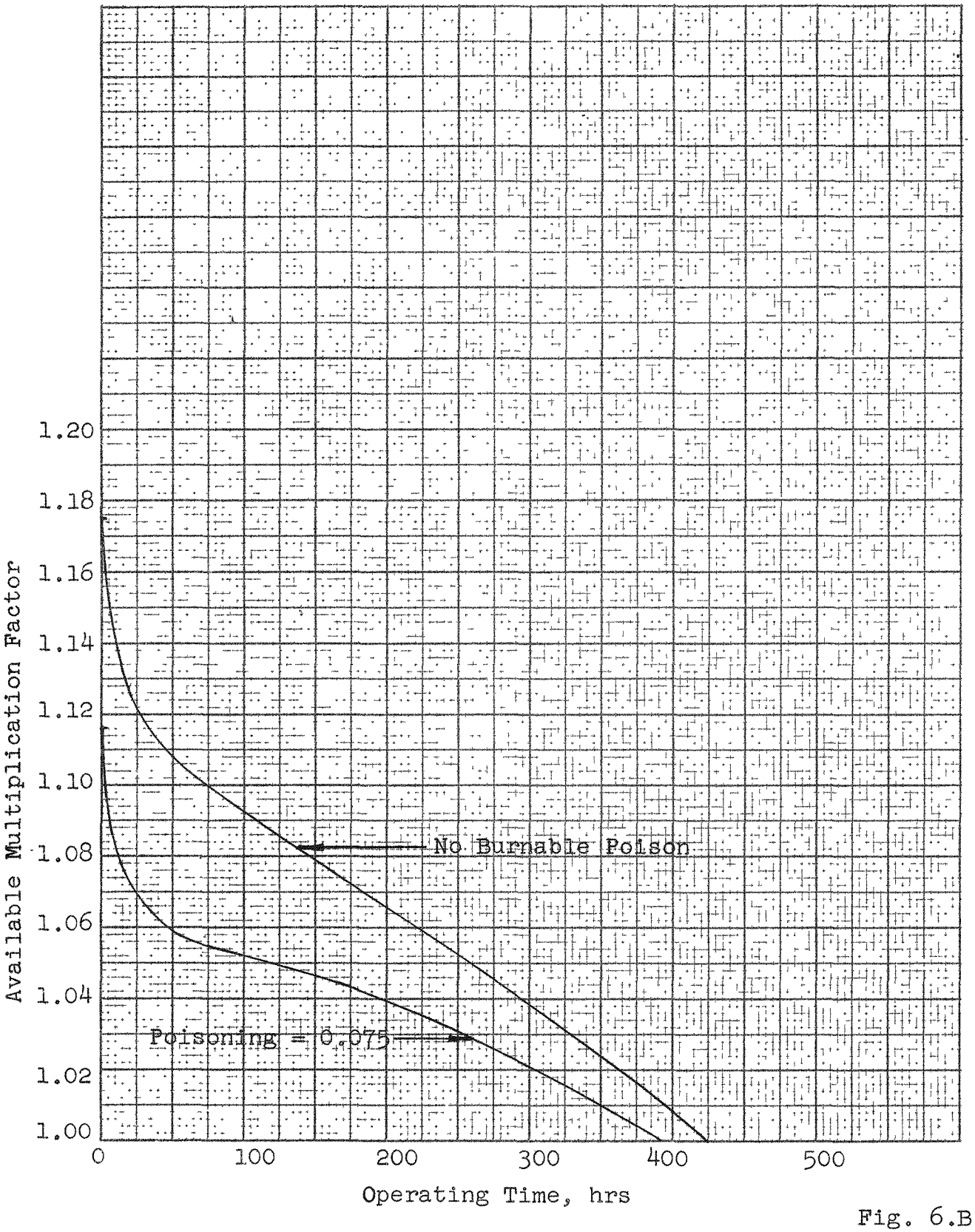

Fig. 6.B

7.0 FUEL ASSEMBLY FABRICATION FEASIBILITY (GRADED FUEL AND POISON)

Letters of inquiry concerning the feasibility of fabricating fuel elements to achieve non-uniform fuel and/or poison distribution in the core of a flux trap type reactor were sent to 14 different firms having fuel element fabrication capability. Enclosures described the core and fuel element configurations and outlined tentative ratios for both radial and axial fuel and/or poison distributions to be achieved. The fabricators were asked to consider two different types of fuel element, the involute plate type and the concentric plate type, in relation to achieving non-uniform fuel and/or poison distribution.

Also enclosed was a list of general questions concerning the fabrication of fuel elements to the specifications outlined. The fabricators were asked to answer these to whatever extent they desired. A copy of the questionnaire appears in Appendix 4.0.

Of the 14 firms queried, there were no replys from six, five replied that they either had no applicable fabricating experience or did not wish to answer, and informative, helpful replies were received from three: Research Division, Curtiss-Wright Corporation, Quehanna, Pennsylvania; Nuclear Division, Combustion Engineering, Inc. Windsor, Connecticut; and Nuclear Materials and Equipment Corporation, Apollo, Pennsylvania.

All of the latter three respondents were unanimous in the opinion that it would be possible to fabricate fuel elements to achieve both radial and axial fuel and poison distributions (in approximately the same ratios and to about the same tolerances as set in the tentative specifications) in an annular reactor core. Opinion was split as to the most appropriate type fuel element with which to achieve the desired distributions. One respondent preferred the involute plate type, another preferred the concentric plate type and the third apparently felt either type would be applicable. All three were of the opinion that the burnable poison should be inserted with the "meat" of the fuel plates. However, different methods of accomplishing this were suggested. Two of the respondents indicated that they felt that inserting fuel alloy of varying fuel content was the most feasible method of achieving non-uniform fuel distribution while the third preferred varying the thickness of the meat.

Only one respondent made definite comments concerning development costs and the cost of fuel elements incorporating non-uniform fuel and poison distributions relative to that of uniformly loaded fuel elements. They indicated that the cost of a fuel fabrication development program, which would include the assembly of a prototype,

would be in the range of $100,000. Upon completion of development, they indicated that the total cost of the non-uniformly loaded fuel assembly would be between 5 to 10 percent higher than that of a uniformly loaded fuel assembly. One respondent indicated that they felt a few pilot runs would be sufficient to establish the effect of extrusion and subsequent hot and cold rolling on the "smearing out" of the fuel and poison distributions but gave no indication as to the probable cost of such a program. The third respondent merely indicated that a fuel fabrication development program would be expensive and that non-uniformly loaded fuel elements would probably be considerably more expensive than uniformly loaded ones.

Further information on the feasibility of non-uniform fuel and poison distribution was obtained in a phone conversation with Mr. John E. Cunningham of the Metallurgy Department of ORNL. Mr. Cunningham indicated that ORNL nas accomplished considerable development work toward achieving non-uniform fuel distribution, radially, in an involute plate. They have been quite successful in achieving a linear fuel concentration change in the radial direction and intend to do some work on achieving a non-linear radial fuel distribution. Mr. Cunningham indicated that it should be relatively easy to achieve both axial and radial non-uniform distribution of fuel. He felt that non-uniform axial fuel distribution would actually be easier to achieve than non-uniform radial fuel distribution. The fuel distribution tolerances quoted by Mr. Cunningham were better than those in the tentative specifications set in the inquiry to industrial fabricators.

In regard to poison distribution, Mr. Cunningham indicated that ORNL had used a uniform poison distribution in the developmental fuel plates produced but felt that a non-uniform poison distribution could also be achieved.

In regard to fuel element fabrication costs, Mr. Cunningham felt that the involute plate type element should prove less expensive to produce than the concentric plate type, even though non-uniform fuel and/or poison distributions were somewhat easier to achieve with the latter type element. He also indicated that the cost of fabricating fuel plates with non-uniform fuel distributions should be less than 150% of that of equivalent plates with uniform fuel distribution.

From the above, it is concluded that there is a high probability of fabricating fuel elements to achieve non-uniform fuel and/or poison distributions in the core of the AETR. It also appears that a good deal of technology, in support of such a development, has been accumulated by both industry and Oak Ridge National Laboratory. In view of this technological background, the cost of a fuel element fabrication development program should not be excessive.

8.0 REFERENCES

1. O. J. Elgert, C. F. Leyse, and D. G. Ott, "Preliminary Investigations for an Advanced Engineering Test Reactor", INTERNUC-9 and Addendum, AECU-3437, Internuclear Company, 1957.

2. C. F. Leyse, et.al., "An Advanced Engineering Test Reactor", INTERNUC-23, AECU-3775, Internuclear Company, 1958.

3. A. M. Larson, et.al., "Experimental and Analytical Studies of Reflector Control for the Advanced Engineering Test Reactor", INTERNUC-47, Internuclear Company, 1959.

4. B. H. Leonard, P. C. Bertelson, E. E. Wade, "AETR Nuclear Mockup Design", INTERNUC-48, Internuclear Company, 1959.

5. T. L. Francis, et.al., "Advanced Engineering Test Reactor Safety Studies", INTERNUC-49, Internuclear Company, 1959.

6. O. J. Elgert, et.al., "Test Requirements for Naval Reactors and Aircraft Nuclear Propulsion (GE) - Applicability of the AETR", INTERNUC-51, Internuclear Company, 1959.

7. A. M. Larson, et.al., "Additional Safety Reflector Drop Tests with the AETR Reflector Control Model", INTERNUC-54, Internuclear Company, 1960.

8. G. G. Bilodeau, et.al., "PDQ An IBM-704 Code to Solve the Two-Dimensional Few-Group Neutron-Diffusion Equations", WAPD-TM-70.

9. M. H. Marlowe, et.al., "WANDA - A One-Dimensional Few-Group Diffusion Equation Code for the IBM-704", WAPD-TM-28, 1956.

10. L. Culpepper, et.al., "CANDLE - A One-Dimensional Few-Group Depletion Code for IBM-704", WAPD-TM-53., 1957.

11. O. J. Marlowe, and P. A. Ombrellaro, "CANDLE - A One-Dimensional Few-Group Depletion Code for IBM-704, Addendum 1, CANDLE-2", WAPD-TM-53 Addendum 1, 1957.

12. H. Bohl, E. B. Gelbard, and G. H. Ryan, "Fast Neutron Spectrum Code for the IBM-704", WAPD-TM-72, 1957.

13. C. H. Westcott, "Effective Cross Section Values for Well Moderated Thermal Reactor Spectra", AECL-407, 1957.

14. "Reactor Physics Constants", ANL-5800, 1958.

APPENDIX 1.0 TWO-GROUP TWO-DIMENSIONAL PDQ CALCULATIONS

The methods used to determine consistent two-group constants and the detailed grid information used for the two-dimensional calculations are discussed in this section.

A1.1 Two-Group Cross Sections

In order to reduce the machine time requirements and increase the efficiency of the two-dimensional calculations for determining the safety reflector worth, a set of two group constants were synthesized from the three group constants used previously. The results using two-group and three-group constants were compared with one-dimensional WANDA calculations for the case with 12 kg U(235) loading, flat fuel distribution, and no shim reflector poisoning. The effective multiplication factors are 1.1797 and 1.1789 respectively. The similarity between the calculated power distributions is illustrated in Figure A1.A. The PDQ results, which coincide with the two-group WANDA results at the reactor midplane, indicate the axial maximum-to-average power density is 1.273 as compared with 1.21 found in previous work.

The diffusion coefficients were prepared using the equation:

$$\bar{D} = \frac{D_1 \phi_1 \Delta u_1 + D_2 \phi_2 \Delta u_2}{\phi_1 \Delta u_1 + \phi_2 \Delta u_2}$$

where

$\bar{D}$ = the two-group epithermal diffusion coefficient, cm

D_1 = the three-group fast diffusion coefficient, cm

D_2 = the three-group intermediate diffusion coefficient, cm

$\phi_1 \Delta u_1$ = the three-group integrated fast flux in the region, n/cm^2-sec

$\phi_2 \Delta u_2$ = the three-group integrated intermediate flux in the region, n/cm^2-sec

The integrated fluxes, $\phi \Delta u$, were taken directly from the output of a three-group WANDA calculation using the constants which are combined to produce the two-group constants. The geometry and three-group constants for the WANDA calculations are summarized in Tables A2.a and A2.b of Appendix 2.0.

The absorption cross sections were prepared using the equation

$$\bar{\Sigma}_a = \frac{\Sigma_{a1}\phi_1\Delta u_1 + \Sigma_{a2}\phi_2\Delta u_2}{\phi_1\Delta u_1 + \phi_2\Delta u_2}$$

where

$\bar{\Sigma}_a$ = the two-group epithermal absorption cross section, cm^{-1}

Σ_{a1} = the three-group fast absorption cross section, cm^{-1}

Σ_{a2} = the three-group intermediate absorption cross section, cm^{-1}

The slowing down cross sections were prepared using the equation

$$\bar{\Sigma}_{sd} = \frac{\Sigma_{sd2}\phi_2\Delta u_2}{\phi_1\Delta u_1 + \phi_2\Delta u_2}$$

where

$\bar{\Sigma}_{sd}$ = the two-group slowing down cross section, cm^{-1}

Σ_{sd2} = the three-group intermediate slowing down cross section, cm^{-1}

The thermal cross-sections for both schemes are identical.

The calculated two-group cross sections used for the two-dimensional calculations are summarized in Tables A1.a and A1.b. For void regions in the PDQ calculations, the epithermal and thermal diffusion coefficients were taken to be 100-cm and the absorption and slowing down constants were set to zero.

Table A1.a

Two Group Constants

WANDA Regions	Material	°F Temp	$\bar{D}$ (cm)	$\bar{\Sigma}_{sd}$ (cm^{-1})	$\bar{\Sigma}_a$ (cm^{-1})	
1	Na	1000	5.5450	0.00020184	0.00019437	Fast
			4.7083	------	0.0058173	Thermal
2	Misc."2"*	170	2.2700	0.0013269	0.00039105	Fast
			1.1904	------	0.017925	Thermal
3	H_2O	170	1.2308	0.035209	0.00036826	Fast
			0.16710	------	0.017470	Thermal
4,5,6	Misc."4"*	170	1.6207	0.0021098	0.00023527	Fast
			0.71060	------	0.012503	Thermal
7 thru 18	Core	170	See Table A1.b			
19	Misc."6"*	170	1.8435	0.0010602	0.00037112	Fast
			1.1429	------	0.011926	Thermal
20	D_2O	170	1.2676	0.0078569	0.00000099897	Fast
			0.88499	------	0.000064700	Thermal
21	Aℓ	170	3.0243	0.00032191	0.00045987	Fast
			3.9640	------	0.011250	Thermal
22	D_2O (clean shim)	170	1.2445	0.0099613	0.0000012665	Fast
			0.88499	------	0.000064700	Thermal
22	D_2O (saturated boric acid)	170	1.244	0.0099613	0.0098141	Fast
			0.88499	------	0.27844	Thermal
23	Aℓ	170	3.2156	0.00036319	0.00051885	Fast
			3.9640	------	0.011250	Thermal
24	D_2O	170	1.2172	0.012447	0.0000015825	Fast
			0.88499	------	0.000064700	Thermal

*Mixtures of water, aluminum, and iron.

Table A1.b

Core Cross Sections

Group	Fast	Thermal
Σ_{sd}	0.017154	------
Σ_a No U(235)	0.00027284	0.014942
Σ_a U(235)	0.0052930	0.21812
Σ_a Core	0.0055658	0.23306
$\nu\Sigma_f$	0.0086806	0.45320
D	1.3913	0.27366

A1.2 Geometry Details

The calculational model for the PDQ two-dimensional calculations is consistent with that shown in Figure 1.D. In terms of mesh units, the geometry is shown in Figure A1.B. The picture is distorted since the mesh unit widths vary. The mesh spacings used in the radial direction are shown in Table A1.c and the mesh spacings used in the vertical direction are shown in Table A1.d

Table A1.c

Mesh Point Spacing in Radial Direction

Mesh Column	Distance From Reactor Centerline (cm)	Δr (cm)
0	-2.9633	
1	2.9633	5.9267
2	5.9266	2.9633
3	8.8899	2.9633
4	10.0709	1.1810
5	11.2519	1.1810
6	12.4968	1.2449
7	13.7417	1.2449
8	14.9866	1.2449
9	15.2481	0.26150
10	15.5096	0.26150

Table A1.c Continued

Mesh Column	Distance From Reactor Centerline (cm)	Δr (cm)
11	15.7711	0.26150
12	16.0326	0.26150
13	16.6054	0.57283
14	17.1783	0.57283
15	17.7511	0.57283
16	18.3239	0.57283
17	18.8968	0.57283
18	19.4696	0.57283
19	20.0424	0.57283
20	20.6152	0.57283
21	21.1881	0.57283
22	21.7609	0.57283
23	22.3337	0.57283
24	22.9066	0.57283
25	23.3713	0.46475
26	23.8361	0.46475
27	24.3008	0.46475
28	24.7656	0.46475
29	26.0356	1.2700
30	27.3056	1.2700
31	28.5756	1.2700
32	29.8456	1.2700
33	31.1156	1.2700
34	32.3850	1.2700
35	33.6556	1.2700
36	34.9256	1.2700
37	35.1636	0.2380
38	35.4016	0.2380
39	37.3066	1.9050
40	39.2116	1.9050
41	41.1166	1.9050
42	43.0216	1.9050
43	43.2596	0.2380
44	43.4976	0.2380
45	48.7761	5.2785
46	54.0546	5.2785
47	59.3331	5.2785
48	64.6116	5.2785
49	69.8901	5.2785
50	75.1686	5.2785
51	80.4471	5.2785
52	85.7256	5.2785

Table A1.d

Mesh Point Spacing in Vertical Direction

Mesh Row	Distance From Core Midplane (cm)	ΔZ (cm)	Mesh Row	Distance From Core Midplane (cm)	ΔZ (cm)
0	+ 76.2002		24	- 20.3200	5.0800
1	+ 69.4268	6.7734	25	- 25.4000	5.0800
2	+ 62.6534	6.7734	26	- 30.4800	5.0800
3	+ 55.8800	6.7734	27	- 35.5600	5.0800
4	+ 53.3400	2.5400	28	- 40.6400	5.0800
5	+ 50.8000	2.5400	29	- 43.1800	2.5400
6	+ 48.2600	2.5400	30	- 45.7200	2.5400
7	+ 45.7200	2.5400	31	- 48.2600	2.5400
8	+ 43.1800	2.5400	32	- 50.8000	2.5400
9	+ 40.6400	2.5400	33	- 55.8800	5.0800
10	+ 38.1000	2.5400	34	- 60.9600	5.0800
11	+ 35.5600	2.5400	35	- 66.0400	5.0800
12	+ 33.0200	2.5400	36	- 76.2000	10.160
13	+ 30.4800	2.5400	37	- 86.3730	10.173
14	+ 27.9400	2.5400	38	- 96.5460	10.173
15	+ 25.4000	5.0800	39	-106.719	10.173
16	+ 20.3200	2.5400	40	-108.2353	1.5163
17	+ 15.2400	5.0800	41	-109.7516	1.5163
18	+ 10.1600	5.0800	42	-111.2679	1.5163
19	+ 5.0800	5.0800	43	-112.7842	1.5163
20	0.0	5.0800	44	-114.3005	1.5163
21	- 5.0800	5.0800	45	-118.1105	3.8100
22	- 10.1600	5.0800	46	-121.9205	3.8100
23	- 15.2400	5.0800			

Figure A1.A

Radial Power Distribution

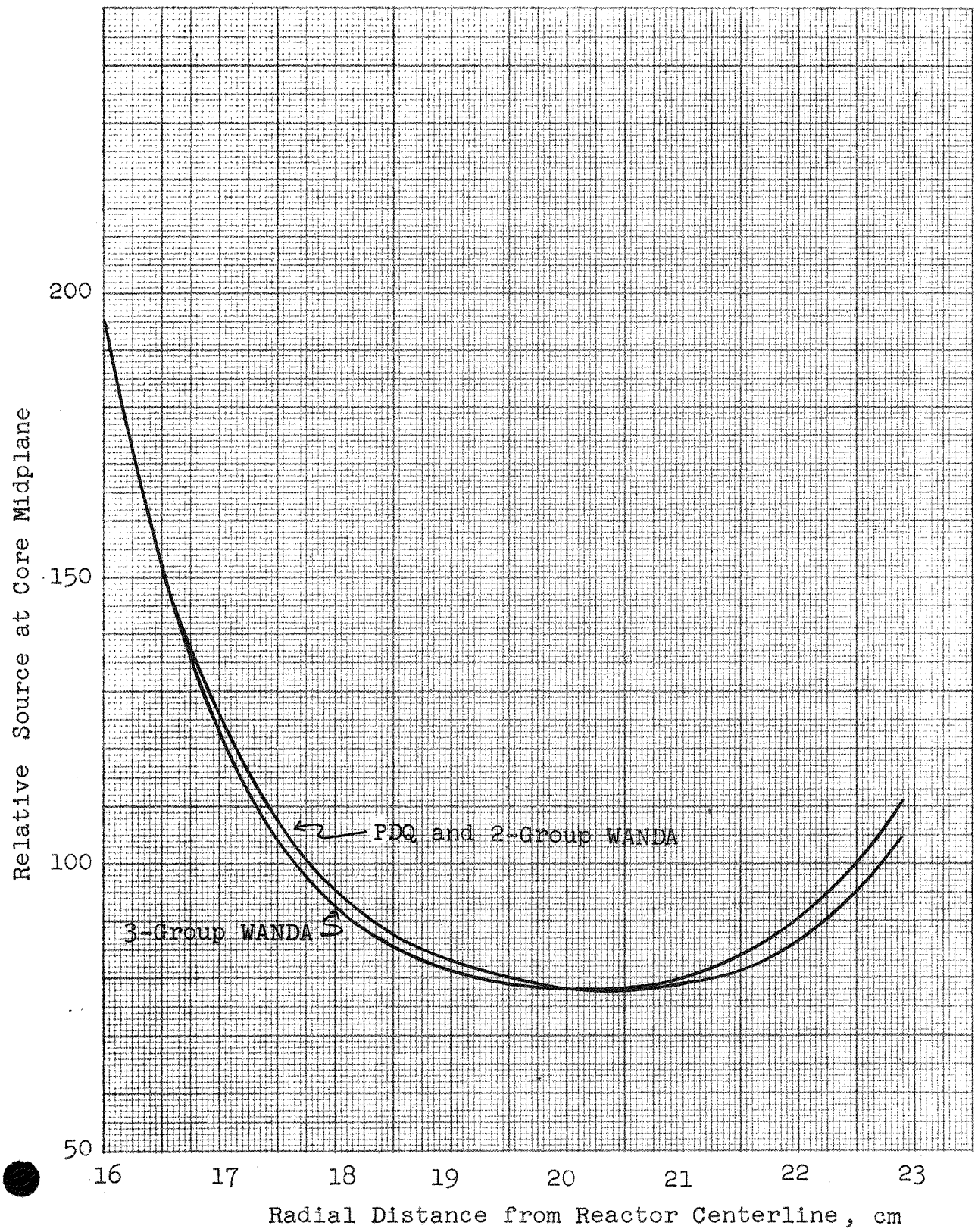

Fig.A1.A

Figure A1.B

Reactor Cross Section in Mesh Units

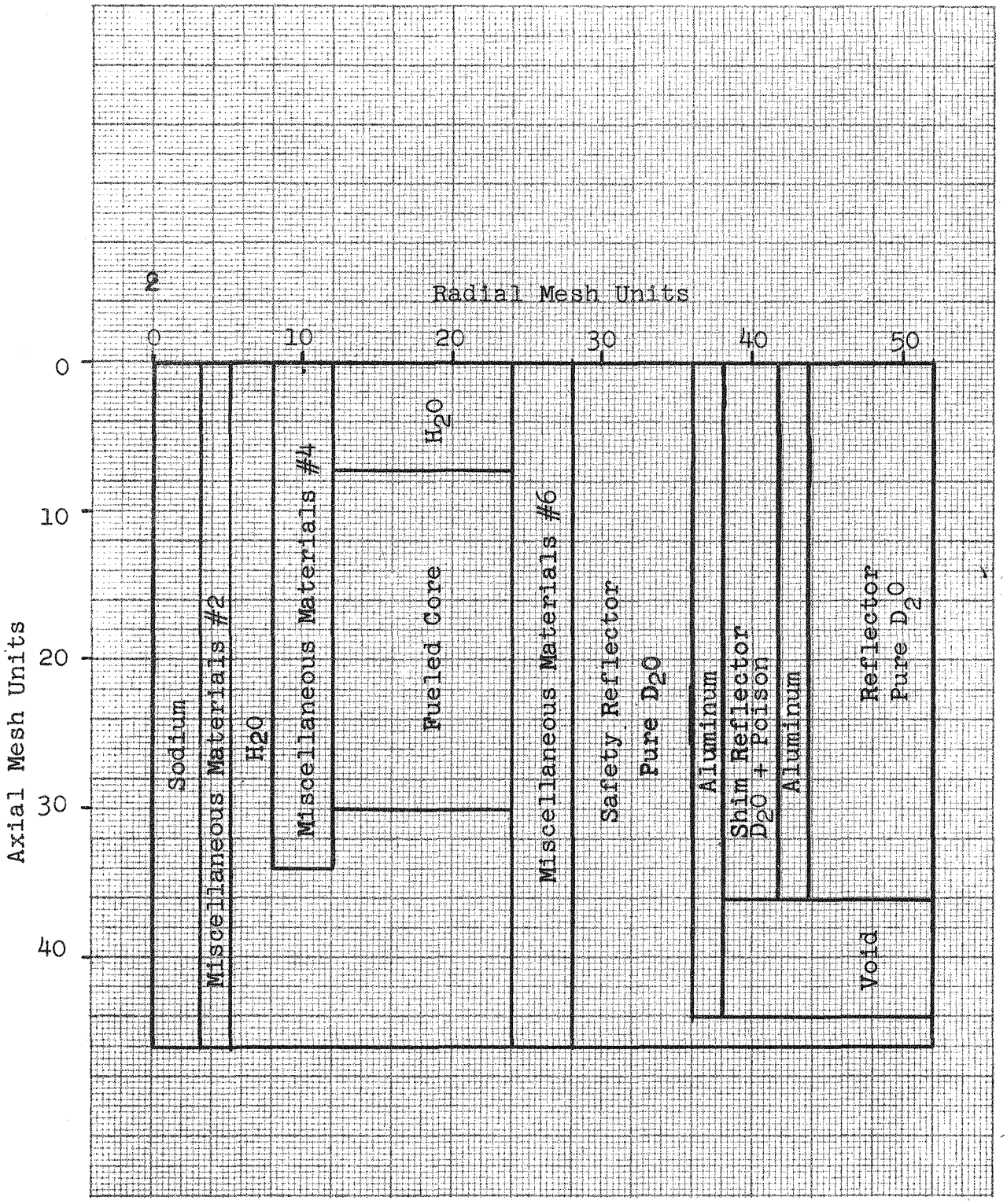

Fig. A1.B

APPENDIX 2.0 METHODS AND PROCEDURES FOR RADIAL POWER FLATTENING

This section describes the method used to determine the fuel distribution which yields a flat power density distribution in the initial AETR core. Detailed geometry and cross sectional data used for the calculations are also included.

A2.1 Method

The AETR core is divided radially into K distinct regions, each of which can have a different homogeneous fuel concentration. The object is to find the distribution of fuel within these K regions which gives identical average power densities in each region. The ideal distribution is then determined from the plot of the K values determined above. The error in this procedure can be reduced by increasing K.

An iterative procedure was selected in which the power distribution is computed using the WANDA diffusion theory code with three energy groups and a poison search in the shim control region for criticality. The power density results from the M^{th} WANDA calculation are used to determine the fuel distribution for the (M+1)st WANDA calculation. In a local region, we can estimate that the power density is proportional to the fuel density and hence, for the (M+1)st iteration,

$$n_k^{M+1} = N_k^M \frac{\bar{p}^M}{p_k^M} \qquad (1)$$

where

n_k = the non-normalized fuel distribution in the k^{th} region

N_k = the normalized fuel distribution in the k^{th} region

$\bar{p}$ = average power density in entire reactor, computed by WANDA

p_k = average power density in the k^{th} fueled region, computed by WANDA

sub k = fueled region index where $1 \leq k \leq K$.

According to the above relationship, when $p_k^M = \bar{p}^M$, the fuel distribution for the (M+1)st iteration is equivalent to the fuel distribution for the M^{th} iteration. Obviously, this is the desired result for a flat power distribution.

The non-normalized fuel distribution, n_k, is related to the normalized distribution by the relation

$$N_k = An_k \tag{2}$$

where A is the normalizing factor. If the average fuel density is $\bar{N}$ in the entire reactor, then

$$\bar{N} = \frac{\sum_{k=1}^{K} N_k V_k}{\sum_{k=1}^{K} V_k} \tag{3}$$

where V_k = volume of the k^{th}region, and the summations are over all fueled regions. Accordingly,

$$\bar{N} = \frac{\sum_{k=1}^{K} An_k V_k}{\sum_{k=1}^{K} V_k} = \frac{A \sum_{k=1}^{K} n_k V_k}{V_T} \tag{4a}$$

or

$$A = \frac{\bar{N} V_T}{\sum_{k=1}^{K} n_k V_k} \tag{4b}$$

where V_T is the total volume of all fueled regions.

Utilizing equations (1), (4b), and (2) the new normalized fuel distribution can be determined. For the first iteration, it is convenient to let

$$N_k^1 = \bar{N}$$

The WANDA output does not include the power densities directly, but rather the power in each region, P_k, and the volume of each region, V_k. The power density is then found by

$$p_k = \frac{P_k}{V_k} . \tag{5}$$

Also, the WANDA program always normalizes its output such that

$$\sum_{k=1}^{K} P_k = 1. \tag{6}$$

The average power density in the reactor is, therefore, always

$$\bar{p} = \frac{\sum_{k=1}^{K} P_k}{\sum_{k=1}^{K} V_k} = \frac{1}{V_T} \quad . \tag{7}$$

Rewriting equation (1), utilizing (5) and (7), we find

$$n_k^{M+1} = \frac{N_k^M V_k}{P_k^M V_T} \tag{8}$$

where N_k^M and P_k^M are the input fuel concentration and output power respectively, for the k^{th} region in the M^{th} WANDA calculation.

A2.2 Geometry and Composition for Calculations

The geometry and composition of the reactor is described in Table A2.a. The regions were arranged such that each of the WANDA constants for all of the fueled core regions could be included on two cards. The regions composed of Misc. "2", Misc."4", and Misc. "6" are composed of mixtures of aluminum, steel and water.

The nuclear constants required by the geometry and composition of Table A2.a are presented in Table A2.b. Table A2.c contains the constants for the fueled regions for the last iteration which produced the flattened power distribution discussed in Section 4.0. Values of D and Σ_{sd} were assumed independent of the fuel concentration.

Table A2.a

Geometry and Composition

Region	Composition	ir (cm)	or (cm)	Region Thickness (cm)	Points	Δr (cm)
1	Na	0	8.890	8.8900	6	1.4817
2	Misc."2"	8.890	11.252	2.3620	4	0.5905
3	H_2O	11.252	14.986	3.7340	6	0.62233
4	Misc."4"	14.986	15.335	0.34866	2	0.17433
5	Misc."4"	15.335	15.683	0.34866	2	0.17433
6	Misc."4"	15.683	16.032	0.34866	2	0.17433
7	Core	16.032	16.605	0.57284	2	0.28642
8	Core	16.605	17.178	0.57284	2	0.28642
9	Core	17.178	17.750	0.57284	2	0.28642
10	Core	17.750	18.323	0.57284	2	0.28642
11	Core	18.323	18.896	0.57284	2	0.28642
12	Core	18.896	19.469	0.57284	2	0.28642
13	Core	19.469	20.042	0.57284	2	0.28642
14	Core	20.042	20.615	0.57284	2	0.28642
15	Core	20.615	21.188	0.57284	2	0.28642
16	Core	21.188	21.760	0.57284	2	0.28642
17	Core	21.760	22.333	0.57284	2	0.28642
18	Core	22.333	22.906	0.57284	2	0.28642
19	Misc."6"	22.906	24.765	1.859	4	0.46475
20	D_2O	24.765	34.925	10.160	20	0.50800
21	Aℓ	34.925	35.401	0.476	2	0.23800
22	D_2O	35.401	43.021	7.620	20	0.38100
23	Aℓ	43.021	43.497	0.476	2	0.23800
24	D_2O	43.497	85.725	42.228	20	2.1114

Table A2.b

Three Group Constants

Constant	Fast Group	Intermediate Group	Thermal Group
	REGION 1 - Sodium at 1000°F		
D, cm	5.7854	4.9920	4.7083
τ, cm^2	6593.0	7493.2	------
Σ_{sd}, cm^{-1}	0.00087750	0.00066620	------
Σ_a, cm^{-1}	------	0.00064153	0.0058173
	REGION 2 - Miscellaneous Material "2" at 170°F		
D, cm	2.2005	2.4312	1.1904
τ, cm^2	1793.1	552.33	------
Σ_{sd}, cm^{-1}	0.0012272	0.0044017	------
Σ_a, cm^{-1}	------	0.0012972	0.017925
	REGION 3 - Water at 170°F		
D, cm	1.4912	0.59720	0.16710
τ, cm^2	29.096	4.9369	------
Σ_{sd}, cm^{-1}	0.051254	0.12099	------
Σ_a, cm^{-1}	------	0.0012655	0.017470
	REGIONS 4, 5, 6 - Miscellaneous Materials "4" at 170°F		
D, cm	1.5258	1.8907	0.71060
τ, cm^2	723.90	233.15	------
Σ_{sd}, cm^{-1}	0.0021077	0.0081094	------
Σ_a, cm^{-1}	------	0.00090430	0.012503
	REGIONS 7 thru 18 - Core with 4×10^{20} at U(235)/cc at 170°F		
D, cm	1.5079	0.91637	0.27366
τ, cm^2	50.195	13.465	------
Σ_{sd}, cm^{-1}	0.030041	0.068056	------
Σ_a, cm^{-1}	0.0	0.022083	0.23306
$\nu\Sigma_f$, cm^{-1}	0.0	0.034440	0.45320
	REGION 19 - Miscellaneous Materials "6" at 170°F		
D, cm	1.5284	2.5272	1.1429
τ, cm^2	1079.8	752.09	------
Σ_{sd}, cm^{-1}	0.0014154	0.0033602	------
Σ_a, cm^{-1}	0.0	0.00086223	0.011926

Table A2.b Continued

Constant	Fast Group	Intermediate Group	Thermal Group
	REGIONS 20, 22, 24 - Heavy Water at 170°F		
D, cm	1.3539	1.1691	0.88499
τ, cm^2	50.419	69.452	------
Σ_{sd}, cm^{-1}	0.026850	0.016831	------
Σ_a, cm^{-1}	0.0	0.0000021400	0.0000343
	REGIONS 21, 23 - Aluminum at 170°F		
D, cm	1.5330	4.1694	3.9640
τ, cm^2	1101.0	7326.0	------
Σ_{sd}, cm^{-1}	0.0013920	0.0005691	------
Σ_a, cm^{-1}	0.0	0.00081300	0.011250

Table A2.c

WANDA Constants for Flat Power Distribution

Region	Σ_{a2} (cm^{-1})	$\nu\Sigma_{f2}$ (cm^{-1})	Σ_{a3} (cm^{-1})	$\nu\Sigma_{f3}$ (cm^{-1})
7	.010310	.015133	.11078	.19914
8	.012753	.019140	.12122	.25187
9	.015738	.024036	.16717	.31629
10	.019194	.029703	.20306	.39086
11	.022849	.035697	.24102	.46974
12	.026182	.041163	.27564	.54166
13	.028510	.044980	.29982	.59190
14	.029257	.046206	.30758	.60804
15	.028244	.044545	.29706	.58617
16	.025776	.040498	.27143	.53292
17	.022479	.035091	.23718	.46177
18	.018992	.029372	.20097	.38651

APPENDIX 3.0 BURNOUT CALCULATIONS USING CANDLE-2

The CANDLE program is a one-dimensional few-group depletion code designed for the study of slab, cylindrical, and spherical reactors. Such a code is of use in estimating reactor lifetimes for given fuel loadings and in determining the time dependence of fuel distributions and flux shapes.

Criticality is maintained during lifetime either by the use of a variable poison cross section or a variable transverse buckling, the former being used in the shim control region in the cylindrical AETR geometry.

Group constants are computed from effective one-velocity microscopic cross sections. The fast group microscopic cross sections are stored on a library tape, whereas the thermal microscopic cross sections are supplied as input for each problem. Other input data required are the initial isotopic number densities, thermal self-shielding factors and group-dependent resonance escape probabilities for U(238). New isotopic number densities are then automatically recomputed at each time step.

CANDLE-2 is the second version of the program and contains certain improvements over the initial version. Detailed descriptions of the codes are available.(10,11)

A3.1 Time Steps

The time steps given in Table A3.a were selected to give approximately equal changes in the multiplication factor for each time increment. The increments at the beginning of the cycle therefore, are shorter in order to follow xenon buildup. The numerical inaccuracies introduced by the finite time step increments are expected to result in very little error.

A3.2 Geometry

The radial geometry of the problems considered is identical to that given in Table A2.a.

A3.3 Region Compositions

The atom number densities for each of the components in each of the reactor regions are given in Table A3.b. The region identification number is that actually used in the CANDLE calculations. Regions 4, 5, and 6 all have the same composition and are designated separately to simplify the mechanics of the problem input and the separation has no physical significance. Regions 7 through 18 are consecutive annular fueled regions, each of which may contain different initial fuel concentrations.

A3.4 Microscopic Cross Sections

Four neutron energy groups were used, the first includes neutron energies above 0.821 Mev; the second covers the range from 5.53 Kev to 0.821 Mev; the third covers the range from 0.625 ev to 5.53 Kev; and the fourth, or thermal group, covers energies below 0.625 ev.

With the addition of three elements not included, the CANDLE-2 cross section library, listed in the manual[11] were used for the calculation. The elements added are deuterium, sodium, and aluminum and their cross sections are listed in Table A3.c which were determined using the MUFT-4[12] program for the IBM-704.

The microscopic thermal cross sections used in the CANDLE calculations are listed in Table A3.c and were selected to produce macroscopic cross sections consistent with those of the previous studies. Some of the elements listed are fission products which are not present in the reactor at startup with a new core.

Cross sections for several of the non - 1/v absorbers were calculated as a function of temperature using the equation

$$\bar{\sigma}(T) = \frac{(\pi)^{1/2}}{2} \left(\frac{T_o}{T}\right)^{1/2} g(T)\, \sigma_o \qquad (1)$$

where $\bar{\sigma}(T)$ is the effective cross section at temperature T,

$T_o = 293.6^{\circ}K$,

T = temperature of medium,

g(T) = non-1/v factor, and

σ_o = cross section at 2200 m/sec (T_o).

Westcott has published[13] values for g(T) over temperature ranges of interest and these were used in the calculations. The results of the calculations are included here for convenient reference as a series of curves showing $\bar{\sigma}(T)$ as a function of T in Figures A3.A through A3.N. The isotopes included are Xe(135), Sm(149), U(235), U(236), U(238), Pu(239), Pu(240), and Pu(241). Two $\bar{\sigma}_a$ curves are shown for Xe(135) using spin parameters of 3/8 and 5/8 respectively. The latter seems to give satisfactory agreement with experiment. It should be recognized that the calculation assumes a non-hardened Maxwell neutron flux, which is consistent with the assumptions made in calculating the other thermal cross sections given in Table A3.d.

A3.5 Summary of Initial Macroscopic Cross Sections

The macroscopic cross sections are calculated from the microscopic data and atom densities given previously by the CANDLE program. Tables A3.e and A3.f summarize the energy and region dependent macroscopic cross sections at the start of burnup for the two cases computed.

A3.6 Miscellaneous Input Data for CANDLE-2

Values for the iodine yield from fission of U(235), U(238), Pu(239), and Pu(241) must be supplied as input. The respective values used are 0.061, 0.055, 0.058, and 0.055.[14]

The epithermal contribution of the absorber used in the shim control region to maintain criticality is the same as that for B(10) given in the CANDLE-2 cross section library. In terms of the thermal absorption cross section, these are

$$\Sigma_{a1} = 0.0001374\ \bar{\Sigma}_{ath},$$

$$\Sigma_{a2} = 0.0007466\ \bar{\Sigma}_{ath}, \text{ and}$$

$$\Sigma_{a3} = 0.05263\ \bar{\Sigma}_{ath}.$$

The low cross section fission products, excluding U(236), contributes 65 barns per atom of U(235) fissioned.

The reactor power is maintained constant at 170 Mw during each time increment.

The transverse buckling factor to account for axial leakage of neutrons is 0.0005225 cm^{-2} and is consistent with previous studies.

The thermal self-shielding factors are assumed to be unity and again the presence of U(238) in the highly enriched fuel is ignored. This latter assumption causes a slight overestimate of the reactivity lifetime and eliminates the presence of Pu(239), Pu(240), and Pu(241) in the reactor during the burnup.

Table A3.a

Time-Step Data for CANDLE Burnout Calculations

Time-Step	Time Elapsed Since Startup hr.	Time Step Interval hr.
0	0	-
1	3.5	3.5
2	10	6.5
3	20	10
4	60	40
5	120	60
6	180	60
7	240	60
8	300	60
9	360	60
10	420	60
11	480	60
12	540	60
13	600	60

Table A3.b

Initial Atomic Densities

Region Identification	Materials	Temperature °F	Atomic Density, 10^{24} atoms/cc
1	Sodium	1000	0.021607
2	Aluminum	170	0.032049
	Hydrogen		0.0060662
	Oxygen		0.0030331
	Iron		0.0036181
	Nickel		0.00050251
	Chromium		0.00090452
3	Hydrogen	170	0.065234
	Oxygen		0.032617
4,5,6	Aluminum	170	0.048124
	Hydrogen		0.013144
	Oxygen		0.006572

Table A3.b Continued

Region Identification	Materials	Temperature °F	Atomic Density, 10^{24} atoms/cc
7 through 18	Aluminum	170	0.024502
	Hydrogen		0.038714
	Oxygen		0.019357
	U(235)		0.0004(average)*
19	Aluminum	170	0.053723
	Hydrogen		0.0070864
	Oxygen		0.0035432
20,22,24	Deuterium	170	0.064818
	Oxygen		0.032409
	Hydrogen		0.00010371
21,23	Aluminum	170	0.06027

*See Figures 4.A and 5.N and Table 4.a for Distribution

Table A3.c

Additions to the CANDLE-2 Library Tape

Element and Group	Cross Section, barns σ_{tr}	σ_r	σ_a
Sodium			
Group 1	2.8850	1.0620	0.000197
Group 2	4.0688	0.31140	0.010330
Group 3	3.1805	0.14699	0.023262
Deuterium			
Group 1	1.7987	1.0968	0.0000
Group 2	2.3108	0.44932	0.0000
Group 3	2.2701	0.27066	0.0000
Aluminum			
Group 1	2.0350	0.28047	0.0033110
Group 2	1.8986	0.036054	0.0048445
Group 3	1.3839	0.0013211	0.016288

Table A3.d

Thermal Microscopic Cross Sections

Material	Temperature °F	Cross Section, barns			
		σ_{tr}	σ_a	σ_f	σ_f
Hydrogen	170	30.579	0.2678	-	-
Oxygen	170	0.00000	0.00016	-	-
Iron	170	9.9099	2.0534	-	-
Nickel	170	9.9145	2.6942	-	-
Aluminum	170	1.3952	0.18666	-	-
Chromium	170	9.9145	1.6974	-	-
Deuterium	170	5.8169	0.000373	-	-
Sodium	1000	3.2766	0.26923	-	-
U(235)	170	545.3	545.3	1133	460.57
U(236)	170	5.70	5.70	-	-
U(238)	170	2.2100	2.2100	0.0000	0.0000
Pu(239)	170	943.00	943.00	1922.0	662.8
Pu(240)	170	249.5	249.5	-	-
Pu(241)	170	1218.5	1218.5	2726.0	890.8
Sm(149)	170	60,330	60,330	-	-
Xe(135)	170	2,685,000	2,685,000	-	-
Fission Products	170	65	65	-	-
B(10)	170	3100.30	3100.30	-	-

Table A3.e

Initial Four Group Constants for CANDLE Calculations

Region	Group	D,cm	Σ_a,cm^{-1}	Σ_{sd},cm^{-1}	$\nu\Sigma_f$,cm^{-1}
1	1	5.3468	0.000004	0.022950	0
	2	3.7911	0.0002232	0.0067330	0
	3	4.8492	0.0005027	0.0029789	0
	4	4.7041	0.0058180	-	0
2	1	3.6447	0.000235	0.019696	0
	2	3.0160	0.000157	0.015169	0
	3	2.2898	0.001191	0.013376	0
	4	1.1904	0.017925	-	0
3	1	2.3176	0.00138	0.10236	0
	2	1.1215	0.00001	0.14725	0
	3	0.60353	0.00093	0.14815	0
	4	0.16710	0.017470	-	0
4,5,6	1	2.6265	0.000438	0.034121	0
	2	2.2038	0.000236	0.031404	0
	3	1.8739	0.000971	0.029600	0
	4	0.71062	0.012503	-	0
*7 through 18 (flat fuel distribution)	1	2.4297	0.001631	0.067675	0.0014580
	2	1.4743	0.001204	0.088271	0.0018966
	3	0.89913	0.014597	0.082320	0.024985
	4	0.23210	0.23306	-	0.45320
19	1	2.6677	0.000328	0.026187	0
	2	2.4823	0.000262	0.017933	0
	3	2.4812	0.000975	0.015814	0
	4	1.1429	0.011926	-	0
20,22,24	1	2.1075	0.001378	0.078927	0
	2	1.1995	0.000000	0.032235	0
	3	1.1667	0.000002	0.019235	0
	4	0.87670	0.00003443	-	0
21,23	1	2.6936	0.000211	0.017688	0
	2	2.8562	0.0002924	0.0033016	0
	3	3.8034	0.00098878	0.00082133	0
	4	3.3542	0.011384	-	0

*See Table A3.f for Distributed Fuel Loading

Table A3.f

Initial Four Group CANDLE Constants for
Fueled Core with Fuel Distributed for Flat Power Density

Region	Group	D,cm	Σ_a,cm^{-1}	Σ_{sd},cm^{-1}	$\nu\Sigma_f$,cm
7	1	2.4495	0.001224	0.067642	0.00064066
	2	1.4860	0.000600	0.088271	0.00083335
	3	0.91160	0.006946	0.085390	0.010979
	4	0.25370	0.11078	-	0.19914
8	1	2.4453	0.001308	0.067649	0.00081031
	2	1.4836	0.000725	0.088271	0.0010540
	3	0.90898	0.008533	0.084753	0.013886
	4	0.24890	0.13616	-	0.25187
9	1	2.4403	0.001412	0.067657	0.0010176
	2	1.4806	0.000878	0.088271	0.0013236
	3	0.90581	0.010474	0.083974	0.017437
	4	0.24327	0.16717	-	0.31629
10	1	2.4345	0.001531	0.067667	0.0012575
	2	1.4771	0.001055	0.088271	0.0016357
	3	0.90216	0.012720	0.083073	0.021549
	4	0.23706	0.20306	-	0.39086
11	1	2.4284	0.001658	0.067677	0.0015113
	2	1.4735	0.001244	0.088271	0.0019658
	3	0.89833	0.014095	0.082120	0.025897
	4	0.23082	0.24102	-	0.46974
12	1	2.4229	0.001773	0.067687	0.0017426
	2	1.4702	0.001415	0.088271	0.0022668
	3	0.89486	0.017261	0.081251	0.029863
	4	0.22542	0.27564	-	0.54166
13	1	2.4191	0.001854	0.067693	0.0019043
	2	1.4679	0.001634	0.088271	0.0024770
	3	0.89246	0.018774	0.080644	0.032632
	4	0.22179	0.29982	-	0.59190
14	1	2.4178	0.001880	0.067695	0.0019562
	2	1.4672	0.001573	0.088271	0.0025495
	3	0.89169	0.019260	0.080449	0.033522
	4	0.22065	0.30758	-	0.60804

Table A3.f Continued

Region	Group	D,cm	Σ_a,cm^{-1}	Σ_{sd},cm^{-1}	$\nu\Sigma_f$,cm
15	1	2.4195	0.001845	0.067692	0.0018858
	2	1.4682	0.001521	0.088271	0.0024530
	3	0.89274	0.018601	0.080714	0.032316
	4	0.22220	0.29706	-	0.58617
16	1	2.4236	0.001759	0.067686	0.0017145
	2	1.4706	0.001394	0.088271	0.0022302
	3	0.89528	0.016998	0.081357	0.029380
	4	0.22606	0.27143	-	0.53292
17	1	2.4291	0.001645	0.067676	0.0014856
	2	1.4739	0.001225	0.088271	0.0019324
	3	0.89871	0.014855	0.082217	0.025458
	4	0.23144	0.23719	-	0.46177
18	1	2.4349	0.001525	0.067666	0.0012435
	2	1.4773	0.001046	0.088271	0.0016175
	3	0.90237	0.012589	0.083126	0.021309
	4	0.23741	0.20096	-	0.38651

Figure A3.A

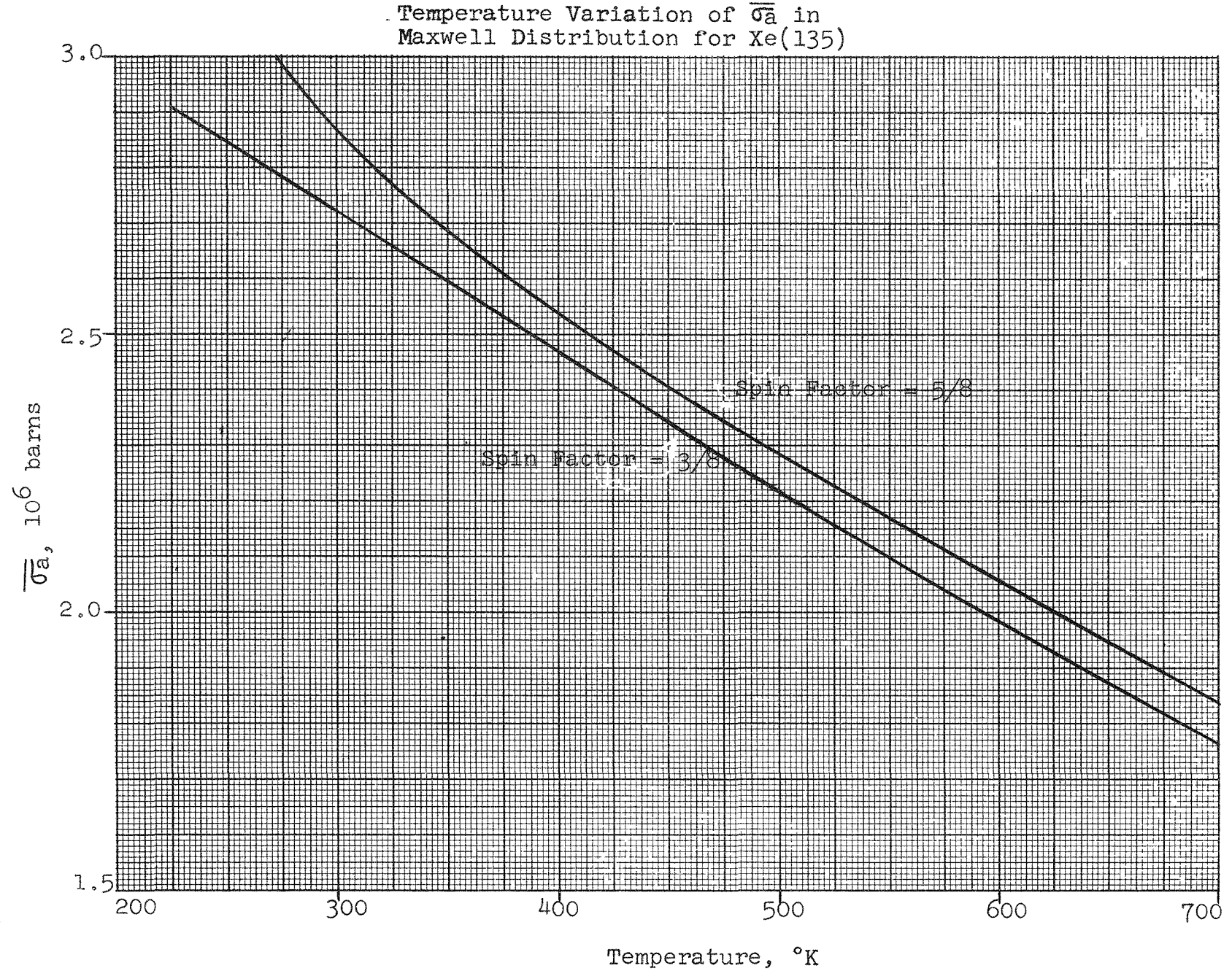

Fig. A3.A

Figure A3.B

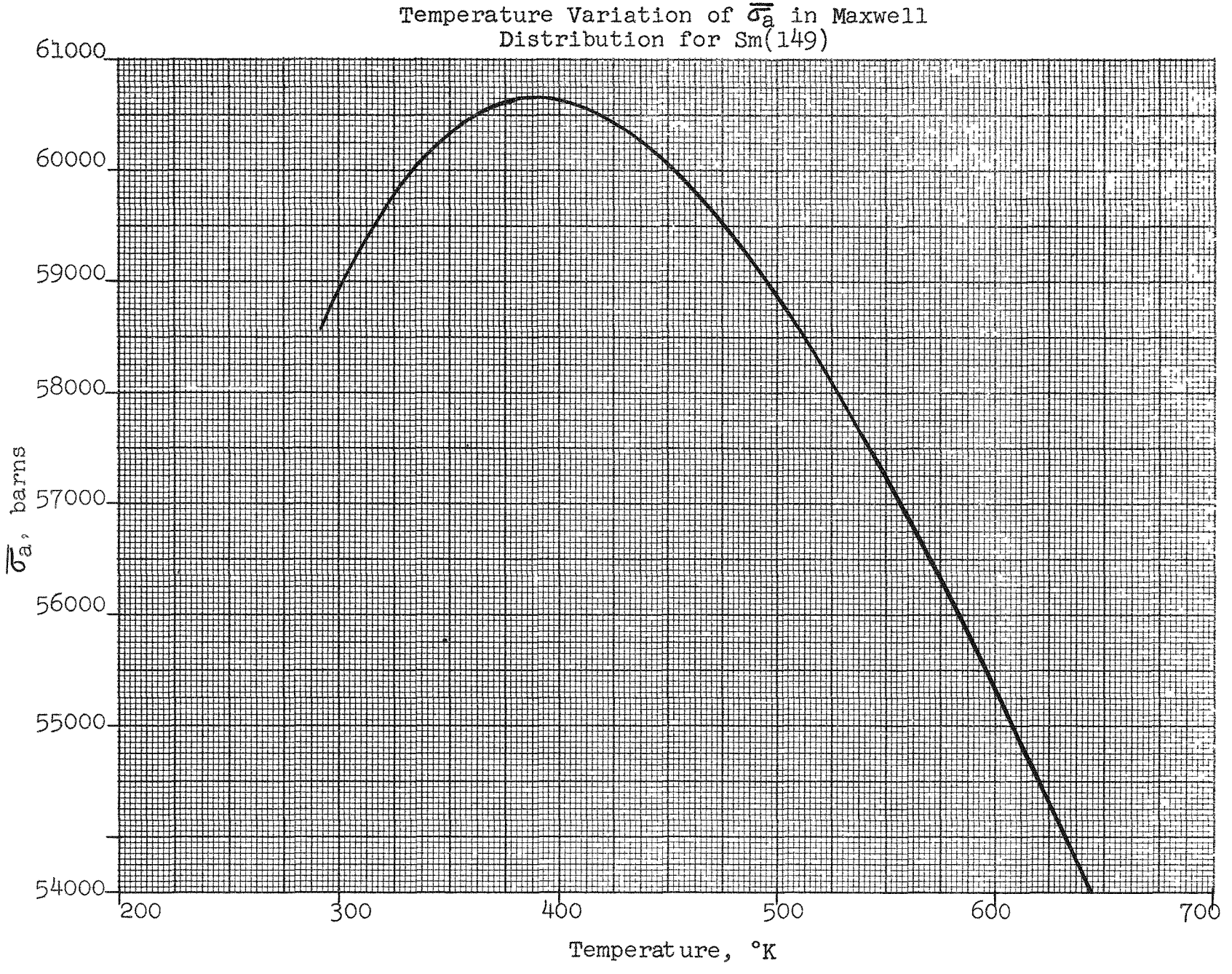

Fig. A3.B

Figure A3.C

Temperature Variation of $\overline{\sigma_a}$ in Maxwell Distribution for U(235)

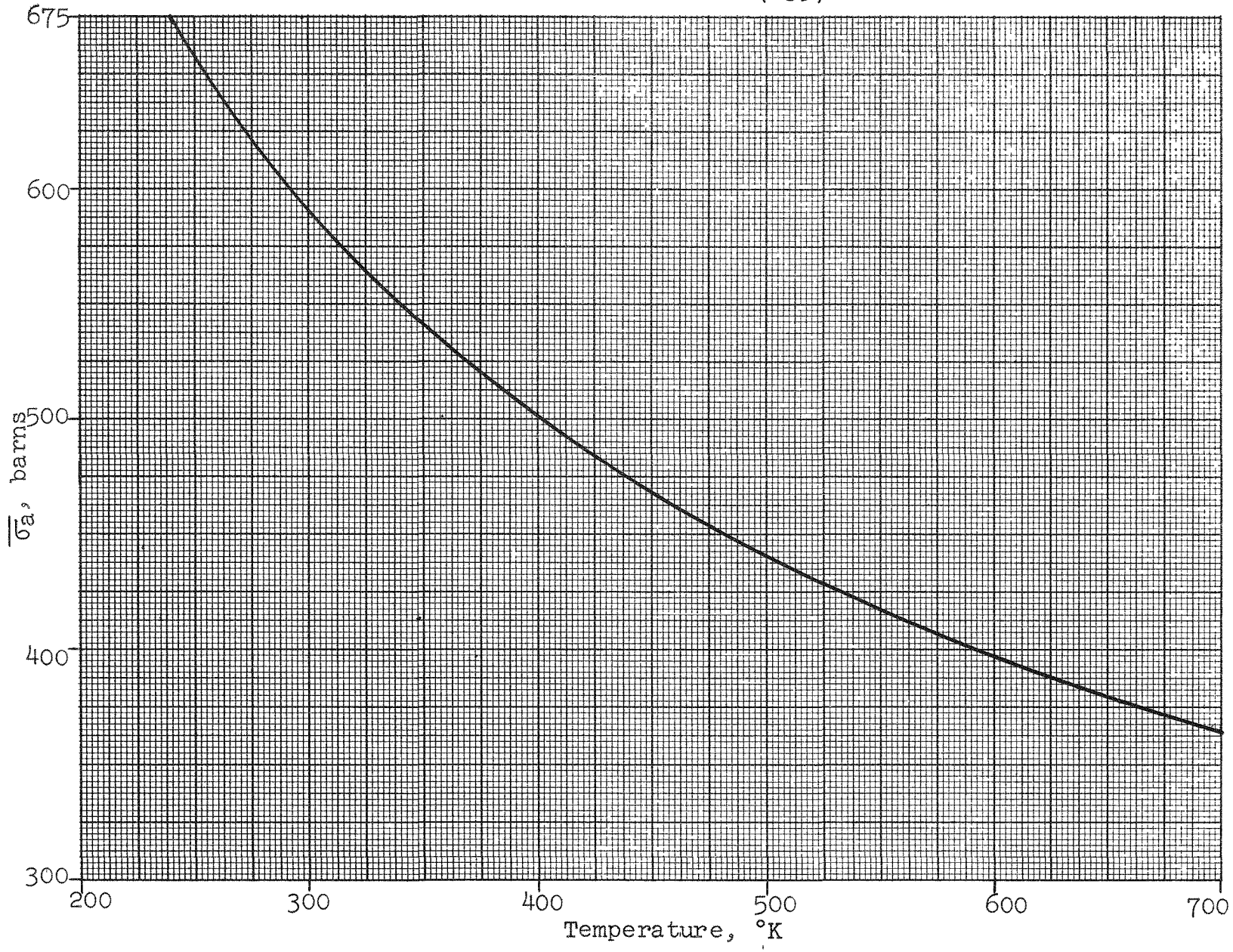

Fig. A3.C

Figure A3.D

Temperature Variation of $\overline{\sigma_f}$ in Maxwell Distribution for U(235)

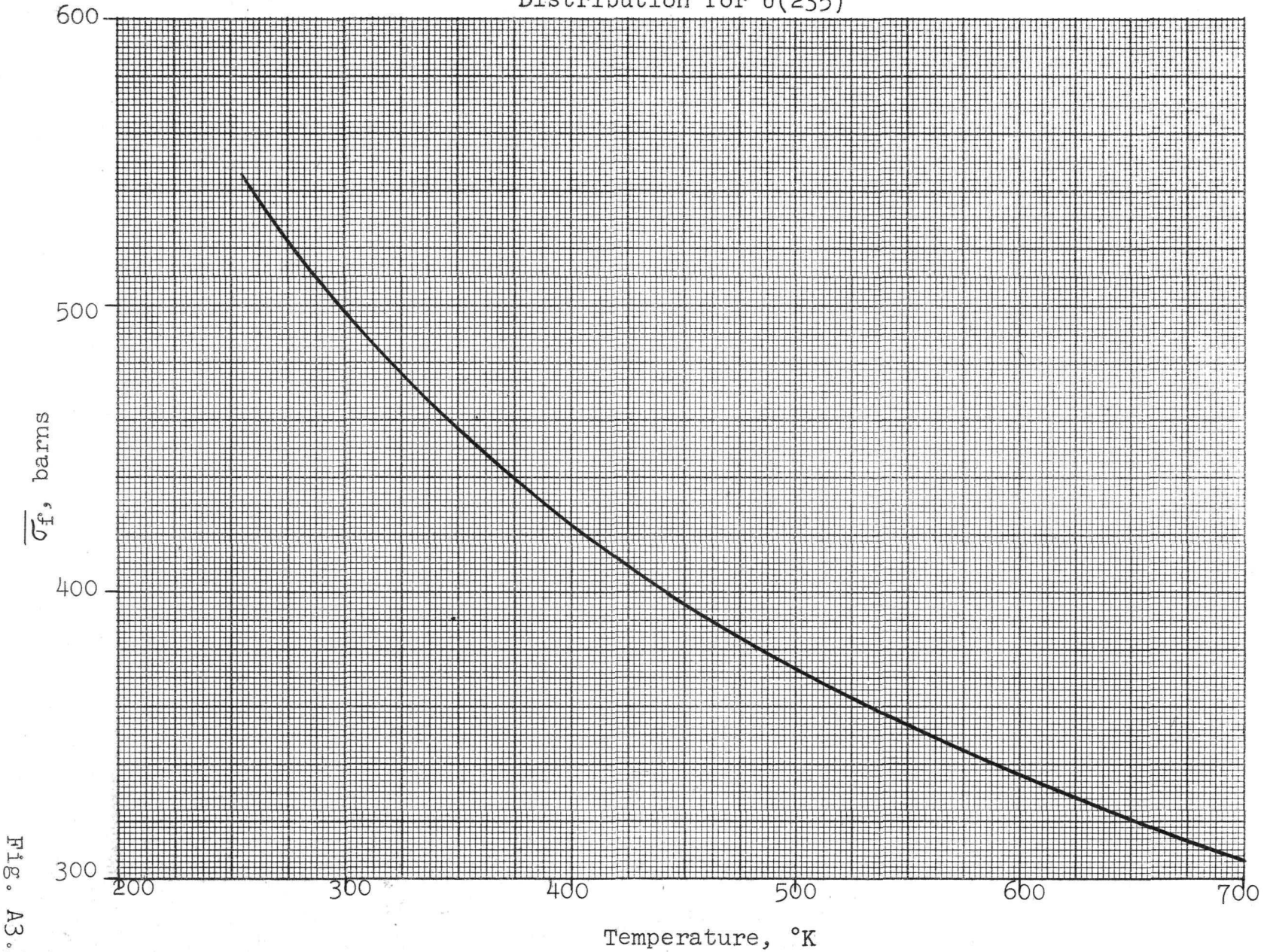

Fig. A3.D

Figure A3.E

Temperature Variation of $\overline{\nu\sigma_f}$ in Maxwell Distribution for U(235)

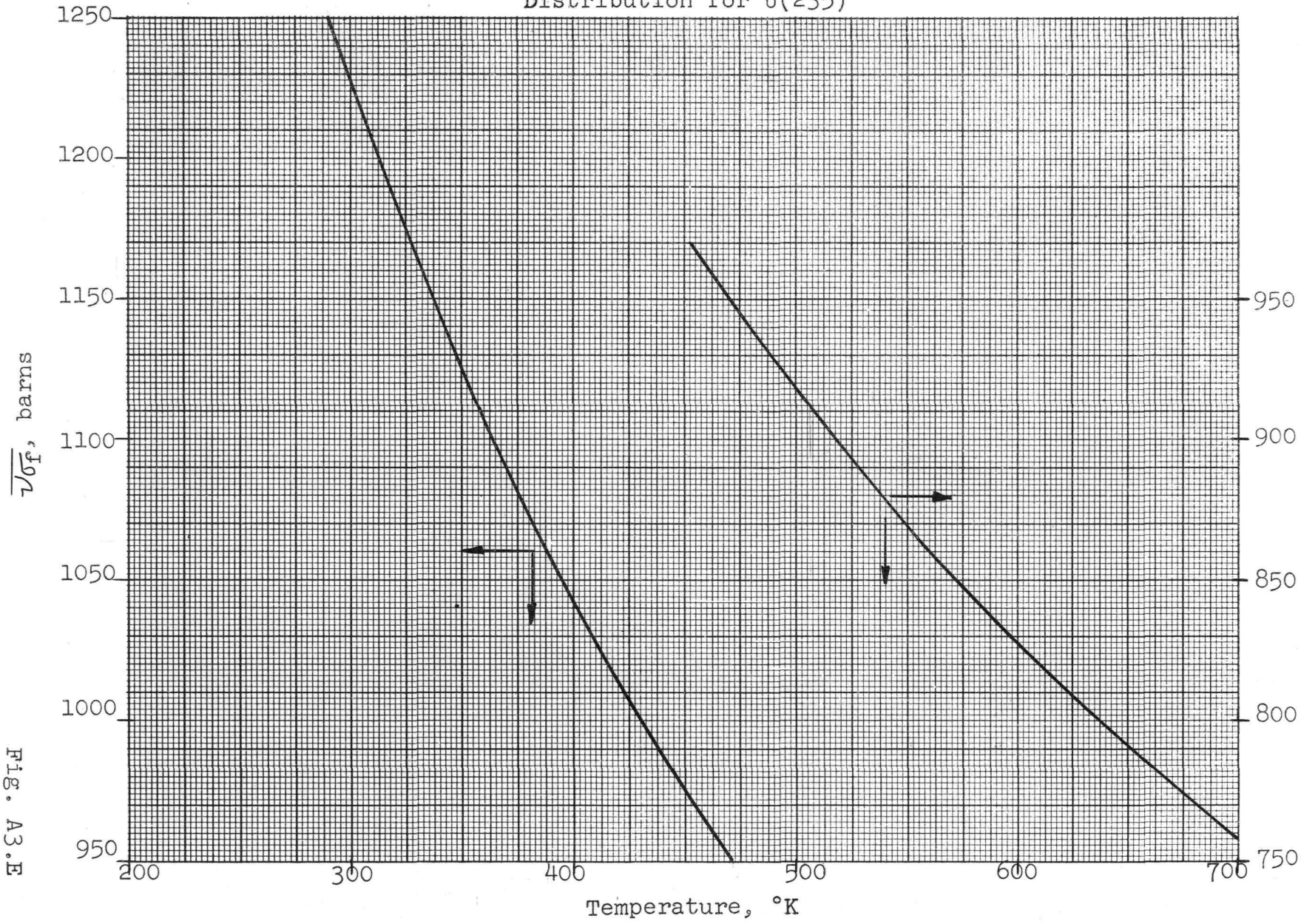

Fig. A3.E

Figure A3.F

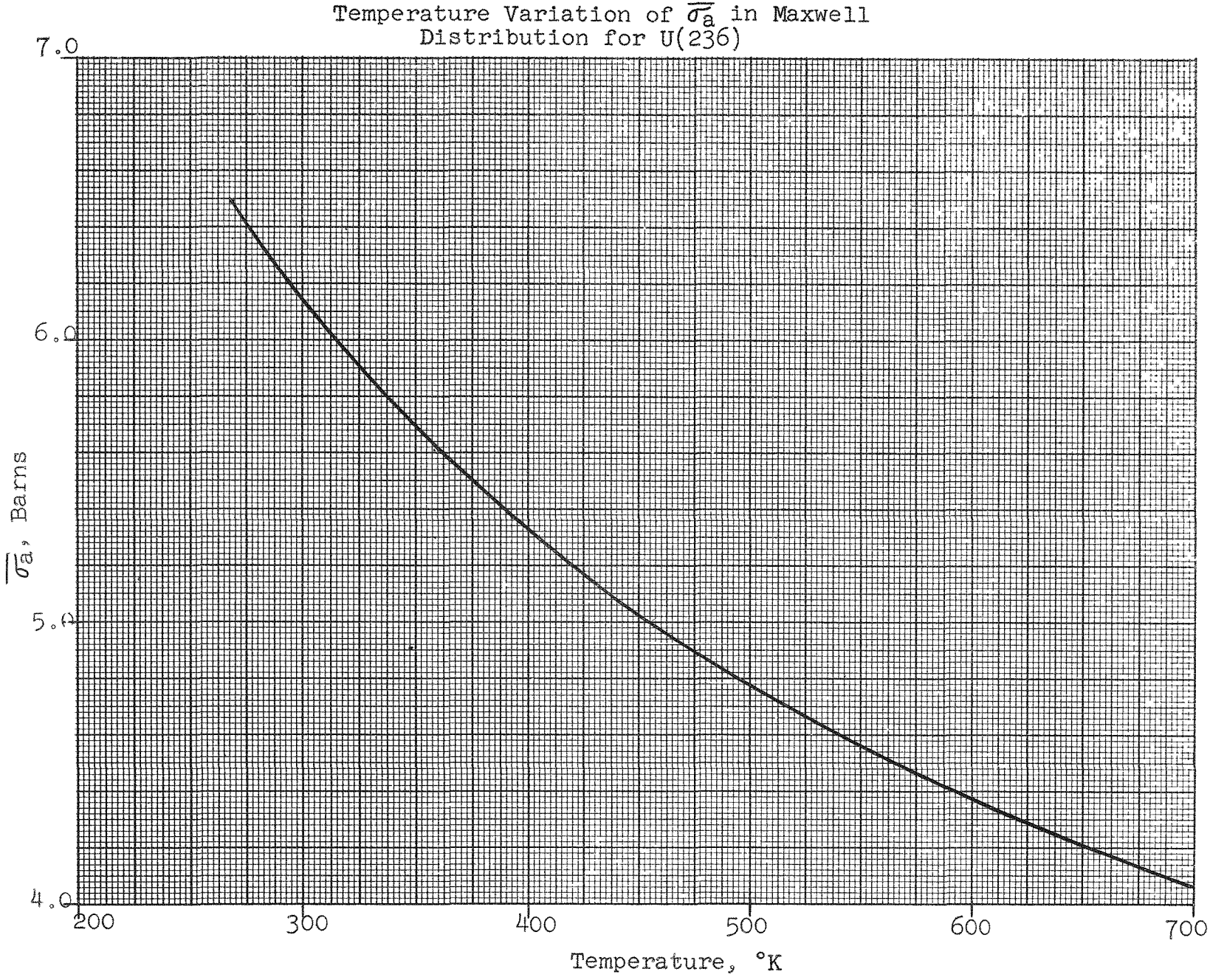

Fig.A3.F

Figure A3.G

Temperature Variation of $\overline{\sigma_a}$ in Maxwell Distribution for U(238)

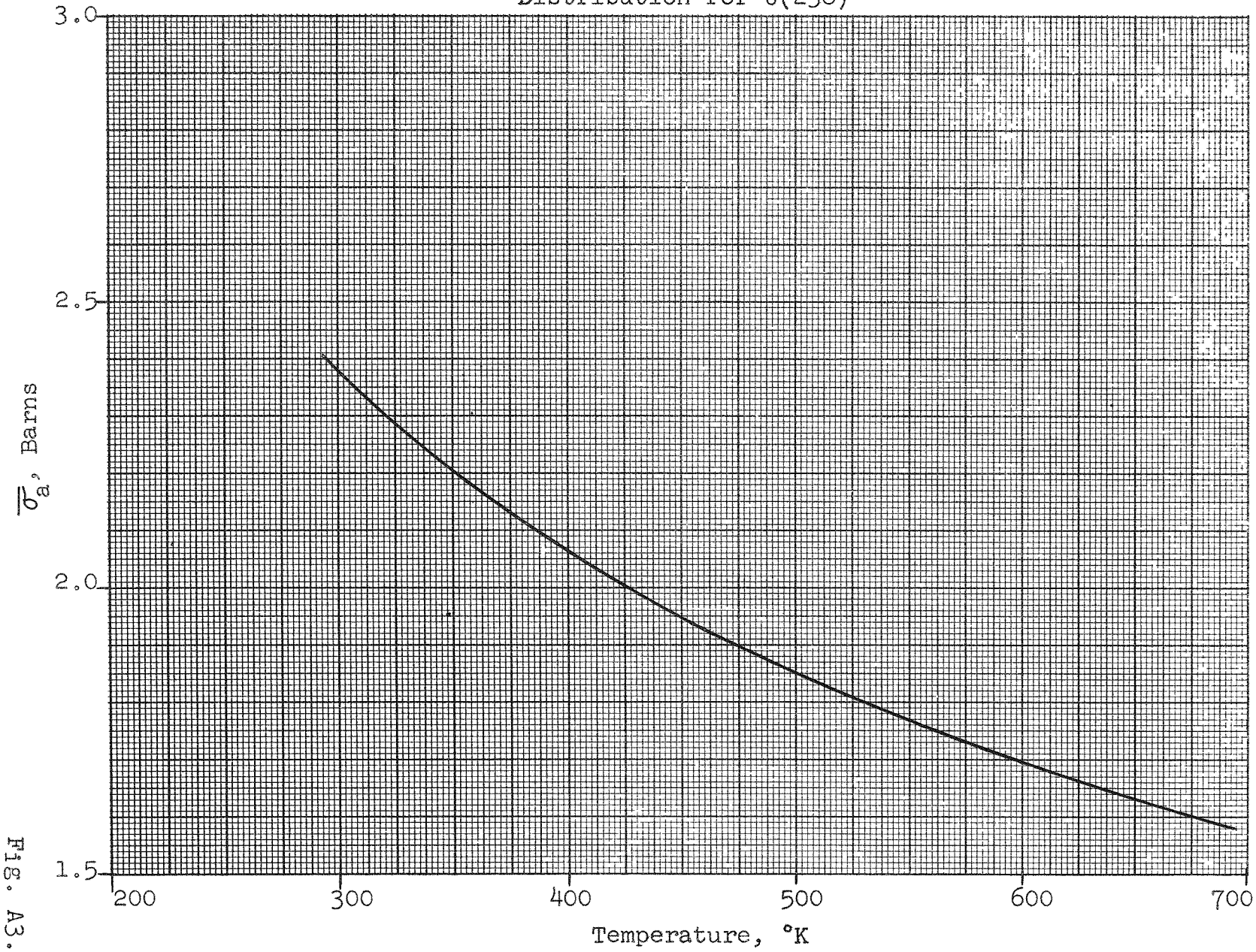

Fig. A3.G

Figure A3.H

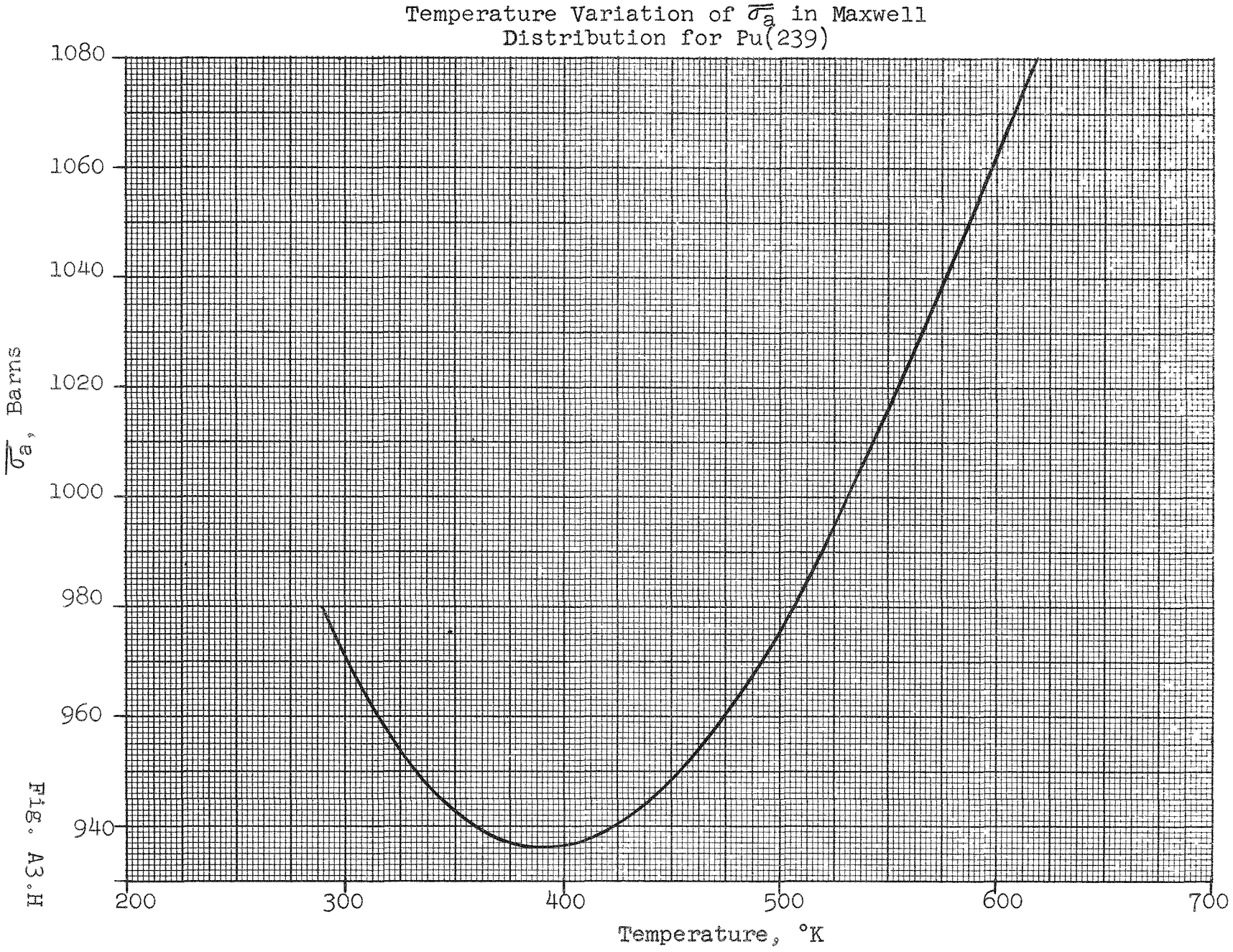

Fig. A3.H

Figure A3.I

Temperature Variation of $\overline{\sigma_f}$ in Maxwell Distribution for Pu(239)

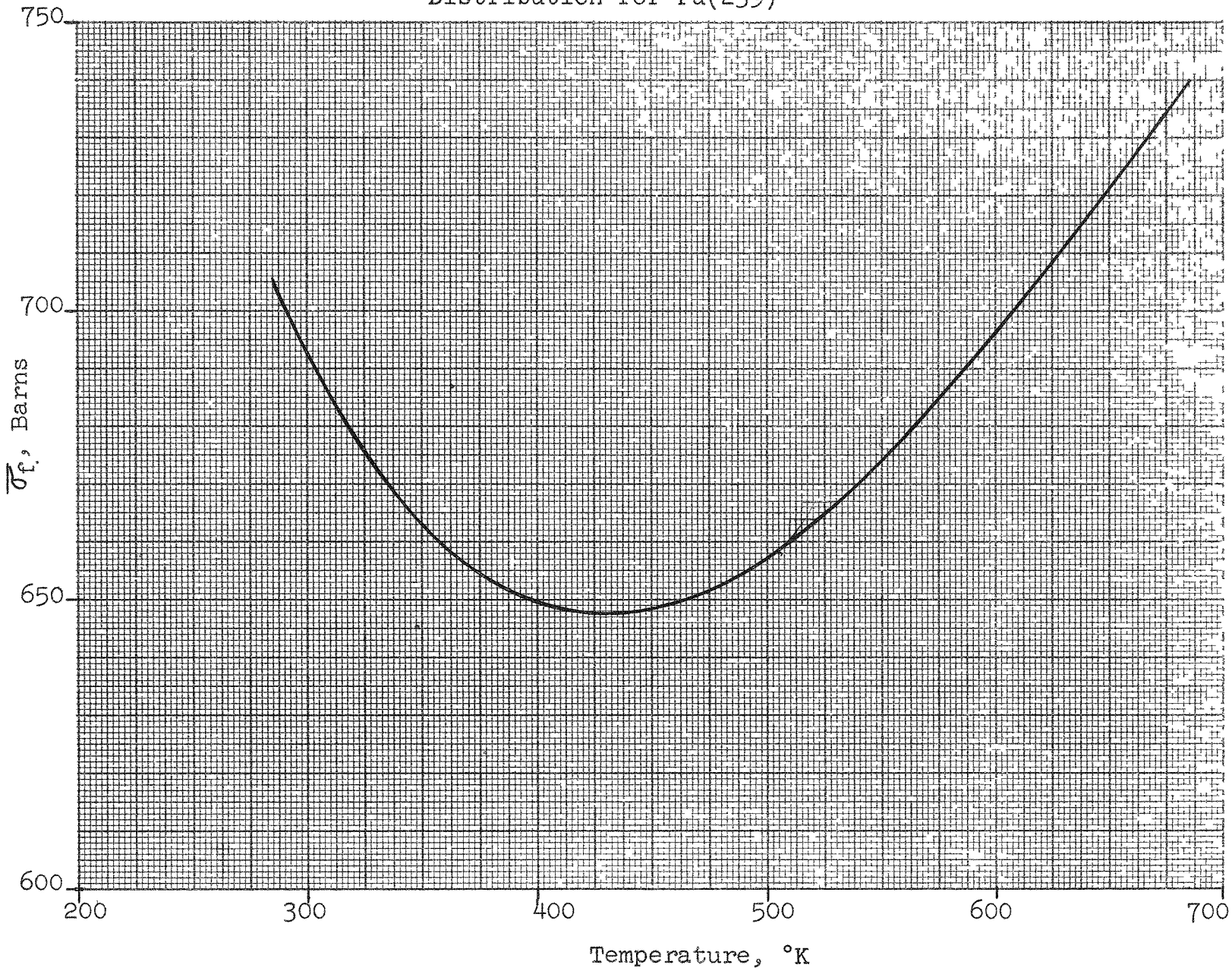

Fig. A3.I

Figure A3.J

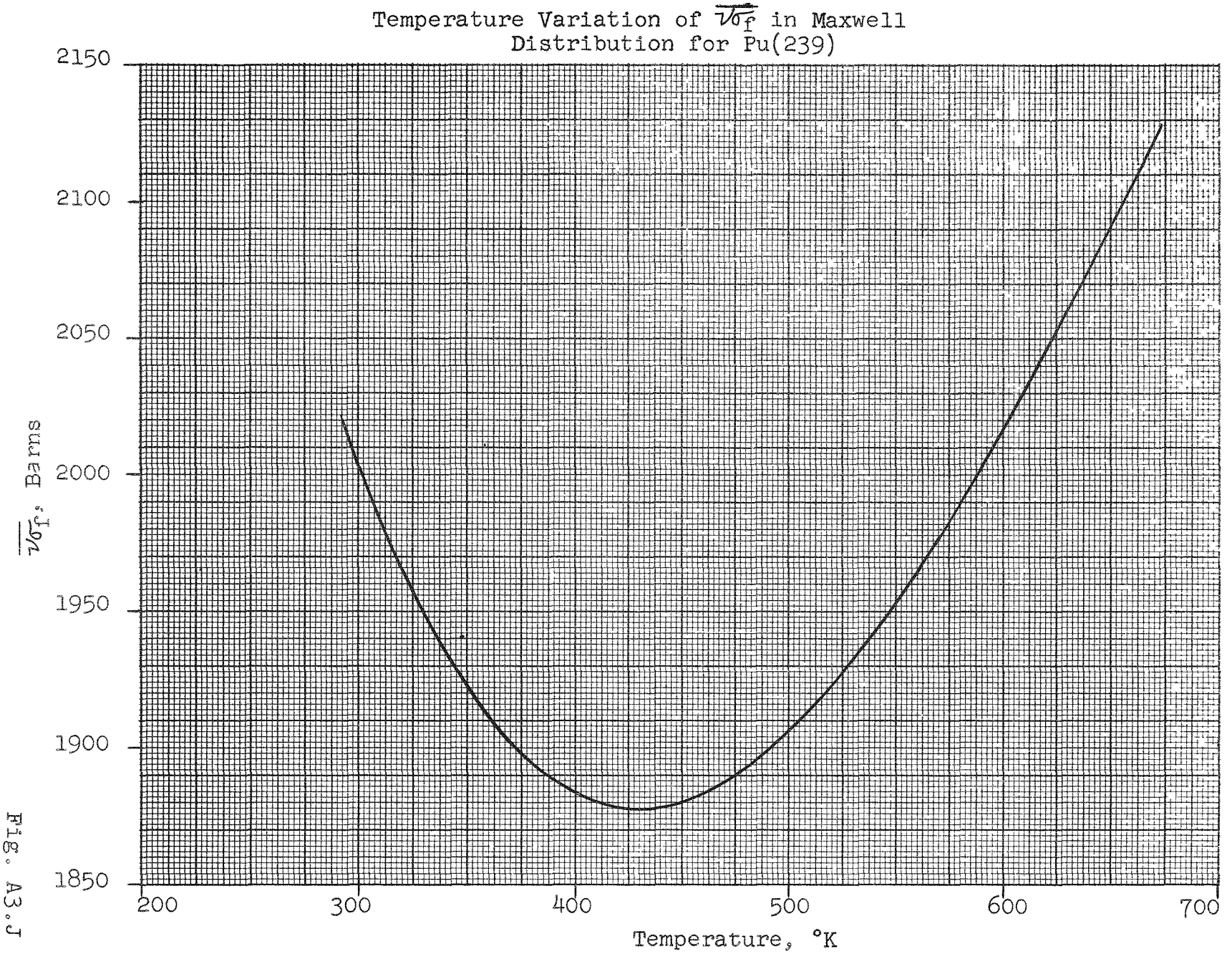

Fig. A3.J

Figure A3.K

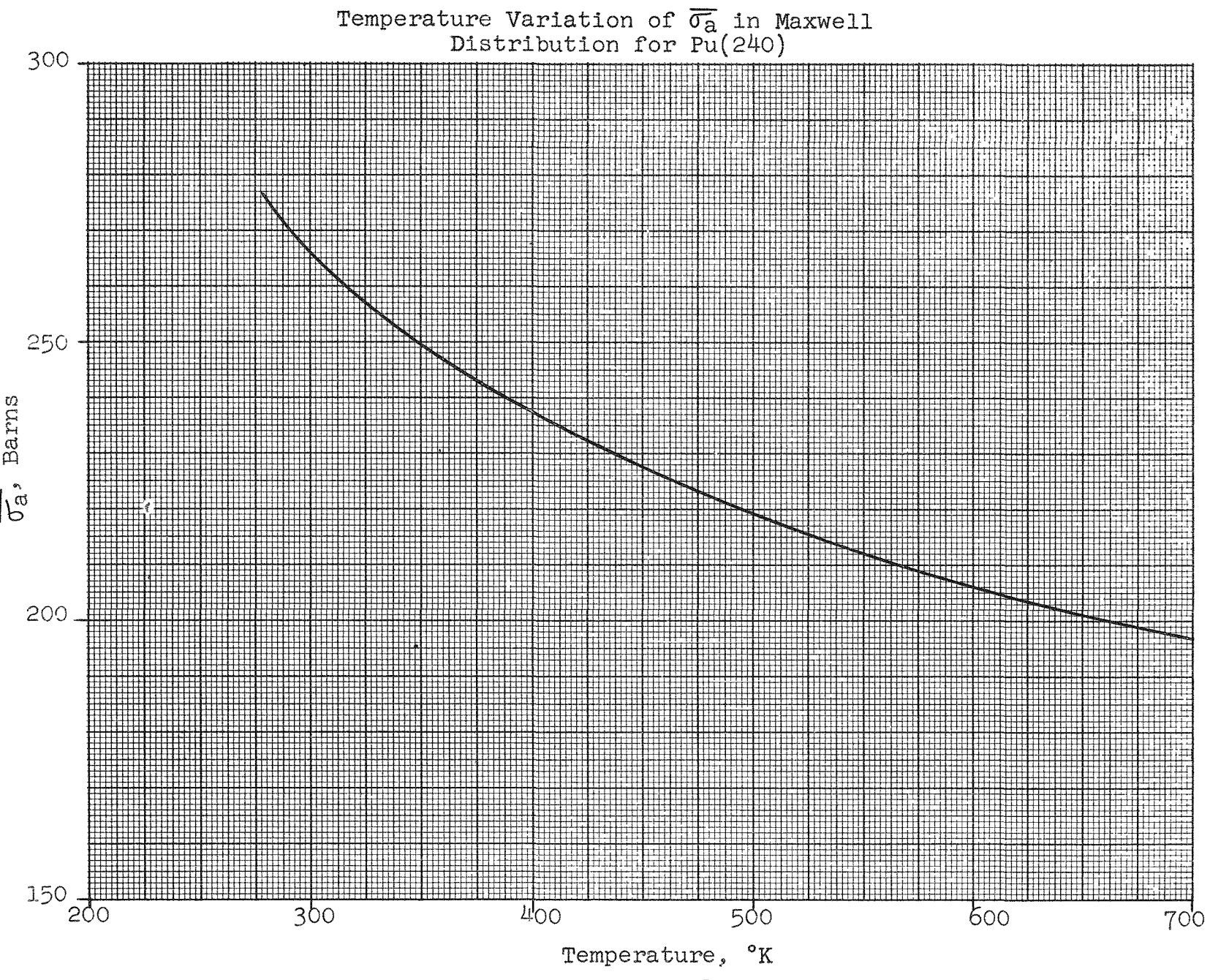

Fig. A3.K

Figure A3.L

Temperature Variation of $\overline{\sigma_a}$ in Maxwell Distribution for Pu(241)

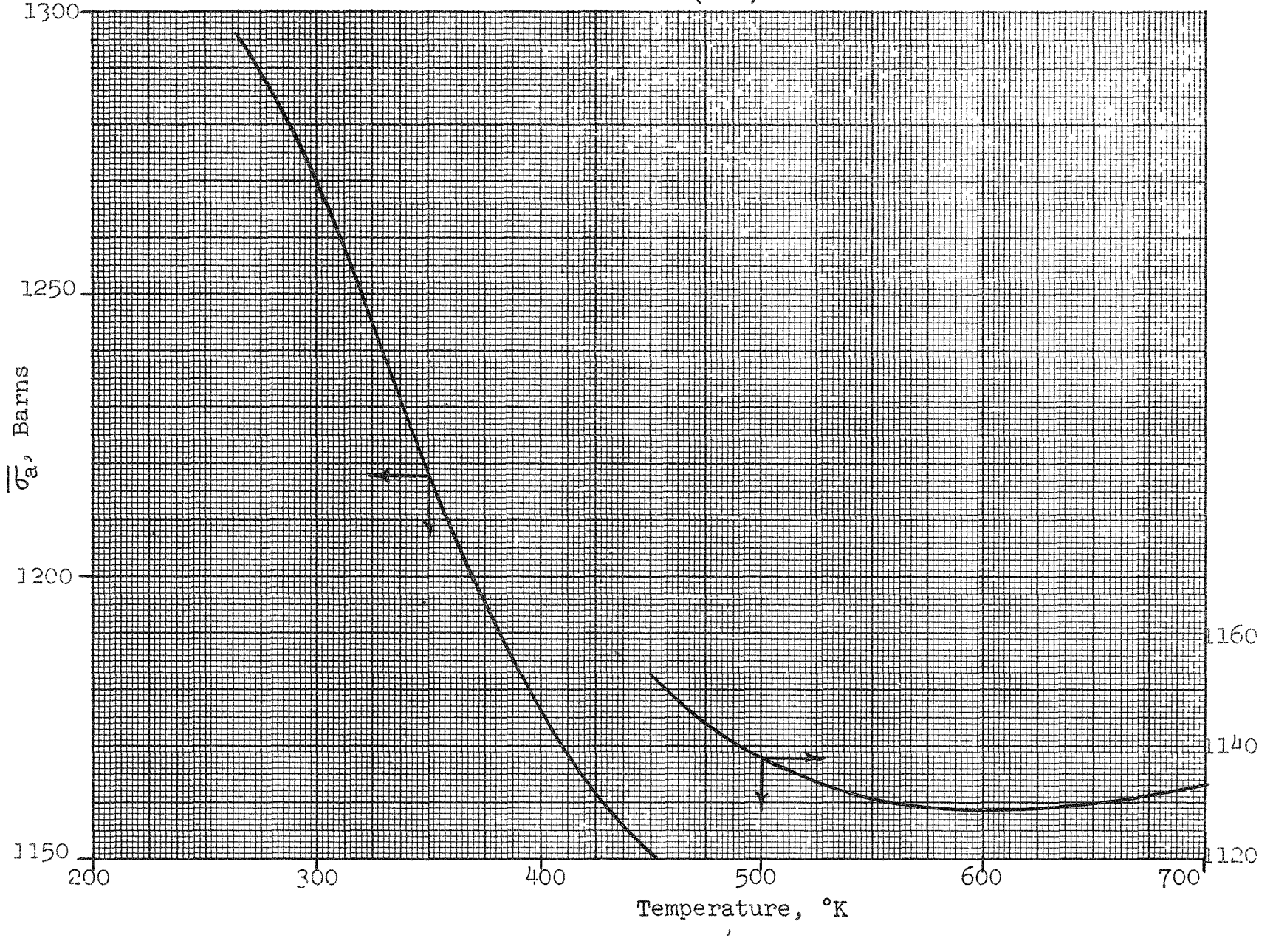

Fig. A3.L

Figure A3.M

Temperature Variation of $\overline{\sigma_f}$ in Maxwell Distribution for Pu(241)

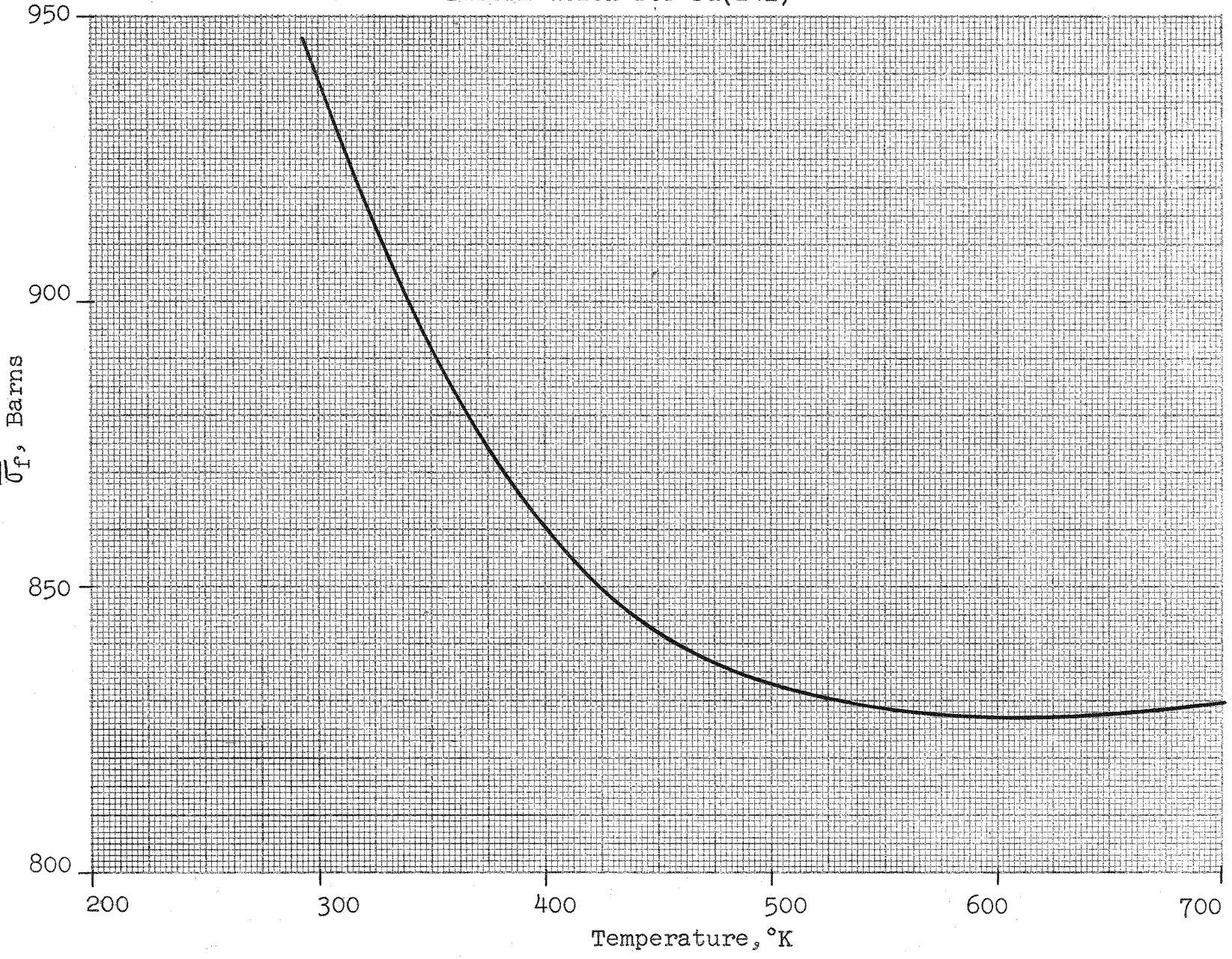

Fig. A3.M

Figure A3.N

Temperature Variation of $\overline{\nu\sigma_f}$ in Maxwell Distribution for Pu(241)

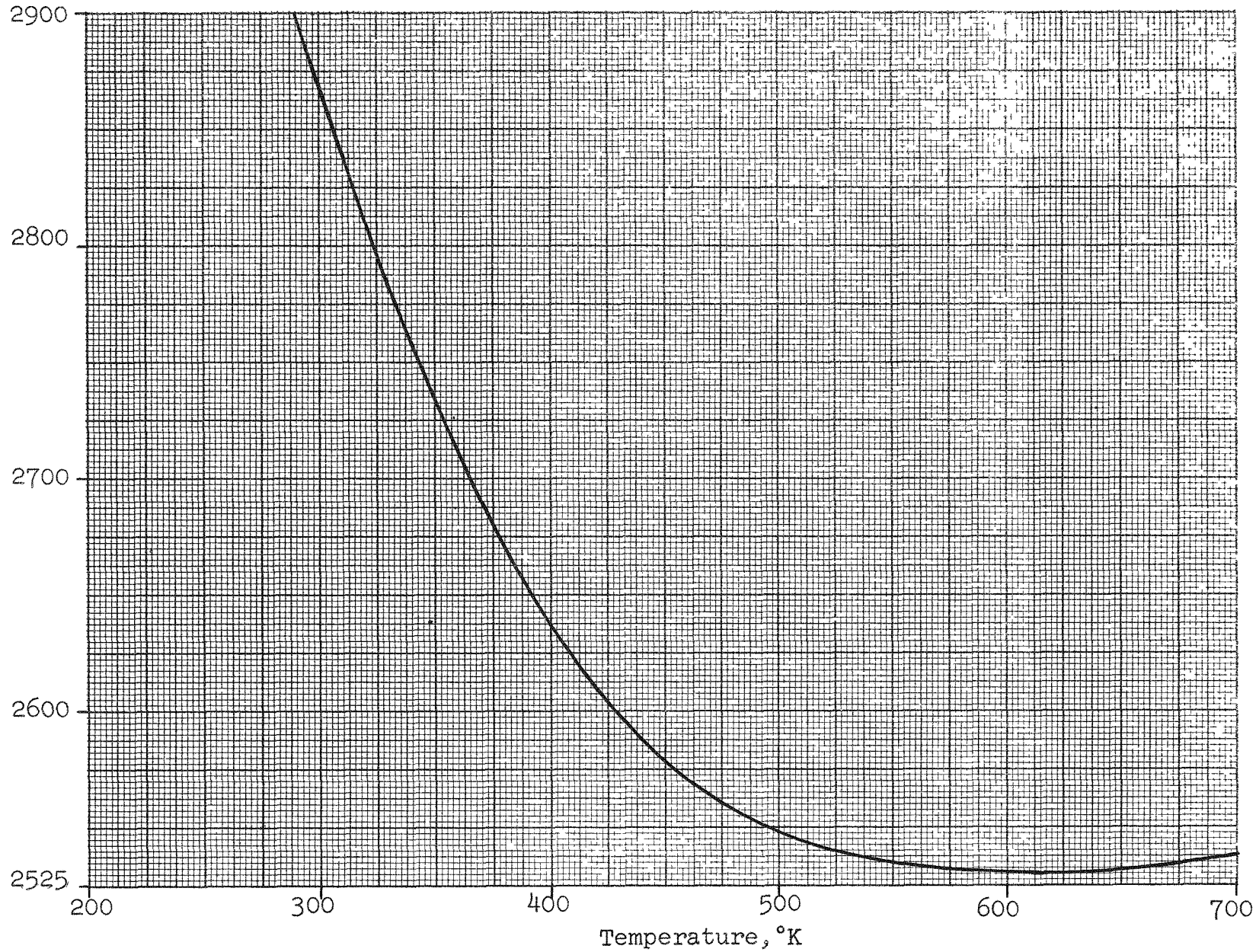

Fig. A3.N

APPENDIX 4.0 QUESTIONNAIRE SENT TO FUEL FABRICATORS

The flux-trap type of engineering test reactor provides very high thermal and/or fast neutron fluxes over a relatively large volume test region. The flux-trap core bascially consists of an annular ring of fuel elements surrounding a central test section. The general configuration of the two types of fuel assembly presently considered most suitable for use in such a core are those having: 1) concentric fuel plates and 2) involute fuel plates, as shown in Figures 1 and 2 respectively. Nominal dimensions and tolerances of the fuel assembly and fuel plate components are indicated in the Figures and in Table 1. The basic material of construction for both types of fuel assembly would be aluminum alloy for both side plates and fuel plate cladding. The fuel alloy would be a U-Al alloy or a metal powder mixture ranging from about 30 w/o U to about 50 w/o U. Highly enriched Uranium(235) would be the fuel material.

We are presently conducting analytical studies of the merit of non-uniform fuel distribution in both the radial and axial directions in the core and of burnable poison in the core.

Since the reactor concept being optimized is for nuclear engineering test purposes, the cost of achieving the design criteria of fuel or poison distribution in the fabricated fuel assembly should not be given much weight in determining feasibility. Rather, it should be used to determine the relative merit of different methods of achieving the desired objectives. If non-uniform fuel distribution (either radially, axially or both) can be achieved in the core by any method of fuel assembly fabrication, that method must be considered feasible. The practicality of the method will depend on such factors as: the strength, the integrity, the mechanical and nuclear tolerances that can be maintained, and finally the cost of the finished fuel assembly produced by the method.

It should be emphasized here that the desired fuel distribution in the fuel plate can be achieved in at least two ways: a) by varying the thickness of the meat (constant fuel concentration in meat), or b) by varying the concentration of fuel in the meat (constant meat thickness). Therefore, although the following data are based on varying the thickness of the meat, we do not mean to imply that this is the method that should be used. If you are aware of any methods of varying fuel concentration, other than those mentioned above, they should also be considered.

It should also be emphasized that the desired poison distribution might be the opposite of fuel distribution. That is, maximum poison concentration might occur at the same place as minimum fuel concentration and vice versa. We do not know at this time what condition may be most desirable in this respect.

PERTINENT INFORMATION

Table 1

Nominal Dimensions: Fuel Assembly and Components

Fuel Assembly		
	Overall length	45 inches
	Overall width (circumferentially around fuel annulus)	Core Size: small / large
	a. Concentric plates	
	Inside	3.28 in / 4.22 in
	Outside	5.06 in / 6.46 in
	b. Involute plates	
	Inside	1.48 in / 1.90 in
	Outside	2.28 in / 2.91 in
	Overall thickness (radially across fuel annulus)	
	a. Small annulus core	2.55 in
	b. Large annulus core	3.20 in
Fuel Plate		
	Overall length	37 in
	Fueled length	36 in
	Width	
	a. Concentric plates	variable, see above
	b. Involute plates	constant, but more than the radial thickness of the fuel annulus
	Thickness	50 mils
Meat		
	Overall length	36 in
	Width	variable or constant (see above) and approximately 0.4 inches less than the overall width of the fuel plate

Thickness	20 mils
Fuel	Highly enriched U(235)
Fuel alloy	30 to 50 w/o U(235) in U-Al alloy or compressed metal powder
Clad	Overall dimensions, other than thickness, same as those of fuel plate
Thickness	15 mils
Composition	Aluminum alloy
Side Plates	Overall dimensions, other than thickness, approximately same as those for fuel assembly
Thickness	0.25 in
Composition	Aluminum alloy

Nominal fuel and poison distribution ranges to be achieved in core:

Fuel distribution range*	
a. radially	0.4 to 1.0 x nom. thickness
b. axially	0.4 to 1.0 x nom. thickness
Poison distribution range**	
a. radially	0.7 to 1.0 x nom. max.conc.
b. axially	0.7 to 1.0 x nom. max.conc.

Guesstimated distribution tolerances (within a given fuel plate)

Fuel distribution tolerances	
a. radially	$\pm$ 0.02 x desired thickness at any point
b. axially	$\pm$ 0.03 x desired thickness at any point
Poison distribution tolerances	
a. radially	$\pm$ 0.02 x desired conc. at any point
b. axially	$\pm$ 0.03 x desired conc. at any point

* Fuel distribution may also be accomplished by varying the fuel concentration in the meat. This should be considered.
**Assume boron as the poison and that the max. poison concentration will be 1% of the max. fuel concentration.

QUESTIONS

On methods of fuel element fabrication to achieve non-uniform distribution of fuel and/or poison radially, axially, or both in an annular reactor core.

1. What would appear to be the most promising place to include burnable poison in the fuel assemblies"

   a. in the fuel alloy
   b. in the side plates
   c. in the clad of the fuel plates
   d. some combination of the above
   e. would either of the two proposed types of fuel element appear to be most promising in this regard?

2. Is it practical (or feasible) to insert burnable poison in a predetermined variable radial and/or axial distribution in the fuel plate and what degree of accuracy might be expected in the distribution?

   a. would either of the two proposed types of fuel element appear to be most promising in this regard?

   b. where would be the most practical (or feasible) place to insert the poison to achieve variable
      radial
      axial
      both radial and axial
      distribution of poison in the core with either of the two proposed types of fuel element?

   c. what degree of accuracy of poison distribution might be expected:

      within a given fuel plate*
      from fuel plate to fuel plate
      from fuel assembly to fuel assembly?

   d. what would be the most practical (or feasible) method or technique of inserting the poison (as in b, above)?

*Note: We have set distribution tolerances on the basis of the fuel thickness (or poison concentration) desired at any given point within one fuel plate.

3. Is it practical (or feasible) to fabricate aluminum fuel assemblies with variable fuel distribution radially and/or axially, and what degree of accuracy can be expected in the distribution?

   a. would either of the two proposed types of fuel element appear to be most promising in this regard?

   b. what would appear to be the most practical (or feasible) method to achieve variable
      radial
      axial
      both radial and axial
      distribution of fuel in the core with either of the two proposed type of fuel elements?

   c. what degree of accuracy of fuel distribution might be expected:

      within a given fuel plate
      from fuel plate to fuel plate
      from fuel assembly to fuel assembly

   d. what would be the most practical (or feasible) method or technique of fuel element fabrication to achieve variable fuel distribution in the core?

4. What are the estimated effects on cost for including variable fuel and/or poison distribution in the fuel assemblies?

5. On the basis of your practical analysis of what we are hoping to achieve, which type of fuel assembly do you feel appears most promising from a fuel assembly fabrication standpoint?

   a. would you estimate it to be feasible or practical?

   b. if it only appears feasible on the basis of your present knowledge, what is the probability of its ultimately becoming practical?

   c. what degree of research and development effort would you estimate to be necessary to make it practical?

6. Are our distribution tolerances realistic? Or should they be based entirely on the nominal thickness (or concentration) of fuel (or poison)? Would you suggest any different basis for fuel (or poison) distribution tolerances?

7. Are our distribution ranges realistic? Could they be widened or should they be narrowed?

8. Are our fuel assembly concepts realistic? Could they be altered to advantage to achieve what is desired? If so, what would you suggest? Should they be changed radically to achieve what is desired? If so, what would you suggest?

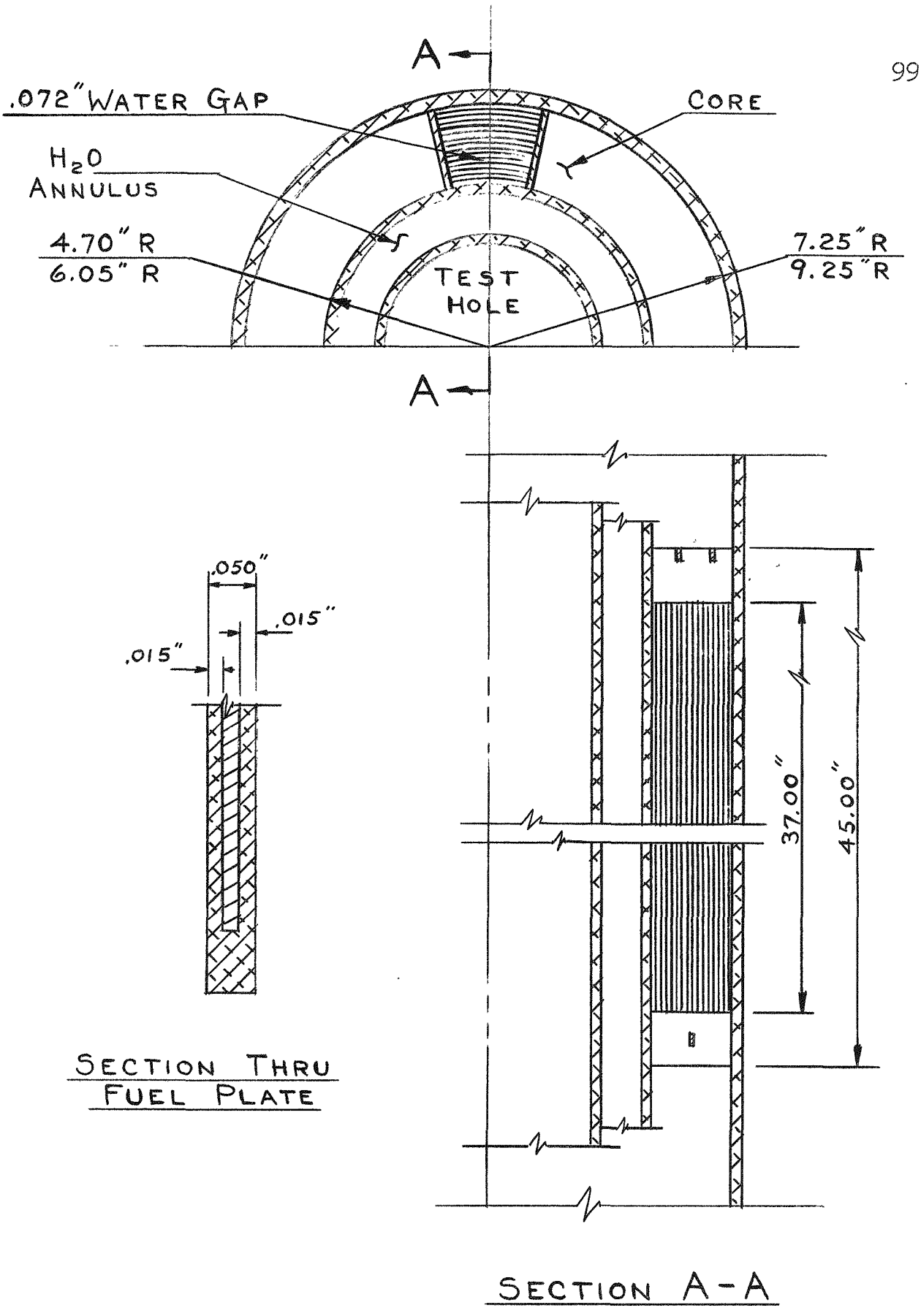

FIGURE 1. CONCENTRIC PLATE TYPE FUEL ELEMENTS

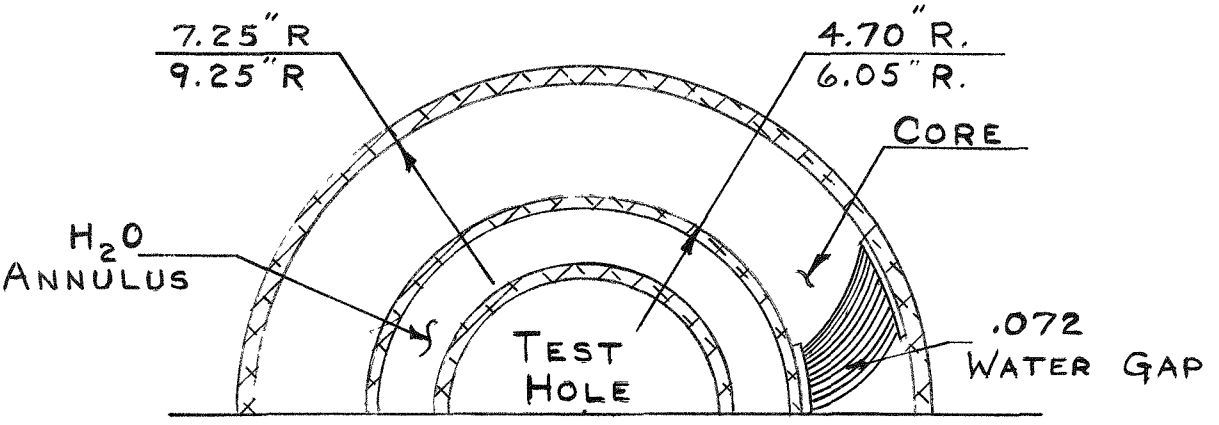

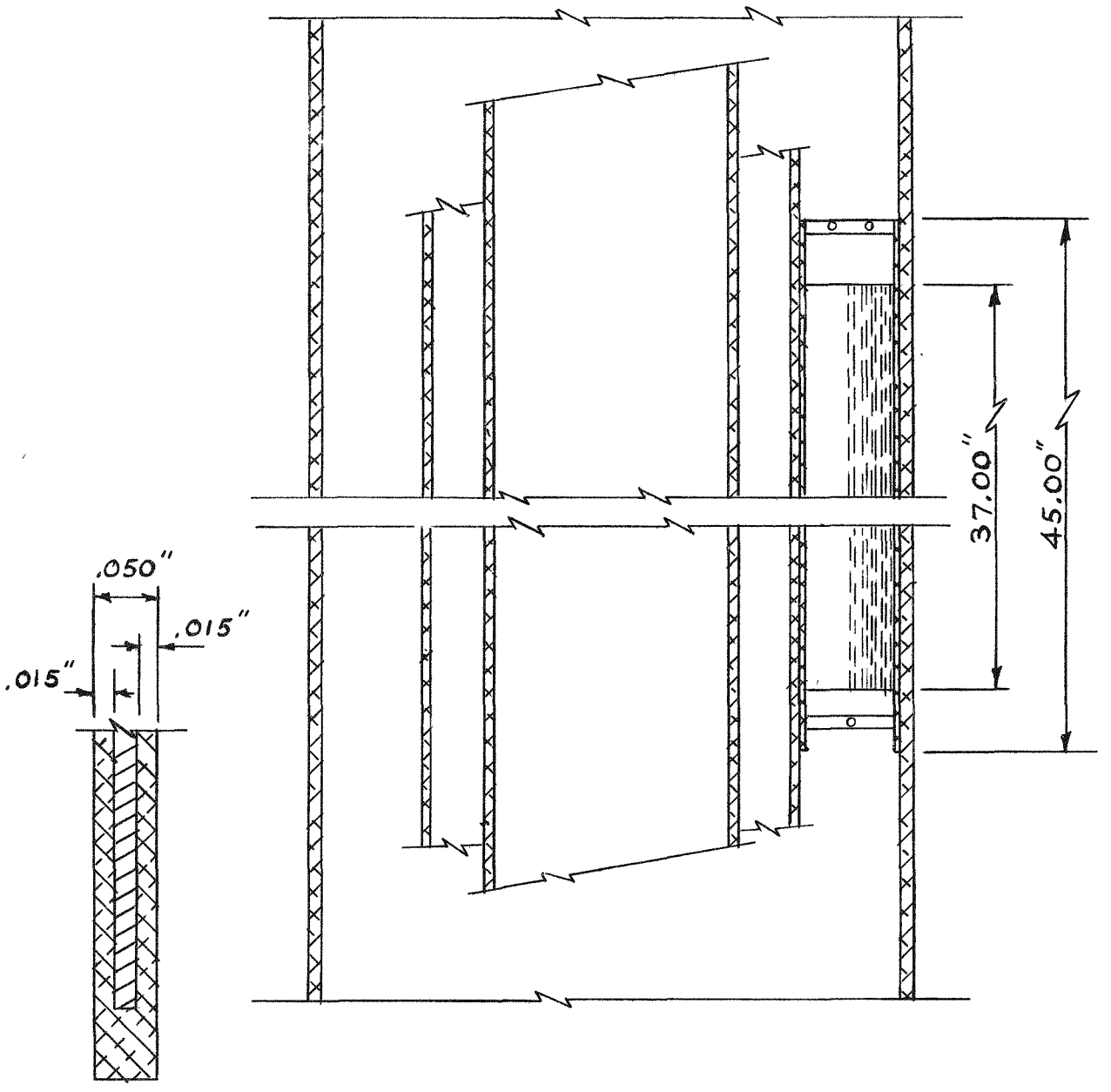

SECTION THRU
FUEL PLATE

FIGURE 2. INVOLUTE PLATE TYPE
FUEL ELEMENTS.